ORGANISATION AND RECOGNITION OF ARTIFICIAL TRANSMEMBRANE PEPTIDES

Dissertation

zur Erlangung des mathematisch-naturwissenschaftlichen Doktorgrades
” Doctor rerum naturalium “
der Georg-August-Universität Göttingen
im Promotionsprogramm Chemie
der Georg-August-University School of Science (GAUSS)

submitted by
ULRIKE ROST
from Leipzig

Göttingen, 2016

Thesis Committee

Prof. Dr. Ulf Diederichsen	*Institute of Organic und Biomolecular Chemistry,* *Georg-August-University Göttingen*
Prof. Dr. Claudia Steinem	*Institute of Organic und Biomolecular Chemistry,* *Georg-August-University Göttingen*

Members of the Examination Commission

Reviewer

Prof. Dr. Ulf Diederichsen	*Institute of Organic und Biomolecular Chemistry,* *Georg-August-University Göttingen*

Reviewer

Prof. Dr. Claudia Steinem	*Institute of Organic und Biomolecular Chemistry,* *Georg-August-University Göttingen*

Additional Members of the Examination Commission

Prof. Dr. Kai Tittmann	*Institute of Molecular Enzymology* *Georg-August-University Göttingen*
Prof. Dr. Dietmar Stalke	*Institute of Inorganic Chemistry,* *Georg-August-University Göttingen*
Dr. Franziska Thomas	*Institute of Organic und Biomolecular Chemistry,* *Georg-August-University Göttingen*
Dr. Inke Siewert	*Institute of Inorganic Chemistry,* *Georg-August-University Göttingen*

Day of the Oral Examination 11 August 2016

The work described in this doctoral thesis has been carried out under the guidance and supervision of Prof. Dr ULF DIEDERICHSEN at the Institute for Organic and Biomolecular Chemistry of the Georg-August-University Göttingen between January 2012 and August 2016.

This work was supported by the DEUTSCHE FORSCHUNGSGEMEINSCHAFT via the Collaborative Research Centre 803 (SFB 803).

ORGANISATION AND RECOGNITION OF ARTIFICIAL TRANSMEMBRANE PEPTIDES

to my family

Publications

Parts of this work have been published in professional journals:

1. U. Rost, Y. Xu, T. Salditt, U. Diederichsen, *ChemPhysChem* **2016**, *17*, 2525-2534.

2. U. Rost, C. Steinem, U. Diederichsen, *Chem. Sci*. **2016**, *7*, 5900-5907.

TABLE OF CONTENTS

1 INTRODUCTION 1

2 SYNTHESIS AND INVESTIGATION OF A NOVEL 7-AZAINDOLE BASED RECOGNITION UNIT 5

2.1 General 5

2.2 7-Azaindole 6
  2.2.1 Fluorescence Spectroscopy 9
  2.2.2 Synthesis and Fluorescence Spectroscopic Analysis of 7-Azaindole and 1-Methyl-7-azaindole 10

2.3 7-Azaindole Building Block 11
  2.3.1 Synthesis of the 7-Azaindole Building Block 12

2.4 Incorporation of the 7-Azaindole Building Block into Model Transmembrane Peptides 14
  2.4.1 Transmembrane Peptides KALP and WALP 14
  2.4.2 Design and Synthesis of Modified KALPs 16

2.5 CD-Spectroscopic Analysis of Modified KALPs 18

2.6 Fluorescence Spectroscopic Analysis of Modified KALP 17 20

2.7 Fluorescence Resonance Energy Transfer (FRET) 21
  2.7.1 Theoretical Background and Evaluation of FRET Data 21
  2.7.2 Determination of Peptide Aggregation State of Modified KALPs using FRET 25

2.8 Synthesis of the 7-Azaindole D-β^3-Building Block 30

2.9 Conclusion 31

3 ARTIFICIAL TRANSMEMBRANE Β-PEPTIDES IN LIPID BILAYERS 33

3.1 General 33
3.1.1 β-Amino Acids 34
3.1.2 β-Peptides 37

3.2 Heavy-Atom Labelled Transmembrane β-Peptides 39
3.2.1 Synthesis of the Iodine-labelled D-β^3-Amino Acid 40
3.2.2 Design and Synthesis of Iodine-labelled Transmembrane β-Peptides 41
3.2.3 CD-Spectroscopic Analysis of the Synthesised β-Peptides 43
3.2.4 X-ray Diffraction Analyses in Model Lipid Multilayer 44
3.2.5 Conclusion 49

3.3 Self-Association of Transmembrane β-Peptides within Lipid Bilayers via Hydrogen-Bond Formation of β-Glutamine 51
3.3.1 Design and Synthesis of ^{h}Gln-functionalised Transmembrane β-Peptides 52
3.3.2 CD-Spectroscopic Analysis of the Synthesised β-Peptides 54
3.3.3 Fluorescence Spectroscopic Analysis of the Synthesised β-Peptides 55
3.3.4 Determination of Peptide Aggregation State of Transmembrane β-Peptides using FRET 57
3.3.5 Conclusion 61

4 SUMMARY 63

5 EXPERIMENTAL PART 69

5.1 General 69

5.2 Characterisation 71

5.3 Standard Operating Procedures (SOPs) 73
5.3.1 SOPs for the Syntheses of the β^3-Amino Acids 73
5.3.2 SOPs for the Syntheses of α- and β-Peptides 74
5.3.3 SOPs for the Preparation of Peptide/Lipid Complexes 77
5.3.4 SOP12: Enantiomeric purity (MARFEY's reagent)[124–127] 78

5.4 Syntheses 79
5.4.1 Synthesis of 1-Methyl-7-azaindole 79
5.4.2 Synthesis of the 7-Azaindole Building Block 80

5.4.3 Synthesis of the 7-Azaindole D-β^3-Building Block 83
5.4.4 Synthesis of the Diiodoallylhomoglycine Building Block 86
5.4.5 Syntheses of the β^3-Amino Acids 90
5.4.6 Syntheses of functionalised KALPs and their non-functionalised Analogues 96
5.4.7 Syntheses of the β-Peptides 103

6 APPENDIX 117

6.1 Concentration dependent Fluorescence Emission Spectra of the KALPs 18-20 at a P/L-ratios 1/500 and 1/1000 at 25 °C 117

6.2 Concentration dependent Fluorescence Emission Spectra of the KALPs 21-23 at a P/L-ratios 1/100, 1/250, 1/500, and 1/1000 at 25 °C and at 60 °C 118

6.3 Concentration dependent Fluorescence Emission Spectra of the β-Peptides 48-50, 51-53 and 54-56 at a P/L-ratio = 1/500 at 25 °C and 60 °C 120

6.4 Concentration dependent Fluorescence Emission Spectra of the β-Peptides 51-53 and 54-56 at the P/L-ratios 1/750 and 1/1000 at 25 °C 122

6.5 Relative Changes in Donor Fluorescence Emission (F/F_0) as a Function of increasing Acceptor Concentration (β-Peptides 51-56) 123

7 ABBREVIATIONS 125

8 REFERENCES 129

9 ACKNOWLEDGEMENTS 137

10 CURRICULUM VITAE 141

INTRODUCTION

Integral membrane proteins represent nearly 30% of the human proteome and take part in a various number of cellular processes.[1,2] Due to the complexity of their protein structures, the precise analysis of their biological activities, functions and mechanisms is limited. If integral membrane proteins want to accomplish their function, they can be either monomeric or they need to associate into oligomeric structures.[3–5] The association of peptides in lipid membranes is based on a variety of noncovalent interactions such as hydrogen bonds, hydrophobic interactions, and electrostatic interactions. As interactions between integral membrane proteins and lipids play an important role in a variety of cellular processes, they build the base for biological functions such as enzyme catalysis, protein-protein binding, signal transduction, flexibility, and stability.[6–11] In order to understand the mechanisms behind these processes that are often complex and thus, poorly understood, simple model transmembrane peptides have been of great interest.[4,12] In addition, specific recognition units have been used as they might help to understand the essentials and molecular details of these transmembrane peptides within the lipid bilayer. To broaden the horizon in the field of peptide chemistry further, the development of new recognition units facilitates the analyses of transmembrane peptides.[5,13–17]

In the first part of this thesis, the design, synthesis and investigation of a novel 7-azaindole based recognition unit are presented. The fluorescence emission and even the fluorescence intensity of the 7-azaindole chromophore are known to be sensitive to their local surrounding.[18–20] Herein, preliminary fluorescence analyses were performed to gain deeper insights into the influences on 7-azaindole on its environment. Furthermore, the synthesis of a 7-azaindole based amino acid residue (**1**) is presented as the latter might be a suitable and promising tool for peptide chemistry.

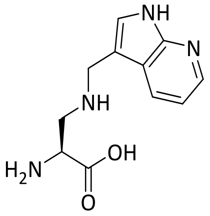

1

Figure 1: Structure of the 7-azaindole based amino acid residue (1).

The novel 7-azaindole based recognition unit (**1**) was further incorporated in a transmembrane model system, *i.e.* KALPs, which was previously presented by KILLIAN and co-workers and analysed by fluorescence spectroscopy. In addition, it is expected that the building block dimerise in hydrocarbon environment such as the inner membrane part. Hence, a possible peptide-peptide association was investigated by fluorescence resonance energy transfer (FRET) experiments in collaboration with C. STEINEM.[3]

Model transmembrane peptides have been used in different ways to analyse basic principles of protein-lipid interactions. Such model systems will help to enable detailed analyses on the structure and dynamics of transmembrane peptides within lipid bilayers. In addition, it is possible to analyse the influence of the length and composition of the inner membrane part on the organisation and dynamics of membrane lipids.[7] During the last three decades, the interest in design and synthesis of artificial β-peptides has risen tremendously as β-peptides are capable of forming more stable secondary structures than α-peptides. Furthermore, they are resistant to proteolytic degradation by proteases and peptidases.[9,21] However, transmembrane β-peptide helices are still widely unexplored and a model transmembrane β-peptide system would be an appreciated tool to investigate peptide-lipid and peptide-peptide interaction, *e.g.* occurring in membrane associated processes.[9,15,21,22]

The second part of this thesis focuses on the rational design, synthesis and investigations of artificial transmembrane β-peptides. The first section addresses the issues of structural parameters such as conformation, orientation and penetration depth of the transmembrane β-peptides incorporated in a membrane environment. Therefore, a novel iodine-labelled D-β^3-amino acid residue (**2**) suitable for Fmoc-solid phase peptide synthesis (SPPS) was synthesised and incorporated in the designed transmembrane β-peptides (Figure 2). This heavy atom building block **2** is expected to provide electron density contrast in the labelled region of the reconstructed electron density profiles during X-ray reflectivity and grazing incidence small-angle X-ray scattering investigations.[13,22] The X-ray diffraction studies were performed in collaboration with Y. XU from the SALDITT research group.

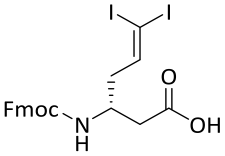

2

Figure 2: Structure of Fmoc-6,6-diiodo-allylhomoglycine (2).

Furthermore, these novel transmembrane β-peptides were used for peptide oligomerisation studies based on hydrogen bond formation within a lipid bilayer as the organisation and assembly of transmembrane β-peptide helices are still widely unexplored.[3,15] In order to investigate if the driving force of these association processes might depend on the lipid environment and/or the interacting molecular species themselves, the novel transmembrane β-peptide system could be an appropriate tool. Herein, hydrogen bond formation was established by placing D-β^3-glutamine recognition units at defined positions within the transmembrane β-peptides (Figure 3).

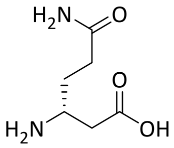

3

Figure 3: Structure of D-β^3-glutamine (3).

D-β^3-Glutamine (**3**) is very similar to asparagine, which has been shown to form hydrogen bonds and thus, allows for self-association of α-peptide helices.[16,23] Here again, the association state was analysed by FRET experiments in collaboration with C. Steinem. The secondary structure of all transmembrane β-peptides reconstituted into unilamellar vesicles was determined by means of circular dichroism spectroscopic measurements (Figure 4).

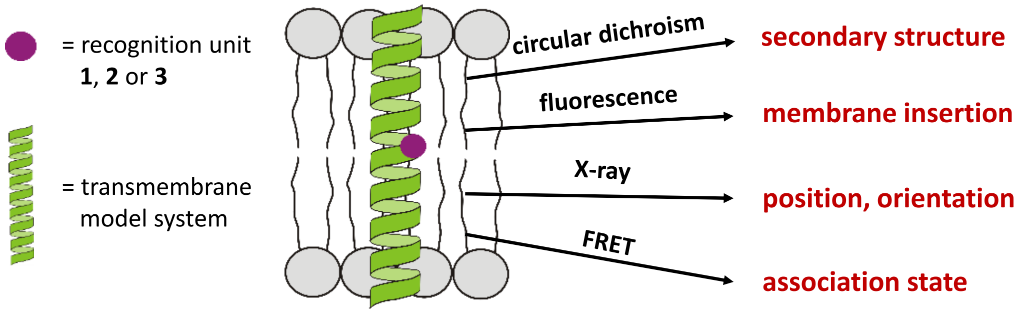
= recognition unit
1, **2** or **3**
= transmembrane
model system
circular dichroism
secondary structure
fluorescence
membrane insertion
X-ray
position, orientation
FRET
association state

Figure 4: Overview of proposed strategies for analysing transmembrane peptides.

SYNTHESIS AND INVESTIGATION OF A NOVEL 7-AZAINDOLE BASED RECOGNITION UNIT

3.1 General

The function, conformation and orientation of integral membrane proteins and peptides are influenced by the surrounding lipid bilayer. The molecular interactions between lipids and these transmembrane proteins and peptides can be described in molecular terms such as hydrophobic interactions, VAN-DER-WAALS interactions, and hydrogen bonding or ionic interactions.[16,24] The influence of these parameters on integral membrane protein interaction are still barely understood and model transmembrane peptides are therefore of great interest.[4,12] In order to design such model systems, different processes have been investigated. Fundamental findings of these studies show that hydrophobic side chains facilitate a membrane insertion. Aromatic and positively charged side chains at the *N*- and *C*-terminal end of a peptide sequence are known to anchor the peptides in a perpendicular orientation inside the membrane.[25–27] Furthermore, helix-helix association inside the membrane is influenced by electrostatic and VAN-DER-WAALS interactions.[28,29] Additional recognition units inside the hydrophobic part of peptides could help to understand the behaviour of transmembrane peptides inside lipid bilayers and their consequential interactions. SCHNEGGENBURGER *et al*. presented heavy-atom labelled transmembrane α-peptides in combination with X-ray diffraction studies to characterise parameters like conformation, orientation and penetration depth of these α-peptides incorporated into lipid membranes. As the heavy atom label the modified amino acid 5,5-diiodo-allylglycine-OH (**4**) was synthesised as recognition unit and integrated into peptides (Figure 5A).[13] Even though transmembrane peptides are dominated by hydrophobic amino acid residues, they also contain polar amino acids that play important structural and functional roles.[30,31] Polar amino acid residues such as Asn, Gln, Glu and Asp are known to control the oligomerisation of transmembrane helices via hydrogen bond formation (Figure 5B, *i*).[32,33]

In addition, BRÜCKNER *et al*. have shown that small β-peptide helices can be organised by nucleobase pairing to acquire more control of the self-association process (Figure 5B, *ii*).[17] Furthermore, amino acid residues like Lys and Glu are able to associate into oligomers via electrostatic interactions (Figure 5B, *iii*).[9]

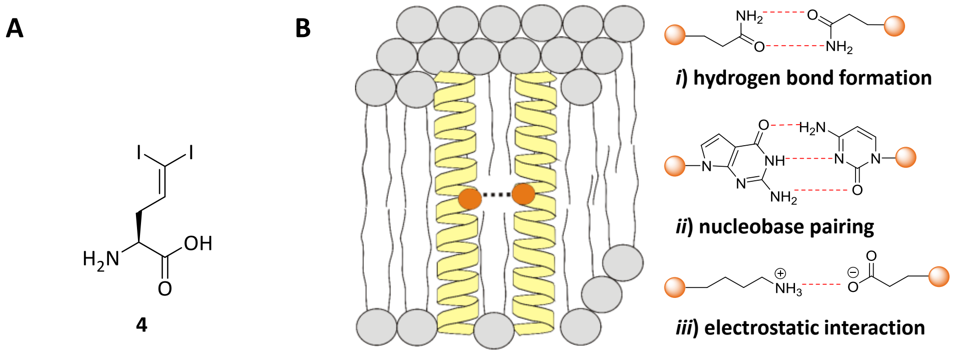

Figure 5: A: 5,5-Diiodo-allylglycine (4). B: Schematic view on different interactions inside the lipid bilayer: *i*) hydrogen bond formation of asparagine, *ii*) nucleobase pairing of guanine and cytosine, and *iii*) electrostatic interaction of lysine and glutamic acid.

All these described interactions are most favoured if the interacting residues are located on the same level in the lipid bilayer which should be considered when designing transmembrane model systems with recognition units.[34]

In order to understand the interactions, conformation and orientation of transmembrane peptides, the development of new recognition units is necessary. Thus, the design, synthesis and analysis of a novel recognition unit **1** with 7-azaindole as recognition unit is presented (Figure 6).

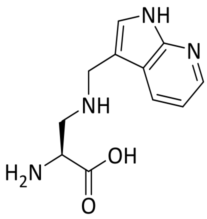

1

Figure 6: Structure of the novel recognition unit (1) with 7-azaindole as basic unit.

3.2 7-Azaindole

7-Azaindole (**5**, 7-AI) is an important model system for different chemical processes.[35] The tryptophan (**6**) analogue 7-azatryptophan (**7**) shows spectral characteristics that are largely determined by the 7-azaindole chromophore (Figure 7). In contrast to tryptophan (**6**), 7-azatryptophan (**7**) has an exponential fluorescence decay that prevents difficulties in interpreting the fluorescence or anisotropy decays when it is integrated in a peptide or protein. In addition, the fluorescence maximum of 7-azatryptophan (**7**) is red-shifted up to 10 nm with respect to that of tryptophan (**6**).[36,37]

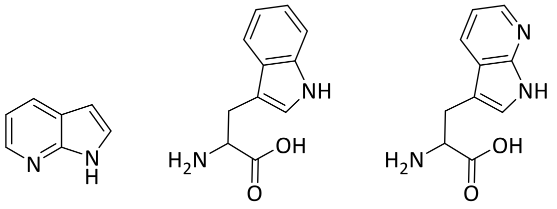

5 **6** **7**

Figure 7: Structure of 7-azaindole (5), tryptophan (6) and 7-azatryptophan (7).

The fluorescence of the 7-azaindole chromophore (**5**) shows a very strong solvent dependence, which can be explained by a longer lifetime in its excited S_1 state, a higher fluorescence quantum yield, and a significantly different electronic distribution than tryptophan. [38,39] Beside the position of the fluorescence maxima, the fluorescence intensity is also influenced by the polarity and proticity of the surrounding solvent. Hence, 7-AI (**5**) derivatives become applicable tools to analyse hydrophobic environments such as lipid bilayers.[19] Photophysics of 7-AI (**5**) have been intensively investigated in many different solvents.[20] The excited-state double-proton transfer (ESDPT) that occurs differently in hydrocarbon and alcohol solvents has been recognized by TAYLOR *et al.* and has already been used as a model for studying photoinduced mutations of DNA base pairs.[40,41] The ESDPT is due to the formation of hydrogen bonded dimers or solute/alcohol complexes, respectively, and results in two fluorescence bands (monomer and tautomer) (Figure 8).[19]

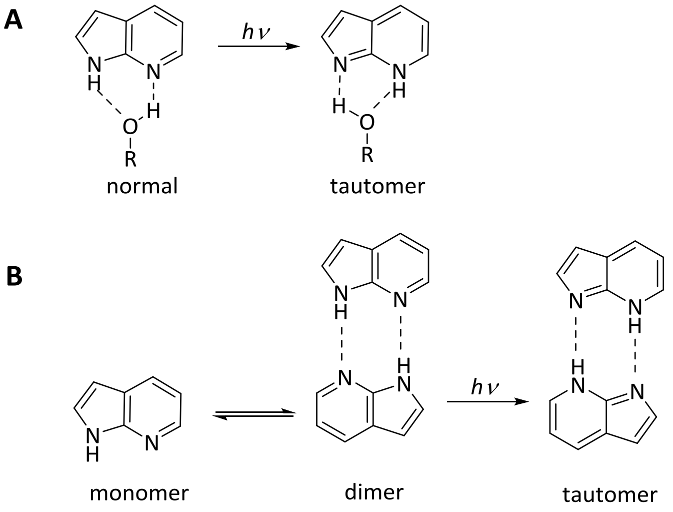

Figure 8: Tautomerisation process of 7-azaindole (5) in alcoholic solvents (A) and in hydrocarbon solvents (B).

Spectroscopic measurements have shown that in hydrocarbon solvents the long-wavelength emission (λ_{max} ~ 490 nm) results from the double-proton transfer of symmetric, hydrogen bonded dimers that give a green tautomer emission (Figure 9).[18–20] These tautomeric fluorescence bands are accessible by steady-state fluorescence spectroscopy or time-resolved fluorescence spectroscopy in the femto-, pico or nano-seconds range.[18,19,35,36,42,43]

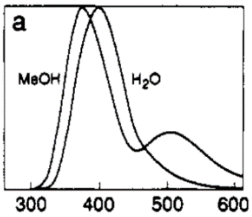

Figure 9: Normalised fluorescence emission spectra of 7-azaindole (1) in water and MeOH.[36]

The other detected fluorescence band (blue-shifted compared to the tautomeric fluorescence) belongs to the monomer or other configurations that are not favourable for proton transfer and result in short-wavelength fluorescence with λ_{max} ~ 340 nm.[19,39] Water exposure results only in one emission band for 7-AI (**5**) with a single-exponential fluorescence decay (Figure 9). Here, only 20% of 7-azaindole (**5**) can undergo the tautomerisation process as most of the solute molecules are inapplicably solvated (Figure 10). In other words, these molecules are 'blocked' from executing an excited-state tautomerisation by the surrounding water molecules.[35] Furthermore, the dimers and tautomers are considered to be planar and cyclic complexes with two NH···N hydrogen bonds. Due to the partial solvation of 7-AI (**5**) (~ 80%), no cyclic transition state could occur.[35] In addition, GUHARAY *et al.* analysed the solvent dependence of 7-azatryptophan (**7**) in micellar environment. They found that an increase in the water/surfactant molar ratio resulted in a red-shifted emission maximum, which is accompanied by quenching of the fluorescence emission and a precise decrease in its quantum yields.[44] This observation is in good agreement with the described solvation by water. After excitation of the water solvated molecules they return to the non-radiative ground state and consequently the quantum yield decreases.[19,35,45]

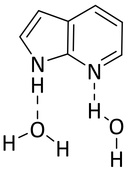

Figure 10: Solvation of 7-azaindole (5) in water.

3.2.1 Fluorescence Spectroscopy

During the past three decades, fluorescence spectroscopy and time-resolved fluorescence spectroscopy have represented useful research tools in biological science like biochemistry and biophysics. Fluorescence spectroscopy is highly sensitive and accessible as the experimental setup is quite simple. In addition, fluorescence imaging is used to gain insights into the structural dynamics of proteins and it can even reveal the localisation of intracellular molecules.[46,47] Fluorescence is the emission of light after the absorption of light. A molecule is excited to an upper electronic state (S_2) and rapidly transfers from S_2 to the lowest excited state S_1 by losing the excess of vibrational energy followed by transition to S_0 (ground state) accompanied by emission of a photon.[47–50] This process has a lifetime of a few nanoseconds (10^{-9} s) and in this period, the molecule can change its position and can interact with its surrounding. Thus, the emission is influenced by the molecule environment and by the dynamics of the molecule.[46] There are various molecules in proteins which show different types of fluorescence, *i.e*. intrinsic, coenzymic, and extrinsic. Aromatic side chains like the indole moiety in tryptophan or the 7-azaindole (**5**) itself are intrinsic chromophores. Some proteins contain a fluorescent coenzyme such as Flavin-adenine dinucleotide. However, sometimes it is necessary to insert suitable chromophores into the protein to be able to use fluorescence spectroscopy.[47] Beside the fluorescence emission, there are other deactivation processes that could occur, which are summarised in the Jablonski diagram.[49] Another process relevant in the present thesis is the fluorescence resonance energy transfer (FRET), in which energy is transferred from one molecule (donor) to another molecule (acceptor) (see 3.7).[50] In the present study (7-nitrobenz-2-oxa-1,3-diazol-4-yl (**8**, NBD) functions as donor, whereas 5(6)-carboxytetramethylrhodamine (**9**, TAMRA) serves as acceptor. These fluorophores were covalently attached to the peptide and represent extrinsic types of fluorescence.

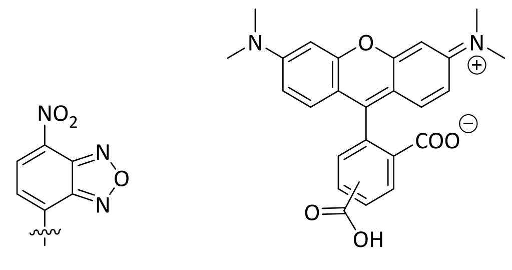

8 **9**

Figure 11: Structure of NBD (8) and 5(6)-TAMRA (9).

3.2.2 Synthesis and Fluorescence Spectroscopic Analysis of 7-Azaindole and 1-Methyl-7-azaindole

In order to get more information on 7-azaindole (**5**) and its solvent dependence, fluorescence spectroscopic investigations were performed. In addition, 1-methyl-7-azaindole (**10**) was introduced and analysed, as it is very similar to 7-azaindole (**5**) but due to its additional methyl group a change in solvent dependence could occur. Thus, it is meaningful to compare the fluorescence of 7-azaindole (**5**) with that of 1-methyl-7-azaindole (**10**) to investigate the influences of different solvents on these building blocks. First of all, 1-methyl-7-azaindole (**10**) was synthesised. Starting with 7-azaindole (**5**), the pyrrole-nitrogen was deprotonated with sodium hydride followed by a nucleophilic substitution using methyl iodide to obtain the methylated compound **10** in 36% yield (Scheme 1).[51]

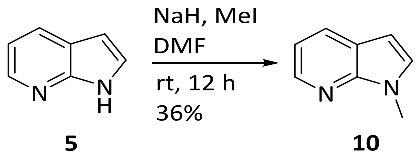

Scheme 1: Synthesis of 1-methyl-7-azaindole (10).[51]

Afterwards, the fluorescence emission spectra of 7-azaindole (**5**) and 1-methyl-7-azaindole (**10**), were recorded in *N*,*N*-dimethylformamide (DMF) and methanol (MeOH) at a concentration of 100 µM at 25 °C (Figure 12). DMF is an aprotic polar solvent and it is expected that DMF has no influence on the fluorescence, whereas MeOH is a protic polar solvent and should influence the fluorescence. The fluorescence spectra of 7-azaindole (**5**) clearly show its solvent dependence with a maximum in DMF at $\lambda_{\max}$ = 362 nm and in MeOH at $\lambda_{\max}$ = 374 nm. These values are in good agreement with the literature known data for the monomer fluorescence.[36,37] Furthermore, the tautomeric-fluorescence is not detectable as the samples might be not concentrated enough and hence, the building block is not able to form solute/alcohol complexes or dimers, that are expected to tautomerise up on excitation. As a consequence, the results demonstrate only the monomer fluorescence of 7-AI (**5**). The fluorescence spectra of 1-methyl-7-azaindole (**10**) show a maximum in DMF at $\lambda_{\max}$ = 372 nm and in MeOH at $\lambda_{\max}$ = 380 nm. The fluorescence spectra of 1-methyl-7-azaindole (**10**) are slightly shifted compared to the spectra of 7-azaindole (**5**), which is a result of the different dielectric constants of DMF and MeOH that influence the two building blocks in a different manner.[52] In both cases, the fluorescence maxima in DMF are almost similar in intensity. Hence, the monomer fluorescence is not influenced by an aprotic polar solvent like DMF as it cannot form hydrogen bonds with the building blocks. The fluorescence spectrum of 7-azaindole (**5**) in MeOH shows a significant decrease in fluorescence intensity due to hydrogen bond formation of 7-AI (**5**) with MeOH.[19] However, 1-methyl-7-azaindole (**10**) does not have such a strong decrease in fluorescence intensity as the 1*H*-position is methylated. Thus, the decrease in fluorescence intensity of 1-methyl-7-azaindole (**10**) is not that strong compared to 7-AI (**5**) in MeOH.

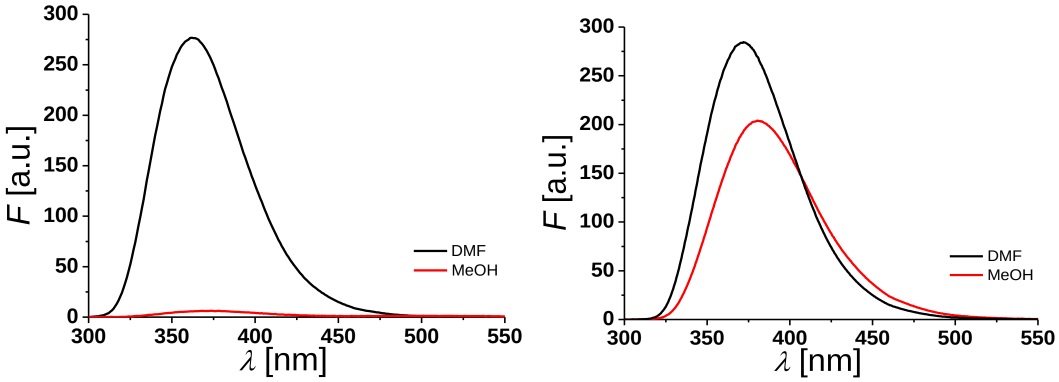

Figure 12: Fluorescence spectra of 7-azaindole (left) and 1-methyl-7-azaindole (right) in DMF (black) and MeOH (red) at *c* = 100 µM.

Nevertheless, the fluorescence intensity of 1-methyl-7-azaindole (**10**) in MeOH is lower than in DMF as the *N*7 could form a hydrogen bond with the solvent, which seems to affect the fluorescence intensity. These findings clearly demonstrate the solvent dependency of the chromophore 7-AI (**5**) during fluorescence spectroscopy. Beside the shift in fluorescence emission, the intensity is also affected by the solvent. Thus, 7-azaindole (**5**) seems to be a suitable recognition unit for analysing hydrophobic environments like lipid bilayers as lipid acyl chains are almost similar to hydrocarbon solvents.

3.3 7-Azaindole Building Block

As already mentioned, 7-azaindole (**5**) seems to be a suitable recognition unit for analysing different environments (see 3.2) and it could be a useful tool in peptide chemistry as it is sensitive to its local surrounding and it is expected to dimerise within the lipid bilayer. Hence, a linkage to the peptide backbone creating a new artificial amino acid facilitates the solid phase peptide synthesis (SPPS). The commercially available 7-azatryptophan (**7**) resembles tryptophan and can be supplied as unprotected D/L-mixtures or as Fmoc-protected D/L-mixtures that need to be purified using enzymatic conditions, which is limited by the price of the required recombinant enzymes. 7-Azatryptophan (**7**) can also be obtained at high cost as the enantiopure amino acid Fmoc-(*S*)-7-azatryptophan.[53–58] LECOINTE *et al*. described the synthesis of (*R*)-7-azaindole purifying the D/L-mixture by enzymatic resolution.[59] NOICHL *et al*. presented a total synthesis of methylated and Fmoc-protected 7-azatryptophans yielding the enantiopure product.[60] During peptide synthesis, tryptophan is generally introduced as Fmoc-Trp(Boc)-OH with a Boc protected 1*H*-position in order to avoid side reactions. Unfortunately, the previously described 7-azatryptophan residues do not contain any protecting group at the 7-azaindole ring and consequently, side reactions could occur during Fmoc-SPPS. In addition, all shown 7-azatryptophan compounds are either expensive or complex to synthesise. Here, a novel synthesis of an enantiopure amino acid with 7-azaindole (**5**) as recognition unit is presented. This amino acid building block **11** can be selectively protected and synthesised in four steps by using commercially available and more convenient starting compounds.

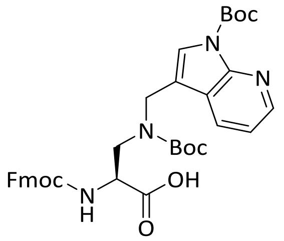

11

Figure 13: Structure of the 7-azaindole building block 11.

3.3.1 Synthesis of the 7-Azaindole Building Block

The synthesis of the 7-azaindole building block (*S*)-2-(9-fluorenylmethyloxycarbonyl)-amino-3-*tert*-butoxycarbonyl-(1'-*ter*t-butoxycarbonyl-7'-azaindole)-3'-(methyl)amino-propanoic acid (**11**) was performed in four steps and resulted in an amino acid building block that is suitable for the synthesis of transmembrane peptides using Fmoc-SPPS. After formylation (Duff reaction) of the commercially available 7-azaindole (**5**) using hexamethylenetetramine, 7-azaindole-3-carboxaldehyde (**12**) was obtained in 67% yield (Scheme 2).[61] The 1*H*-position was protected using 4-dimethylaminopyridine (DMAP) and di-*tert*-butyl dicarbonate (Boc_2O) to receive 1-*tert*-butoxycarbonyl-7-azaindole-3-carboxaldehyde (**13**) in 91% yield.[62]

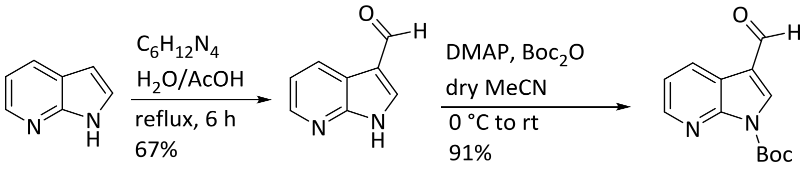

5 **12** **13**

Scheme 2: Synthesis of 1-*tert*-butoxycarbonyl-7-azaindole-3-carboxaldehyde (13).

In a second reaction, Fmoc-Asn-OH (**14**) was converted to Fmoc-Dap-OH (**15**) by a Hofmann rearrangement using (diacteoxyiodo)benzene (PIDA) in 66% yield (Scheme 3).[63]

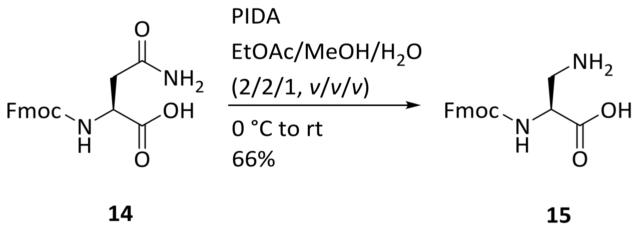
PIDA
EtOAc/MeOH/H_2O
(2/2/1, *v*/*v*/*v*)
0 °C to rt
66%
Fmoc
NH_2
OH
N
H
O
14
15

Scheme 3: Synthesis of Fmoc-Dap-OH (15).

The final step was a reductive amination of Fmoc-Dap-OH (**15**) with the Boc-protected aldehyde **13** (Scheme 4). The Boc-protection was necessary as no product was formed during synthesis using the unprotected aldehyde **12**. This might be due to interactions of the unprotected building block (**12**) with surrounding solvent molecules (see 3.2). In order to perform the reductive amination, **13** and **15** were treated with *N*,*N*-diisopropylethylamine (DIPEA) to give the imine, which was reduced to the secondary amine using $NaBH_4$. The secondary amine was further Boc-protected using Boc_2O in aqueous sodium carbonate/dioxane solution to obtain the final amino acid building block (*S*)-2-(9-fluorenylmethyloxy-carbonyl)-amino-3-*tert*-butoxycarbonyl-(1'-*tert*-butoxycarbonyl-7'-azaindole)-3'-(methyl)amino-propanoic acid (**11**) in 56% yield over two steps. This 7-azaindole (7-AI) building block **11** is suitable for Fmoc-SPPS and can be incorporated in transmembrane peptides.

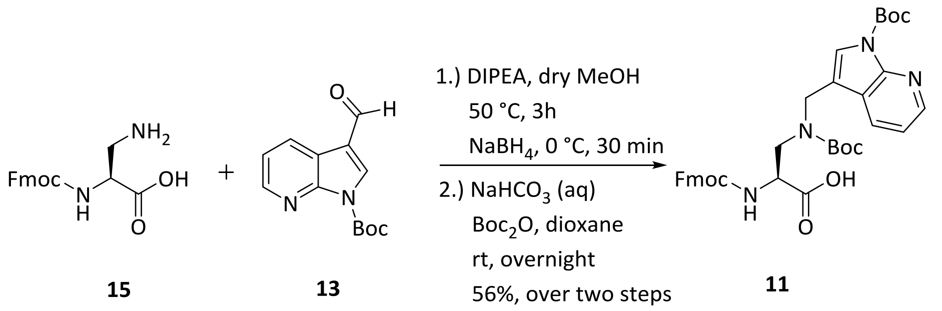
1.) DIPEA, dry MeOH
50 °C, 3h
$NaBH_4$, 0 °C, 30 min
2.) $NaHCO_3$ (aq)
Boc_2O, dioxane
rt, overnight
56%, over two steps
Fmoc
NH_2
OH
O
H
N
Boc
15
13
11

Scheme 4: Final step of the synthesis of (*S*)-2-(9-fluorenylmethyloxycarbonyl)-amino-3-*tert*-butoxycarbonyl-(1'-*tert*-butoxycarbonyl-7'-azaindole)-3'-(methyl)amino-propanoic acid (11).

3.4 Incorporation of the 7-Azaindole Building Block into Model Transmembrane Peptides

In order to investigate the potential of the synthesised 7-AI building block **11** incorporated in a peptide, a well-established model system had to be found. As the fluorescence of the 7-AI building block **11** should be detected only, it is necessary to find a system without any other aromatic amino acids. Thus, KALP23 (KAL-peptide, **16**, Figure 14) presented by KILLIAN and co-workers is used as it is known to form a stable secondary structure (α-helix) and it is incorporated into lipid bilayers in a transmembrane orientation.[64–68]

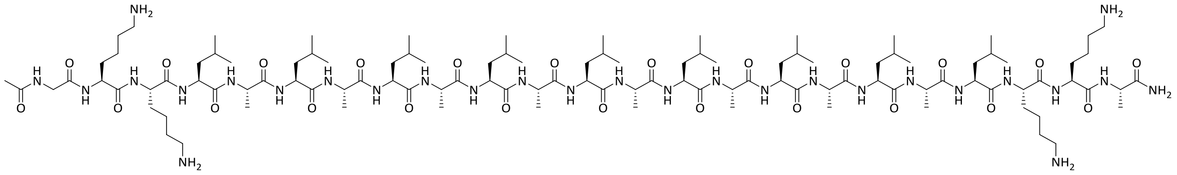

16

Figure 14: Structure of KALP23 (16).[67]

3.4.1 Transmembrane Peptides KALP and WALP

KALPs and WALPs were presented by KILLIAN and co-workers as model transmembrane peptide systems.[64–68] In both cases, the hydrophobic core (differing in length) is composed of alternating leucine (L) and alanine (A). The peptides are flanked at each side either of a sequence containing two charged lysine (K) residues (KALPs) or two polar tryptophan (W) residues (WALPs) (Table 1).[66,69] Lysine side chains are known to interact with the lipid head groups and thus, they facilitate the solubility in aqueous systems.[70] Tryptophan residues with its indole moieties arrange the peptide in the polar/apolar interface of the lipid membrane.[71]

Table 1: Amino acid sequence of KALP and WALP (Etn = ethanolamine, *n* = number of LA residues in the sequence).

Peptide	Sequence
KALP	Ac-GKKLA(LA)$_n$LKKA-NH$_2$
WALP	Ac-GWWLA(LA)$_n$LWWA-Etn

KALPs and WALPs form a stable α-helical secondary structure if embedded in membrane environment influencing the thickness of the membrane in a different manner.[67] Hence, KALPs and WALPs were used to analyse the effect of changes on lipid membranes due to different hydrophobic peptide length (*n* × LA).[7] If the length of the hydrophobic part of the peptide and that of the inner membrane part do not correspond, a hydrophobic mismatch does arise.[69,72] The peptides and lipids are able to offset a hydrophobic mismatch by several adaptations (Figure 15, Figure 16). A positive hydrophobic mismatch, *i.e*. the hydrophobic part of the peptide is longer than the thickness of the lipid bilayer, can be alleviated by the adaptions described in Figure 15.[73]

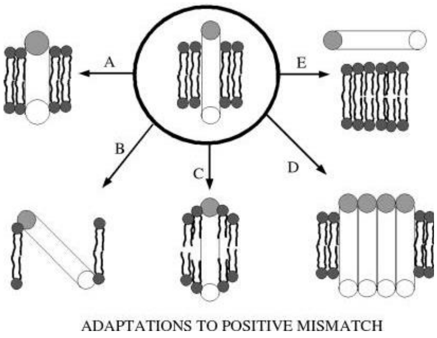

A: Decrease of the hydrophobic length of the helix.

B: Tilting of the peptide.

C: Ordering of the acyl chain near the peptide, that increases the local bilayer hydrophobic width.

D: Aggregation or oligomerisation.

E: Expulsion of the peptide from the membrane.

Figure 15: Possible adaptions to positive mismatch.[69]

If the hydrophobic part of the peptide is small as compared to the bilayer thickness, a negative hydrophobic mismatch is the result.[66] This negative hydrophibic mismatch can be alleviated by the adaptions presented in Figure 16.[69] Furthermore, the flanking polar and charged residues of the peptide can also compensate the hydrophobic mismatch, as they prefer certain positions and orientations inside the lipid/water interface.

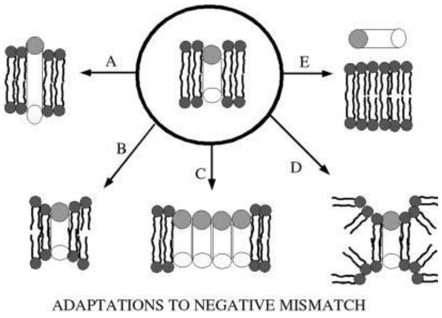

A: Increase of the hydrophobic length of the helix.

B: Decrease of the bilayer width next to the peptide, by acyl chain disordering.

C: Aggregation or oligomerisation.

D: Non-lamellar phase formation.

E: Expulsion of the peptide from the membrane.

Figure 16: Possible adaption to negative mismatch.[69]

KALPs do not show the same tendency towards hydrophobic mismatch as WALPs, due to the long and flexible side chains of lysine whioch can easily compensate a smaller or larger hydrophobic thickness of the lipid bilayer. In order to optimize the interaction of positive charged lysine residues with negative charged phosphate groups, the lysine side chains are able to stretch themselves in the right postion, so called 'snorkeling'.[69,70,72] KALPs and WALPs represent perfect transmembrane model systems to analyse different influences such as peptide length or lipid composition on hydrophobic mismatch. KILLIAN and co-workers used these kinds of artificial peptides with variable length and analysed a wide range of mismatch situations after incorporation of these peptides in lipid bilayers of varying thickness.[65–67,71,74] They found, that a mismatch of about 7.0 Å could be tolerated if the hydrophobic part of the peptide is shorter than the bilayer thickness (negative mismatch) and if the peptide was too long, a positive hydrophobic mismatch of more than 13 Å could be alleviated. In addition, hydrophobic peptides with a positively charged *N*-terminus like KALPs are known to be better incorporated in a transmembrane orientation in lipid bilayers than uncharged peptides.[74] Hence, KALPs with all their characteristics seem to be a suitable model system to analyse the potential of a novel building block within lipid membranes.

3.4.2 Design and Synthesis of Modified KALPs

As mentioned before, KALP23 was used as model transmembrane peptide system to investigate the novel designed building block **11** in a membrane environment. KALP23 has a hydrophobic stretch of 25.5 Å and is well-established in lipids composed of 1,2-dimyristoyl-*sn*-glycero-3-phosphocholine (DMPC), which have a hydrocarbon thickness of 23.0 Å.[66,67] As KALP23 is slightly longer than DMPC it is expected that the peptide spans the entire hydrophobic core of the lipid bilayer. The peptide is composed of leucine (L) and alanine (A) in an alternating arrangement ($(LA)_8L$) and flanked with two lysine (K) residues to facilitate the solubility in aqueous systems.[70] The 7-AI building block **11** was incorporated in the middle of the sequence using Fmoc-SPPS by replacing one leucine and the resulting peptide **17** was used to perform preliminary analysis (Figure 17).

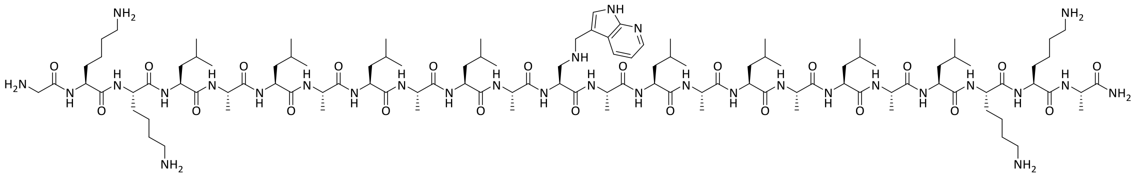

17

Figure 17: Structure of the modified KALP23 (17) with the 7-azaindole recognition unit 11 incorporated in the middle of the sequence.

In order to investigate if the α-peptides with the incorporated 7-AI recognition unit **11** associate inside the membrane, fluorescence resonance energy transfer (FRET) studies were performed. For FRET-analysis, two different fluorophores (NBD (**8**) and TAMRA (**9**)), serving as a donor-acceptor pair, were attached to the α-peptides. Two sets of α-peptides were designed, where the first set has no recognition unit and functions as reference (Figure 18, left), whereas the second set has one recognition unit (7-AI building block **11**, Figure 18, right). As the FRET effect should be unrestricted by the 7-azaindole building block **11**, it was placed accordingly replacing one leucine (Figure 18, left). For the attachment of the fluorophores, one additional lysine with an Alloc-protecting group (orthogonal to Fmoc-SPPS) at the side chain was introduced either to the *C*- or *N*-terminus. The fluorophores (**8**, **9**) were attached to the side chain of the additional lysine as it is known that free peptide termini are required for membrane insertion and that during fluorescence labelling a conformational restriction could occur.[15] The α-peptides were arranged antiparallel and the recognition unit **11** was placed accordingly (Figure 18).

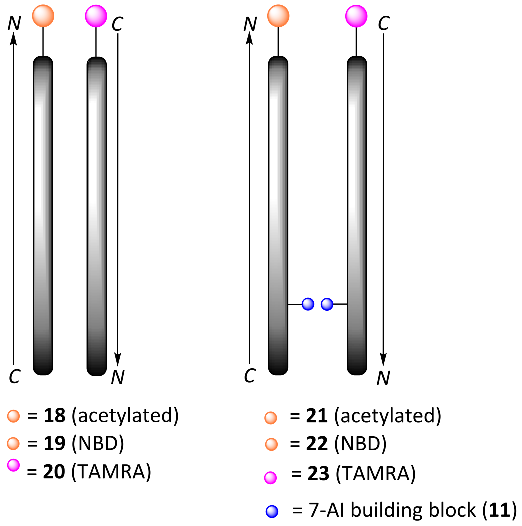
N
C
C
N
N
C
C
N
● = 18 (acetylated)
● = 19 (NBD)
● = 20 (TAMRA)
● = 21 (acetylated)
● = 22 (NBD)
● = 23 (TAMRA)
● = 7-AI building block (11)

Figure 18: Schematic view on the modified KALP23 for FRET analysis with no recognition unit (18/19/20, left) and with recognition unit (21/22/23, right).

All peptides (**18**-**23**) were synthesised on a rink amide MBHA resin using automated microwave assisted Fmoc-SPPS. Therefore, lysine was used with an orthogonally protected side chain (Boc, Alloc) to avoid side reactions. The *N*-terminal Fmoc-group was deprotected with piperidine in DMF (20%). Each single coupling step was performed with the respective amino acid (5.00 eq) activated by Oxyma® in DMF (1.0 M) and DIC in DMF (0.5 M) or by HBTU/HOBt in NMP (0.49 M/0.5 M) and DIPEA in NMP (2.0 M) (Figure 19). During Alloc-deprotection using $Me_2NH \cdot BH_3$ (40.0 eq) and $Pd(PPh_3)_4$ (0.10 eq) in dry DMF, the *N*-terminal Fmoc-group was also deprotected. Hence, the final amino acid of the sequence was coupled as Boc-protected residue.

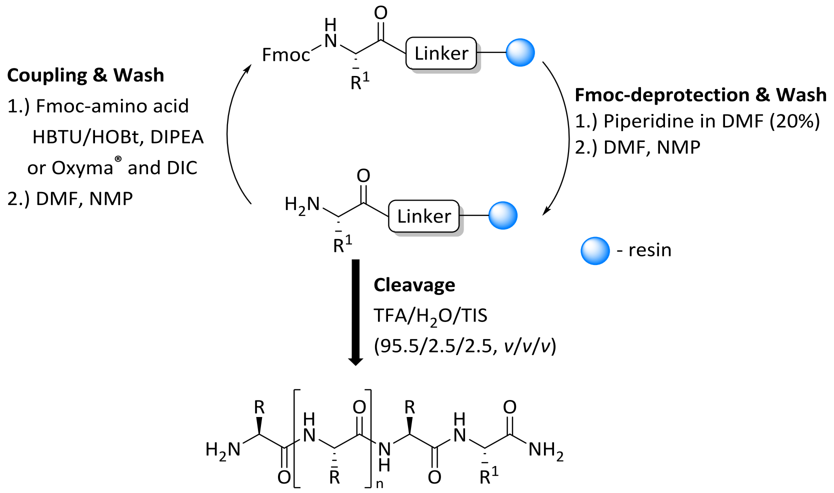
Coupling & Wash
1.) Fmoc-amino acid
HBTU/HOBt, DIPEA
or Oxyma® and DIC
2.) DMF, NMP
Fmoc
H
N
O
R1
Linker
Fmoc-deprotection & Wash
1.) Piperidine in DMF (20%)
2.) DMF, NMP
H2N
O
R1
Linker
● - resin
Cleavage
TFA/H2O/TIS
(95.5/2.5/2.5, v/v/v)
R
H2N
O
H
N
R
O
n
N
H
R
O
H
N
R1
O
NH2

Figure 19: Schematic view on the synthesis of α-peptides using Fmoc-SPPS.

After successful Alloc-deprotection of the lysine next to the *C*-terminal end, TAMRA (**9**) was attached to the sequence. Therefore, 5(6)-TAMRA (**9**) (5.00 eq) in DMF was activated by PyBop® (4.70 eq) and DIPEA (9.80 eq) and allowed to react at rt overnight. Similarly, Alloc-deprotection of the lysine next to the *N*-terminal end, NBD (**8**) was followed by labelling. Thus, NBD–Cl (3.00 eq) in DMF was activated by DIPEA (20.0 eq) and allowed to react at rt overnight. As during FRET-experiments the total peptide concentration had to be kept constant, the free side chain amino functionality of the *N*-terminal lysine was acetylated with DMF/Ac_2O/DIPEA (18:1:1, *v*/*v*/*v*) at rt for 10 min, too. Afterwards, cleavage from the solid support and simultaneous removal of the protecting groups was carried out using TFA/H_2O/TIS (95.5/2.5/2.5, *v*/*v*/*v*) followed by HPLC purification. In total, three different types of peptides were designed and synthesised: *i*) **17** with recognition unit **11** in the centre of the sequence, and for FRET analysis *ii*) **18**/**19**/**20** without recognition unit and *iii*) **21**/**22**/**23** with recognition unit **11** (Table 2).

Table 2: Synthesised α-peptides.

No.	Modified KALP23
	Recognition unit 11 in the centre of the sequence
17	H-GKKLALALALA(**11**)ALALALALKKA-NH_2
	No recognition unit
18	H-GK(acetyl)KKLALALALALALALALALKKA-NH_2
19	H-GK(NBD)KKLALALALALALALALALKKA-NH_2
20	H-GKKLALALALALALALALALALKKK(TAMRA)A-NH_2
	With recognition unit 11
21	H-GK(acetyl)KKLALALALALALA(**11**)ALALKKA-NH_2
22	H-GK(NBD)KKLALALALALALA(**11**)ALALKKA-NH_2
23	H-GKKLALA(**11**)ALALALALALALKKK(TAMRA)A-NH_2

3.5 CD-Spectroscopic Analysis of Modified KALPs

Circular dichroism spectroscopy is a standard and well-established method to analyse secondary structure elements of peptides and proteins.[75] Here, the synthesised KALPs **18** (with recognition unit) and **21** (without recognition unit) were analysed in different membrane environments, *i.e.* small unilamellar vesicles (SUVs) composed of DMPC (T_m = 23 °C) or large unilamellar vesicles (LUVs) composed of 1,2-dioleoyl-*sn*-glycero-3-phosphocholine (DOPC, T_m = -17 °C) at a P/L-ratio of 1/20 and a peptide concentration of 38 µM in TRIS® buffer (Figure 20).[76] The CD-spectra of the peptides **18** and **21** show a pattern with two minima at 209 nm and 223 nm, a zero-crossing around 202 nm and a maximum near 198 nm. These characteristics are in very good agreement with the literature known CD-values of an α-helix.[77] In addition, CD-spectroscopic investigation of KALP23 and the similar WALP23 described by PLANQUE *et al*. and WEISS *et al*. show an approximately identical pattern as the presented CD-spectra of the peptides **18** and **21** in DMPC and DOPC.[64–66]

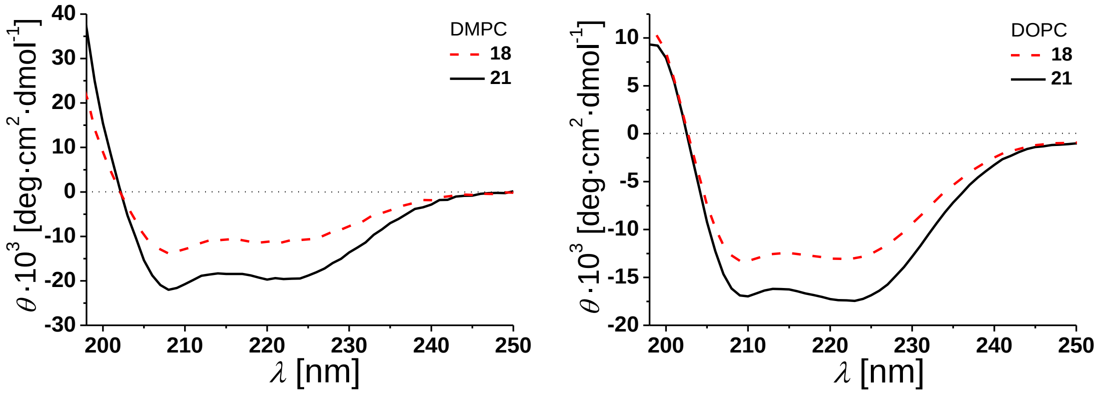

Figure 20: CD-spectra of 18 and 21 in DMPC SUVs (left) at 30 °C and DOPC LUVs (right) at 25 °C (P/L-ratio = 1/20, peptide concentration: 38 µM, TRIS® buffer).

In addition to determining the secondary structure (α-helix), the CD-spectra of both α-peptides (**18** and **21**) reconstituted in DMPC (SUVs) and DOPC (LUVs) clearly demonstrate no influence of the recognition unit **11** on the secondary structure formation.

In order to analyse the thermal stability of the secondary structure of the synthesised KALPs **18** and **21**, CD-spectra of both α-peptides embedded in DOPC (LUVs, peptide concentration: 38 µm, P/L-ratio = 1/20) were measured at 25 °C and 60 °C (Figure 21). Here again, the CD-spectra show the characteristic CD pattern of an α-helix confirming that the secondary structure of the peptides **18** and **21** is almost unaffected by an increase in temperature. Hence, the synthesised KALPs **17**-**23** seem to be a good model system as they are thermally stable and unaffected by the incorporated recognition unit **11**.

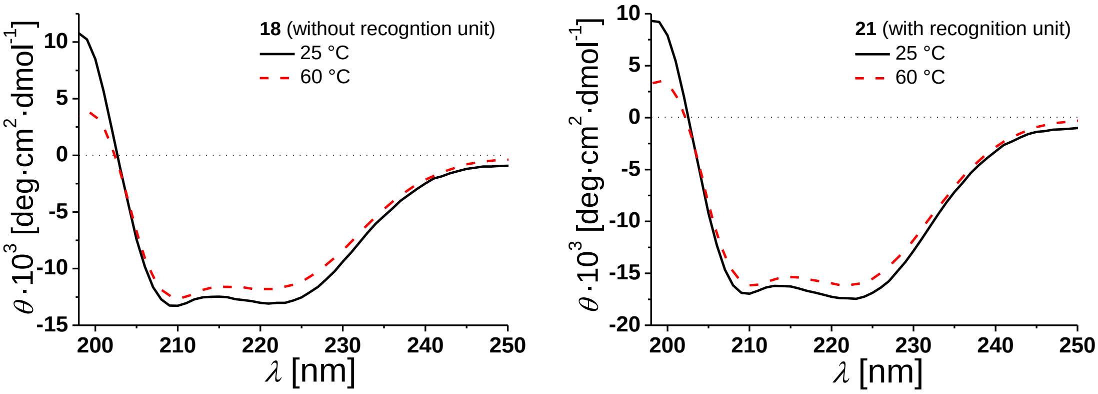

Figure 21: CD-spectra of 18 (left) and 21 (right) in DOPC LUVs (P/L-ratio = 1/20, peptide concentration: 38 µM, TRIS® buffer at 25 °C and 60 °C).

3.6 Fluorescence Spectroscopic Analysis of Modified KALP 17

In order to analyse the solvent dependence of the modified transmembrane KALP **17**, fluorescence spectroscopic measurements (see also 3.2.1) were performed detecting the intrinsic 7-azaindole fluorescence of the incorporated recognition unit **11**. Therefore, the synthesised KALP **17** was studied in a membrane environment, *i.e.* small unilamellar vesicles (SUVs) composed of DMPC at a peptide concentration of 100 µM, and a P/L-ratio of 1/30 in aqueous TRIS® buffer at 25 °C (Figure 22, blue curve). In addition, KALP **17** was analysed in MeOH (100 µM) and TRIS® buffer (aq, 100 µM) at 25 °C (Figure 22, red and black curves). The fluorescence spectra of the modified KALP **17** show a maximum in DMPC at λ_{max} = 372 nm and in MeOH and TRIS® buffer a maximum at λ_{max} = 380 nm. The maximum of KALP **17** in DMPC is slightly shifted compared to the maxima in MeOH and TRIS® buffer (aq) due to the differences in the dielectric constants of the used solvents.[52] KALP **17** in DMPC shows a similar value to 7-azaindole (**5**) in DMF, whereas the maxima of KALP **17** in MeOH and TRIS® buffer (aq) are related to the values of 7-AI (**5**) in MeOH (see 3.2.2). Here again, the tautomeric-fluorescence is not detectable as the samples might be not concentrated enough and hence, the 7-AI building block **11** is not able to form these solute/alcohol complexes in MeOH or dimers in hydrocarbon environment, which consequently results only in fluorescence of the monomeric form of the 7-AI building block **11**.

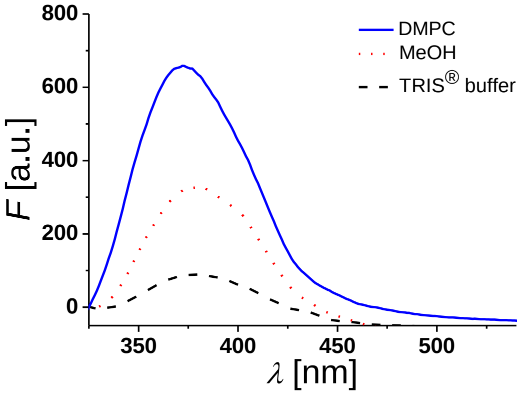

Figure 22: Fluorescence spectra of the modified transmembrane KALP 17 in DMPC (SUVs) (blue) at a peptide concentration of 30 µM and a P/L-ratio of 1/30, MeOH (red) and TRIS® buffer (black).

Furthermore, the fluorescence spectra clearly demonstrate the dependency of the modified KALP **17** on its local environment. The fluorescence emission of KALP **17** in TRIS® buffer (aq) is almost quenched as the 7-AI building block **11** seems to be 'blocked' by the water molecules. However, an increase in fluorescence intensity is observed in MeOH and in DMPC, which is more pronounced in DMPC than in MeOH. These observations are in very good agreement with the preliminary investigations on 7-azaindole (**5**) (see 3.2.2). Here again, the fluorescence intensity of the building block

11 with its 7-AI chromophore seems to be influenced by MeOH and thus, a decrease in intensity is determined compared to the observation in DMPC. As the building block **11** was introduced in the middle of the peptide sequence, the significant increase in fluorescence intensity and the blue-shift of KALP **17** embedded in DMPC (compared to KALP **17** in MeOH) confirms a similarity to a hydrocarbon environment like the acyl chains of lipids. Hence, a successful incorporation of this peptide **17** in the lipid membrane can be assumed.

These results clearly demonstrate the dependence of KALP **17** on its local environment and they present a suitable application of the new 7-azaindole building block **11** in the field of peptide research. Even though no tautomeric fluorescence band was detectable an association of the 7-AI building **11** inside lipid bilayers cannot be completely excluded. Thus, the association state of the peptides was studied by fluorescence resonance energy transfer (FRET) experiments.

3.7 Fluorescence Resonance Energy Transfer (FRET)

3.7.1 Theoretical Background and Evaluation of FRET Data

Beside the fluorescence emission described in 3.2.1, there are other processes that could occur. A singlet-singlet energy transfer, in which the energy is transferred to an acceptor molecule, so called fluorescence resonance energy transfer (FRET) was described for the first time in 1948 by FÖRSTER.[50,78] In detail, after excitation of the donor molecule to an upper electronic state (S_2), the molecule rapidly goes from S_2 to the lowest excited state S_1 by losing the excess of vibrational energy. Before it relaxes to the S_0 (ground state) accompanied by emission of a photon, the energy is transferred to an acceptor molecule by dipole-dipole interactions.[47–50,79] Thereby, the fluorescence emission of the donor molecule is quenched and only the fluorescence emission of the acceptor molecule is detected as it emits a photon in returning to the ground state (S_0).[48] This non-radiative energy transfer between a donor and an acceptor species is described as resonance phenomenon. Therefore, the absorption spectrum of the acceptor molecule has to overlap with the emission spectrum of donor molecule, which means that the fluorophores have to be located close to each other with an optimum distance of approximatively 1-10 nm.[48,80,81] The energy transfer between both dipoles decreases with the 6th power of the distance between donor and acceptor (R). Thus, the transfer rate constant k_T is

$$k_\mathrm{T} = \frac{1}{\tau_\mathrm{D}}\left(\frac{R_0}{R}\right)^6 \tag{2.1}$$

where τ_D terms the fluorescence lifetime of the donor in absence of the acceptor molecule.[80,82]

R_0 denotes the FÖRSTER radius at which the energy transfer process between donor and acceptor provides an efficiency of 50%.[83,84] In order to analyse the distance R between donor and acceptor, the energy transfer efficiency is determined, which is described as:

$$E = \frac{1}{1+(R/R_0)^6} \tag{2.2}$$

The energy transfer efficiency can be estimated via measuring the fluorescence intensity of the donor in the presence (F) and in absence (F_0) of the acceptor (2.3).[85]

$$E = 1 - \frac{F}{F_0} \tag{2.3}$$

Hence, the distance R between donor and acceptor is given as:

$$R = \left(\frac{F}{F_0 - I}\right)^{\frac{1}{6}} \cdot R_0 \tag{2.4}$$

During the last decades, fluorescence resonance energy transfer (FRET) experiments were used to assess the oligomeric state of peptides.[86–88] In order to perform FRET analysis the peptides have to be labelled with a suitable donor-acceptor pair. The degree of association becomes accessible by measuring the decrease in fluorescence emission intensity of the donor as a function of the acceptor concentration while keeping the total peptide-lipid concentration constant by adding unlabelled peptide. In the absence of an association process no energy transfer is expected.[15,23,88] An oligomerisation state of the peptides within the vesicles would result in a decrease in fluorescence emission intensity of the donor with an increasing mole fraction of acceptor (χ_A). This dependence allows the determination of the number of subunits in the peptide assembly.[88] In order to model the data obtained from FRET-measurements the following assumptions were made: *i*) labelling does not influence the association of the peptides, *ii*) all peptides are located in the lipid bilayer, *iii*) the interaction of the peptides is random, *iv*) one acceptor has the ability to quench all donors within that oligomer, and *v*) the number of donors and acceptors in the aggregates is random.[15,23,88,89] According to the model described by ADAIR *et al.*, the measured fluorescence, F, of the acceptor is given by

$$F = f_D(N_D - N_Q) + f_Q N_Q \tag{2.5}$$

where f_D is the molar fluorescence of unquenched donor, f_Q is the molar fluorescence of quenched donor, N_D gives the total moles of donor, and N_Q gives the moles of quenched donor.[88]

Whereas, the fluorescence in the absence of acceptor, F_0, is given by

$$F_0 = f_D N_D \tag{2.6}$$

Combining the equations (2.5) and (2.6) the energy transfer efficiency, E, can be written as

$$E = 1 - \frac{F}{F_0} = \left(1 - \frac{f_Q}{f_D}\right)\frac{N_Q}{N_D} \tag{2.7}$$

Following the previous described assumptions, the number of oligomers with any donor and acceptor concentration can be determined by a binominal distribution, in which the total number of quenched donors, N_Q, is given by

$$N_Q = \sum_{j=1}^{n-k}\sum_{k=1}^{n-1} k \frac{n!}{k!j!(n-k-j)!}\chi_{\mathrm{D}}^{\mathrm{k}}\chi_A^{\mathrm{j}}\chi_{\mathrm{U}}^{\mathrm{n\text{-}k\text{-}j}} \tag{2.8}$$

with n as the number of units in the oligomer, χ_D the mole fraction of the donor, χ_A the mole fraction of the acceptor and χ_U the mole fraction of the unlabelled species with the relationship $\chi_D + \chi_A + \chi_U = 1$. k counts the number of donors except for $k = 0$, in which the oligomer contains acceptors and unlabelled species and $k = n$, where the oligomer contains only donor species. The number of acceptor species is counted by j except for $j = 0$, where the oligomer contains only acceptor and unlabelled species. The total number of donors, N_D, is

$$N_D = \sum_{j=0}^{n-k}\sum_{k=1}^{n} k \frac{n!}{k!j!(n-k-j)!}\chi_{\mathrm{D}}^{\mathrm{k}}\chi_A^{\mathrm{j}}\chi_{\mathrm{U}}^{\mathrm{n\text{-}k\text{-}j}} \tag{2.9}$$

Assuming a monomer-oligomer equilibrium and the combination of equations (2.8) and (2.9) with (2.7) a monomer-dimer equilibrium can be written in terms of fluorescence intensities resulting from the monomeric species $(F/F_0)_\mathrm{m}$ and from the dimeric species $(F/F_0)_\mathrm{dimer}$ as

$$\frac{F}{F_0} = m\left(\frac{F}{F_0}\right)_{\mathrm{m}} + (1 - m)\left(\frac{F}{F_0}\right)_{\mathrm{dimer}} \tag{2.10}$$

$$\text{with } \left(\frac{F}{F_0}\right)_{\mathrm{dimer}} = 1 - \chi_{\mathrm{A}} \tag{2.11}$$

with m as the fraction of molecules in the monomeric state and $(1 - m)$ as the fraction of molecules in the oligomeric state, where m is given as

$$m = \frac{n_\mathrm{m}}{n_0} \tag{2.12}$$

$$\text{with } n_\mathrm{m} = \frac{N_\mathrm{m}}{n_\mathrm{lip}} \text{ and } n_0 = \frac{N_0}{n_\mathrm{lip}} \tag{2.13}$$

N_{m} is the number of peptides in the monomeric state, N_0 is the total number of peptides and n_{lip} is the total amount of lipid molecules. Due to the occurrence of FRET without the formation of aggregates, $(F/F_0)_{\mathrm{m}}$ can be estimated applying the approximation of WOLBER and HUDSON, that is given as

$$\left(\frac{F}{F_0}\right)_m = A_1 \exp\left(-k_1 \chi_{\mathrm{A}} \frac{N_0}{A} R_0^2\right) + A_2 \exp\left(-k_2 \chi_{\mathrm{A}} \frac{N_0}{A} R_0^2\right) \qquad (2.14)$$

where A_1, A_2, k_1, k_2 are constants. A describes the area of one vesicle.[83]

Combining the equations (2.8) and (2.9) with (2.7) a monomer-trimer equilibrium is given in terms of the fluorescence intensities resulting from the monomeric-trimer species $(F/F_0)_{\mathrm{trimer}}$ by

$$\frac{F}{F_0} = m\left(\frac{F}{F_0}\right)_{\mathrm{m}} + (1-m)\left(\frac{F}{F_0}\right)_{\mathrm{trimer}} \qquad (2.15)$$

$$\text{with } \left(\frac{F}{F_0}\right)_{\mathrm{trimer}} = (\chi_{\mathrm{A}} - 1)^2 \qquad (2.16)$$

Combining the equations (2.8) and (2.9) with (2.7) a monomer-tetramer equilibrium is given in terms of the fluorescence intensities resulting from the monomeric-tetramer species $(F/F_0)_{\mathrm{tetramer}}$ by

$$\frac{F}{F_0} = m\left(\frac{F}{F_0}\right)_{\mathrm{m}} + (1-m)\left(\frac{F}{F_0}\right)_{\mathrm{tetramer}} \qquad (2.17)$$

$$\text{with } \left(\frac{F}{F_0}\right)_{\mathrm{tetramer}} = (1 - \chi_{\mathrm{A}})^3 \qquad (2.18)$$

In order to describe the strength of the interaction between two molecules (binding affinity) the dissociation constant K_{D} is used, which is defined as

$$K_{\mathrm{D}} = \frac{(m\,\chi_{\mathrm{P}})^{\mathrm{n}}}{\left((1-m)\frac{\chi_{\mathrm{P}}}{n}\right)} \qquad (2.19)$$

where χ_{P} represents the lipid-to-peptide ratio. K_{D} is expressed in units of peptide/lipid mole fraction (MF).[5,15,23,83,87,88,90,91] Applying a global fit analysis, the dissociation constant can be estimated assuming a FÖRSTER radius of R_0 = 5.1 nm.

Analyses of the obtained FRET data and calculations concerning the statistically occurring FRET were performed by C. STEINEM. These evaluations of the FRET data are prerequisite for analysing association process of transmembrane peptides.

3.7.2 Determination of Peptide Aggregation State of Modified KALPs using FRET

The association state of the modified KALPs **18**-**23** reconstituted into DOPC vesicles using the 7-azaindole building block **11** as a potential recognition unit was investigated by fluorescence resonance energy transfer (FRET) experiments (see 3.7). The first FRET experiments where performed in DMPC vesicles yielding low quality data, which made it difficult to analyse the latter. One possible reason could be the non-constant main transition temperature T_m of DMPC vesicles (T_m = 23 °C) during sample preparation. In order to incorporate peptides into lipid membranes it is necessary that lipids exhibit the liquid crystalline phase.[92] Hence, temperature fluctuations of around 5 °C result in changes from the gel to the liquid crystalline phase (for DMPC), which influences sample preparation and consequently the data obtained from FRET experiments. To circumvent such problems DOPC vesicles (T_m = -2 °C) were used.[76,92]

In order to perform FRET measurements peptides were labelled with a donor- (NBD, **8**) acceptor (TAMRA, **9**) pair.[78,93] As an example, the fluorescence emission spectra of the peptides **18**/**19**/**20** (without recognition unit) and **21**/**22**/**23** (with recognition unit) at a P/L-ratio of 1/500 at 25 °C are shown in Figure 23 (for all fluorescence emission spectra at different P/L-ratios see 7.1 and 7.2).

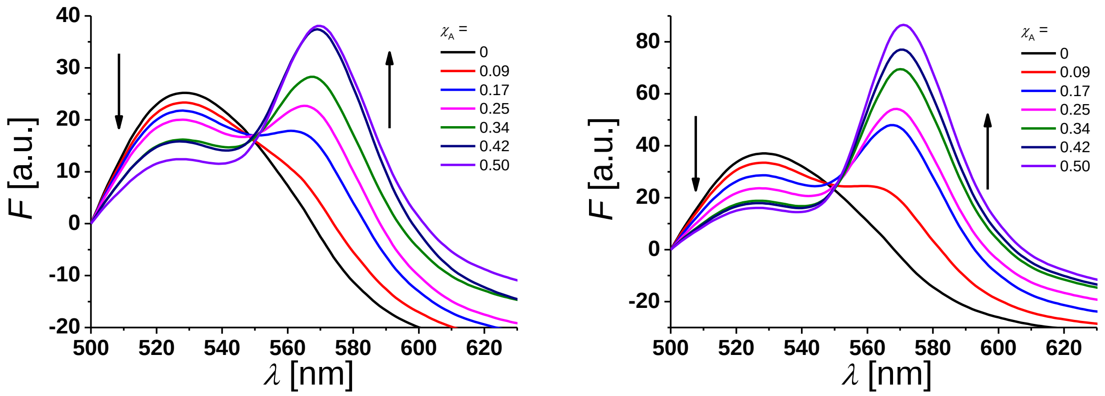

Figure 23: Fluorescence emission spectra of 18/19/20 without recognition unit (left) and 21/22/23 with recognition unit (right). The spectra show NBD-labelled β-peptides (donor, 6.0 µM) with varying amounts of TAMRA-labelled species from 0-0.5 determined at 25 °C. The non-labelled compound was added to keep the total peptide concentration constant (12 µM) and the P/L-ratio at 1/500 (DOPC).

The degree of peptide association becomes available by measuring the ratio of NBD-fluorescence intensity F at 530 nm in the presence of TAMRA-labelled peptides and NBD fluorescence intensity F_0 at 530 nm in its absence as a function of the TAMRA-labelled peptides concentration. The total peptide/lipid-ratio was kept constant by adding the respective acetylated non-labelled peptide. Figure 24 shows the ratio F/F_0 for the peptides **18**/**19**/**20** (without recognition unit) as a function of the mole fraction (χ_A) of the acceptor at 25 °C and a P/L-ratio of 1/500 (red) and 1/1000 (green). The spectra show an almost identical decrease in the ratio F/F_0 with increasing mole fraction (χ_A) of the acceptor of the peptides for both P/L-ratios. The statistical occurrence of FRET in DOPC vesicles was calculated according to WOLBER *et al.*, which was performed by C. STEINEM.[15,83]

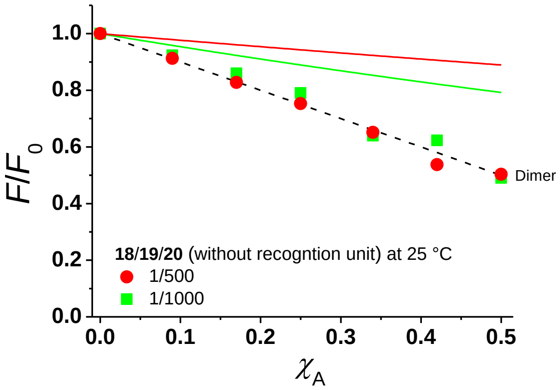

Figure 24: Relative changes in NBD-fluorescence emission (*F*/*F*₀) as a function of increasing acceptor concentration (χ_A) are plotted for 18/19/20 (without recognition unit) at a P/L-ratio of 1/500 (red) and 1/1000 (green) at 25 °C. The red solid line (1/500) and the green solid line (1/1000) are results of a modelling according to WOLBER *et al.*, by taking only statistical occurrence of FRET in vesicles into account without the formation of aggregates.[15,83] A monomer-dimer equilibrium does not explain the obtained data. The black dashed line is the result of the global fit analysis taking a pure dimer into account.

The red solid line (1/500) and the green solid line (1/1000) are results of a global fit analysis assuming peptide monomers in DOPC vesicles (LUVs, 100 nm) with a FÖRSTER radius R_0 = 5.1 nm. The calculated plots are not in accordance with the obtained data. In addition, no agreement between the data and the plots were found for a monomer-dimer equilibrium (plots are not shown) as both data sets show the same signals. Taking a pure dimer into account the global fit analysis could explain the obtained data (Figure 24, black dashed line). This result shows that the peptides **18**/**19**/**20** without recognition unit do not exist in a monomeric state as expected, but they seem to associate into dimers. An explanation for the observed association could be the compensation of a negative hydrophobic mismatch (see also 3.4.1). The modified KALPs have a hydrophobic stretch of 25.5 Å and DOPC has a hydrocarbon thickness of 26.8 Å.[94] Hence, the hydrophobic part of the peptides is slightly shorter (1.3 Å) compared to the hydrophobic thickness of the lipids and therefore, both adjust their hydrophobic part to achieve a match. A negative hydrophobic mismatch can be alleviated amongst other adaptions by an oligomerisation of the peptides.[69] KILLIAN and co-workers have shown that negatively mismatching peptides that are flanked with lysine residues tend to form dimers in the lipid bilayer.[67] They found that the deepest acceptable membrane position of a charged moiety is around the lipid phosphate region, where it can interact with negatively charged phosphate groups and hence, it might induce oligomerisation. Under negative hydrophobic mismatch conditions lysine flanked analogues undergo a reduced incorporation or induce non-lamellar phases.[67,72] In addition, due to negative hydrophobic mismatch, the membrane thickness of DOPC is significantly decreased in the proximity of the peptides by acyl chain disordering.[69,95] These results demonstrate that a mismatch of 1.3 Å, which is less than one additional amino acid, significantly influences the association behaviour of the synthesised peptides **18**/**19**/**20** (without recognition unit).

The ratio F/F_0 for the peptides **21**/**22**/**23** (with recognition unit) as a function of the mole fraction (χ_A) of the acceptor at 25 °C and different P/L-ratios (1/100, 1/250, 1/500 and 1/1000) together with the results of a global fit analysis assuming a monomer-tetramer equilibrium (grey solid lines) resulted in the data sets depicted in Figure 25A. No agreements between data and plots were found for a monomer-tetramer equilibrium. As the peptides without recognition unit (**18**/**19**/**20**) exist in a dimer formation a global fit analysis assuming a dimer-tetramer equilibrium (grey dashed lines) was performed (Figure 25B). Here again, no accordance between data and plots were obtained. However, the spectra of the peptides **21**/**22**/**23** show a decrease in the ratio F/F_0 with increasing mole fraction (χ_A) of the acceptor of the peptides for all P/L-ratios. In addition, a decrease in energy transfer (F/F_0) with increased P/L-ratio was detected. Both observations suggest the formation of more complex oligomers than the presented dimer formation of the peptides without recognition unit (**18**/**19**/**20**) indicating an association of the 7-azaindole building block **11** inside the peptides.

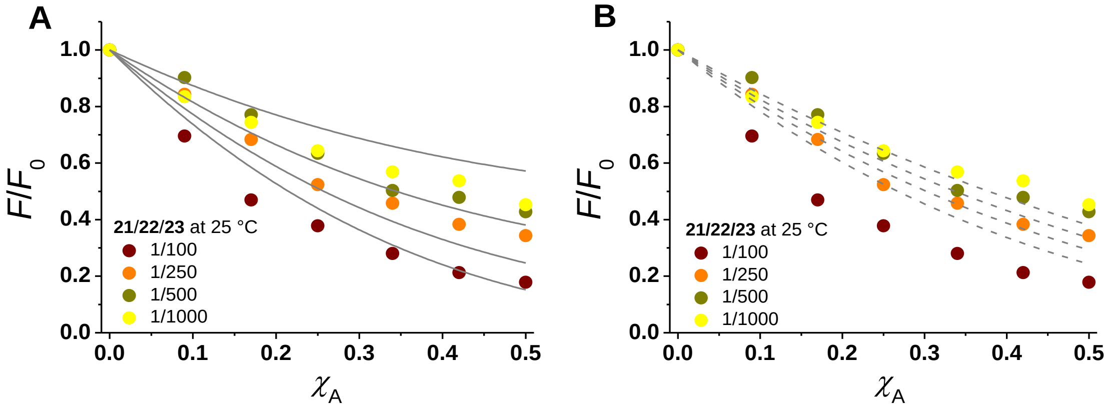

Figure 25: Relative changes in NBD-fluorescence emission (*F*/*F*₀) as a function of increasing acceptor concentration (χ_A) are plotted at different P/L-ratios (1/100, 1/250, 1/500 and 1/1000) for 21/22/23 (with recognition unit) at 25 °C. The grey solid lines are the results of a global fit analysis assuming (A) a monomer-tetramer equilibrium and (B) a dimer-tetramer equilibrium with the FÖRSTER radius R_0 = 5.1 nm and assuming that the FRET occurs statistically.[15,83]

Unfortunately, it could not be verified what kind of association occurs as the global fit analyses do show an inconclusive result. In addition, the observed association could be due to NH···N hydrogen bond formation or π-stacking of the aromatic system of the 7-AI building block **11**, the latter seems more consistent as no tautomeric fluorescence band was detected during fluorescence spectroscopy of KALP **17** (see 3.6).[96–98] Furthermore, it cannot be ruled out that the negative hydrophobic mismatch influences the association processes and hence, complicates the global fit analyses.

In order to analyse the influence on the association properties in more detail, the temperature was varied, as hydrogen bond formations as well as π-stacking interactions are known to become weaker at higher temperatures.[99–101] Fluorescence emission spectra of the peptides **21/22/23** (with recognition unit) reconstituted in a lipid membrane (DOPC) at different P/L-ratios (1/100, 1/250, 1/500 and 1/1000) were measured at 60 °C (see 7.2). To avoid any temperature effects, such as the temperature dependency of the extinction coefficients of the fluorophore NBD and TAMRA, the relative changes in fluorescence intensity F/F_0 are considered.[15] The results obtained at 60 °C for the peptides **21/22/23** are depicted in Figure 26 together with the expected F/F_0 (χ_A) for dimeric peptides **18/19/20** (black solid line).

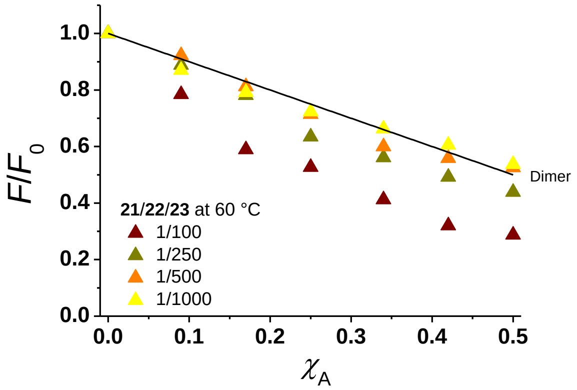

Figure 26: Relative changes in NBD-fluorescence emission (F/F_0) as a function of increasing acceptor concentration (χ_A) are plotted at different P/L-ratios (1/100, 1/250, 1/500 and 1/1000) for 21/22/23 (with recognition unit) at 60 °C. The black line is the result of the global fit analysis of 18/19/20 (without recognition unit) taking a pure dimer into account.

In all four cases the FRET effect is reduced at 60 °C compared to that at 25 °C. At the P/L-ratios 1/500 and 1/1000 the peptides **21/22/23** dissociate into dimers, whereas at 1/250 and 1/100 an association is still observable. This effect is more pronounced at a P/L-ratio of 1/100 with the highest peptide concentration of all analysed P/L-ratios. Hence, the observed FRET effect at a P/L-ratio of 1/100 seems to be influenced by the high amount of peptides in the lipids, that might provide a peptide association. As the peptides **21/22/23** only dissociate into dimers (P/L-ratio of 1/500 and 1/1000) at higher temperature it can be assumed that due to the negative hydrophobic mismatch a dissociation into monomers is not possible as the structure of the lipid bilayer is influenced by this mismatch, too (see 3.4.1). In addition, CD-spectroscopic measurements of the peptide **21** at 25 °C and 60 °C have shown that peptide **21** forms a stable secondary structure, even at a higher temperature. Thus, an unfolding of the secondary structure of the peptides **21**/**22**/**23** due to an increase in temperature can be ruled out. It can therefore be concluded that the observed association/dissociation processes are a result of an interaction of the 7-AI building block **11** inside the peptides. To understand the influences on a negative hydrophobic mismatch in more details, FRET analyses of the peptides without recognition unit at higher and lower P/L-ratios, *e.g.* 1/2000 and 1/250, seems necessary. In addition, it cannot be ruled out, that the 7-azaindole building block **11** itself can have any impact on the result of the FRET experiments. Therefore, it might be advisable to analyse the 7-azaindole recognition unit **11** in more details. As no tautomeric fluorescence band was detected during fluorescence spectroscopy of KALP **17**, it might be reasonable to reconsider the design of the 7-AI building block **11**. It cannot be excluded that the connection of the 7-AI chromophore (**5**) with the peptide backbone is not flexible enough and hence, no dimerisation did occur. In order to increase the flexibility of the 7-AI recognition unit Fmoc-Orn-OH (ornithine) or Fmoc-Lys-OH (lysine) could be used instead of Fmoc-Dap-OH (**15**) as they have two or three additional CH_2-groups, respectively.

Furthermore, the design of the modified KALPs should be reconsidered as a negative hydrophobic mismatch is unfavourable for lysine flanked peptides.[67] KALPs can easier compensate a positive mismatch than a negative mismatch (see 3.4.1). Hence, the hydrophobic stretch of the modified KALPs should be slightly longer than the hydrophobic thickness of the lipid bilayer. DOPC seems to be a suitable lipid system as during sample preparation and FRET measurements no problems occur. In order to design a useful peptide-lipid system one or two amino acids should be added to the hydrophobic stretch of the peptide (Table 3).

Table 3: Comparison of the hydrophobic stretch/thickness of amino acid sequences of the used model system and the new proposed model system with DOPC.[a]

	Sequence	Hydrophobic stretch/thickness
used model system	H-GKKLA(LA)$_7$LKKA-NH_2	25.5 Å
new model system	H-GKKLA(LA)$_8$LKKA-NH_2	28.5 Å
DOPC		26.8 Å

[a] It is assumed that each amino acid has a length of 1.5 Å.

To handle any kind of problems with the used KALPs an alternative way could be to enhance knowledge within the field of β-peptides by choosing another transmembrane model system. The field of β-peptides offers a broad range of possibilities in peptide chemistry and will be described in details in the third chapter of the present thesis (*ARTIFICIAL TRANSMEMBRANE β-PEPTIDES IN LIPID BILAYERS*). Therein, the design, synthesis and analyses of a novel transmembrane β-peptide model system is described in details. This model system could be used to analyse the potential of the 7-azaindole building block **11** as it shows some advantages compared to α-peptide model systems (see 4.2 and 4.3). In order to use transmembrane β-peptides a D-β^3-7-azaindole building block **24** has to be synthesised (see 3.8).

3.8 Synthesis of the 7-Azaindole D-β^3-Building Block

Having the proof for the 7-azaindol recognition unit **11** being sensitive to its local surrounding and hence, useful to confirm a transmembrane insertion of peptides in the lipid bilayer the concept should be extended to the field of β-peptides. Therefore, the synthesis of the 7-azaindole D-β^3-building block **24** is presented as it will be used to investigate transmembrane β-peptides. Starting with Fmoc-D-Asn-OH (**25**), Fmoc-D-Dap-OH (**26**) was obtained by a HOFMANN rearrangement as described before (see Scheme 3, bottom).[63] Afterwards, Fmoc-D-Dap-OH (**26**) was Boc-protected using Boc_2O in an aqueous sodium carbonate/dioxane solution to obtain **27** in 92% yield.[102] When moving from Fmoc-D-Dap(Boc)-OH (**27**) to Fmoc-D-β^3-Dap-OH (**28**) the ARNDT-EISTERT homologation method was utilized (for details see 4.1.1.1), followed by Boc-deprotection with 4.0 M HCl in dioxane. This reaction was performed in 68% yield over three steps (Scheme 5).[103,104]

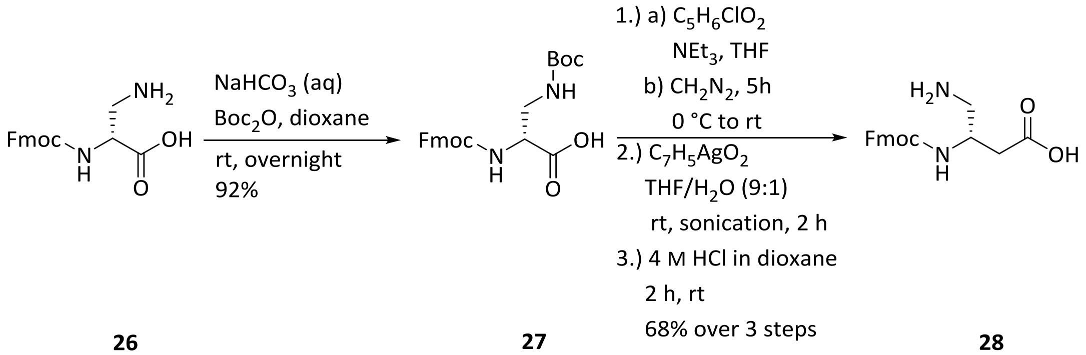

26 **27** **28**

Scheme 5: Synthesis of Fmoc-D-β^3-Dap-OH (28).

After a reductive amination of Fmoc-D-β^3-Dap-OH (**28**) with the Boc-protected aldehyde **13** under the same conditions as described in 3.3.1 the final amino acids residue (*S*)-3-(9-fluorenylmethyloxycarbonyl)-amino-4-*tert*-butoxycarbonyl-(1'-*tert*-butoxycarbonyl-7'-azaindole)-3'-(methyl)-amino-propanoic acid (**24**) was obtained with 56% yield over two steps. This D-β^3-7-azaindole building block **24** is suitable for Fmoc-SPPS and can be incorporated in transmembrane β-peptides (Scheme 6).

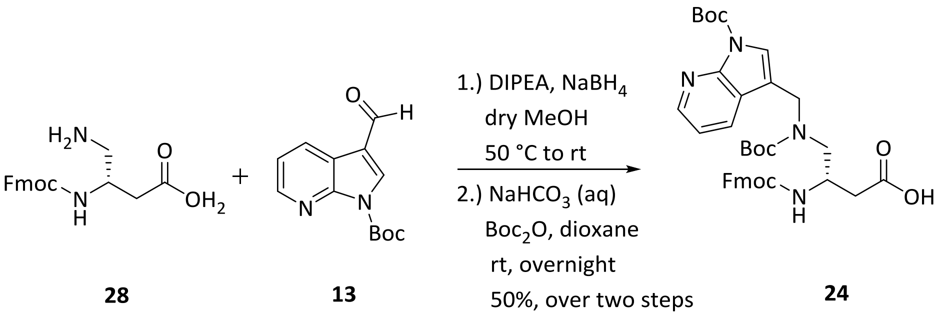

Scheme 6: Final step of the synthesis of (*S*)-3-(9-fluorenylmethyloxycarbonyl)-amino-4-*tert*-butoxycarbonyl-(1ˈ-*tert*-butoxycarbonyl-7ˈ-azaindole)-3ˈ-(methyl)amino-butanoic acid (24).

3.9 Conclusion

A novel 7-azaindole building block **11** has been synthesised and incorporated into model transmembrane peptides, *i.e*. KALPs using Fmoc-SPPS. Initially, the secondary structure of the synthesised peptides reconstituted into unilamellar vesicles composed of DMPC (SUVs) or DOPC (LUVs) was determined to be an α-helix by means of CD spectroscopy. In addition, the CD-spectra clearly indicated that the secondary structure of the peptides is almost unaffected by an increase in temperature. In order to analyse the solvent dependence of the 7-azaindole modified KALP **17**, fluorescence spectroscopic measurements were performed detecting the intrinsic 7-azaindole fluorescence of the incorporated recognition unit **11**. Results clearly demonstrate the dependence of KALP **17** on its local environment as in TRIS® buffer the fluorescence emission is almost quenched, whereas in DMPC vesicles a significant increase in fluorescence intensity is observed. However, no tautomeric fluorescence band could be detected indicative of no dimer formation due to the 7-AI building block **11** inside the peptide. As an association of the 7-AI recognition unit **11** cannot be completely excluded FRET experiments were performed to investigate a possible association state. The results show that peptides **18**/**19**/**20** (without recognition unit) already assemble into dimers as a result of an occurring of a negative hydrophobic mismatch. The peptides **21**/**22**/**23** (with recognition unit) form more complex oligomers, which dissociate into dimers by increasing temperature. Unfortunately, the kind of association state could not be verified by global fit analysis. It could not be clearly established whether the NH···N hydrogen bonds formation or a π-stacking of the aromatic system of the 7-AI building block **11** take place in the association process. The latter seems more consistent as no tautomeric fluorescence band was detected during fluorescence spectroscopy of KALP **17**.

ARTIFICIAL TRANSMEMBRANE β-PEPTIDES IN LIPID BILAYERS

4.1 General

The prerequisite for many biological functions of proteins is the folding of peptide strands into well-defined, active and compact secondary structures.[21,105] These secondary structures play a vital role in protein architecture and are often involved in recognition and binding processes between proteins or peptides.[17] Information of proteins such as their biological activities, functions and mechanisms on a molecular level are sometimes limited due to the complexity of protein structures and have attracted attention of many chemists, biophysicists and biochemists.[4,12] As chemical and biological questions have become intertwined, the interest in the design and synthesis of unnatural oligomers that fold into specific and well-defined three-dimensional structures has increased substantially during the past few years.[103,106,107] These artificial oligomers are a good way to understand biological processes like enzyme catalysis, protein-protein and protein-nucleic acids binding, protein folding, flexibility and stability.[9] Hence, a various number of synthetic proteins composed of α-amino acids with defined conformations similar to those in natural peptides and proteins have previously been investigated.[9,12,108] Beside α-peptides, SEEBACH, GELLMAN and DEGRADO have already reported that β-peptides are able to fold into well-defined and extremely stable secondary structures.[21,109,110] These artificial β-peptides provide a novel approach to analyse the mechanism of protein folding processes and structural stabilization. In addition, they seem to be an excellent medium for the design of new biomimetic structures with useful applications in the field of pharmaceuticals and materials science.[111] Unnatural β-peptides are also known to be stable towards enzymatic degradation both *in vitro* and *in vivo*, by *e.g.* proteolytic and metabolising enzymes in microorganisms and insects. As β-peptides consist of β-amino acid residues, these β-amino acid building blocks could be useful in peptidomimetic drug design.[112,113] Hence, the design, synthesis and investigations of artificial β-peptides are of great interest for many different research fields to gain new insights into peptide-peptide and peptide-lipid interactions.[114]

4.1.1 β-Amino Acids

The wide spectrum of applications of α-amino acids arouses the interest towards synthetic approaches for both natural and unnatural amino acids.[115] β-Amino acids occur relatively seldom in nature compared to α-amino acids. Similarly, their synthesis must be enantiomerically pure since in most amino acids only one enantiomeric form is biologically active. [109,116] β-Amino acid residues can function as key components of medically useful molecules like Taxol®, an anti-tumour agent or Bestatin®, an immunological response modifier.[117] In contrast to α-amino acids, β-amino acids have one additional α-methylene group, which results in various numbers of possible constitutional and configurational isomers since β-amino acids have four options of substitution.[109,116] There are three general types of chiral β-amino acids differing in position and number of substituents. Substituents could take place at *i*) the carbon bearing the carboxyl group (α-position), *ii*) the carbon bearing the amino group (β-position), or *iii*) both positions.[118,119] In order to distinguish positional isomers, SEEBACH and co-workers have suggested the terms β^2- and β^3-amino acids where the number specifies the position of the side chains (Figure 27).[120,121]

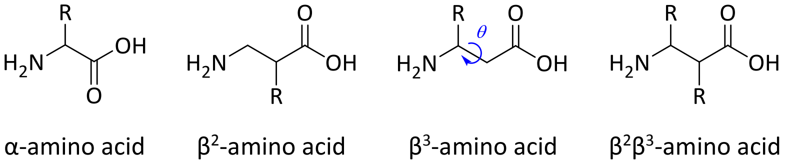

Figure 27: Schematic view on an α-amino acid, a β^2-amino acid, a β^3-amino acid, and a β^{2}β^3-amino acid.[118]

Due to homologation, an additional rotation axis with the torsion angle θ exists in a β-amino acid (see Figure 27). This C_α-C_β-bond angle θ and the possibility to have four different substituents enable a wide variety of secondary structure formations.[112] The synthesis of β^3-amino acids has been intensively investigated during the last few decades and many different methods are available for their synthesis.[109,119] Herein, they were made by implementing the ARNDT-EISTERT homologation methods converting an α- to a β^3-amino acid.[3]

4.1.1.1 Synthesis of β^3-amino acids

As β-amino acids are much less frequent in nature than α-amino acids, they need to be synthesised from their α-amino analogues.[116] Starting with the commercially available D-α-amino acid, the D-β^3-amino acid residues were synthesised in excellent yields by an optimised ARNDT-EISTERT homologation method (Scheme 7).[104,109,122] Therefore, the protected D-α-amino acid (PG: Boc or Fmoc) was activated with isobutylchloroformate to obtain a mixed anhydride.

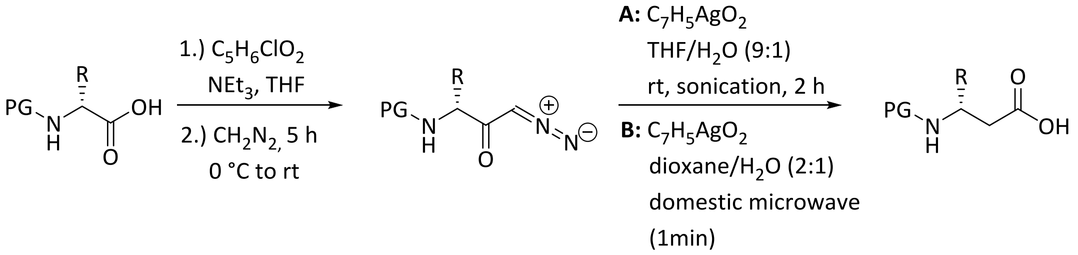

Scheme 7: Schematic view on the synthesis of protected D-β^3-amino acids (PG: Boc or Fmoc) using an optimised ARNDT-EISTERT homologation method.[123]

The diazomethane carbon is acetylated by this mixed anhydride to give an α-diazo ketone, which was used without further purification and in quantitative yields.[103,104] The key step of the ARNDT-EISTERT homologation method is the WOLFF-rearrangement of the α-diazo ketones to ketenes, which was accomplished by silver(I) catalysis. The reaction is conducted in the presence of water to yield the carboxylic acid. Two different silver(I) catalysed methods of the WOLFF-rearrangement are presented. Method A was performed in an ultrasonic bath for two hours and method B in a domestic microwave for one minute.[103,122] In both cases the resulting crude product was precipitated in ice-cold pentane to obtain the desired protected D-β^3-amino acid in excellent yields and without the necessity for further purification steps (Table 4).

Table 4: Synthesised D-β^3-amino acids, the obtained yield over two steps (^{A} sonication; ^{B} domestic microwave) and their further on used abbreviation.

D-β^3-amino acid	yield in %	Abbreviation of the unprotected D-β^3-amino acid
Fmoc-D-β^3-Val-OH (**29**)	94^B	^{h}Val
Fmoc-D-β^3-Lys(Boc)-OH (**30**)	83^B	^{h}Lys
Boc-D-β^3-Lys(Fmoc)-OH (**31**)	72^A	
Fmoc-D-β^3-Lys(Alloc)-OH (**32**)	70^A	
Fmoc-D-β^3-Trp(Boc)-OH (**33**)	75^A	^{h}Trp
Fmoc-D-β^3-Gln(Trt)-OH (**34**)	72^A	^{h}Gln
Boc-D-β^3-Asp-OBzl (**35**)	83^B	^{h}Asp
Fmoc-D/L-β^3-Trp(Boc)-OH (**36**)	68^A	–

4.1.1.2 Enantiomeric purity of aromatic D-β^3-amino acids

The synthesis of aromatic β^3-amino acids is prone to racemisation.[117,123] Therefore, the enantiomeric purity of Fmoc-D-β^3-Trp(Boc)-OH (**33**) was analysed using MARFEY's reagent (**37**) (1-fluoro-2,4-

dinitrophenyl-5-L-alanine amide, FDAA).[124,125] MARFEY's reagent was introduced in 1984 and provides a simple and effective analytical method for structural characterisation in peptide synthesis and detection of small quantities of amino acids.[124] FDAA (**37**) is a derivatisation reagent that reacts with primary amino groups of optical isomers to form diastereomeric derivatives which can be separated by conventional high performance liquid chromatography (HPLC) (Scheme 8).[125,126]

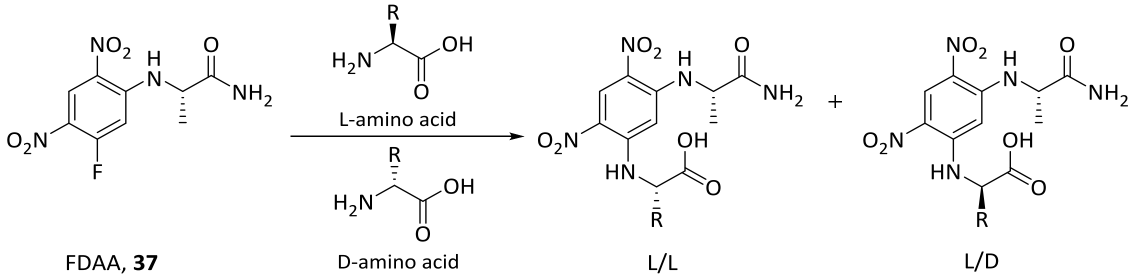

Scheme 8: Synthesis of L/L- and L/D-diastereomers using MARFEY's reagent (37).[127]

FDAA derivatives of D-amino acids exhibit strong intermolecular hydrogen bonding, which reduces their polarity compared to the corresponding L-amino acid derivatives. Consequently, L/D-diastereomers are selectively retained on reverse phase columns and elute much later than corresponding L/L-diastereomers.[127] The diastereomeric derivatives have an absorption maximum at 340 nm with an extinction coefficient $\varepsilon = 30000\ \mathrm{cm^{-1} \cdot M^{-1}}$, and thus, can be detected by UV spectroscopy with nanomole sensitivity.[125,127]

Fmoc-D-β^3-Trp(Boc)-OH (**33**) and Fmoc-D/L-β^3-Trp(Boc)-OH (**36**, racemate), which was synthesised as a reference (see 4.1.1.1), were analysed using MARFEY's reagent. The respective β^3-amino acid was treated according to the procedure of MARFEY *et al.* and BHUSHAN *et al.* (see 6.3.4).[126,127] The resulting diastereomeric derivatives were analysed using HPLC (Figure 28). The HPLC chromatogram showed the L/L-diastereomere (t_R = 46.7 min) and the L/D-diastereomere (t_R = 48.6 min) after reaction with MARFEY's reagent, as expected for Fmoc-D/L-β^3-Trp(Boc)-OH (**36**, racemate).

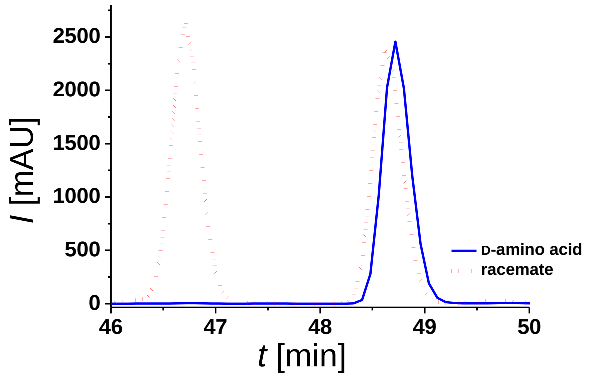

Figure 28: HPLC chromatogram of the D/L-mixture (36, red) and the D-amino acid (33, blue) after the reaction with MARFEY's reagent.

After reaction of Fmoc-D-β^3-Trp(Boc)-OH (**33**) with FDAA only the L/D-diastereomere (t_R = 48.7 min) was detected in the HPLC chromatogram, demonstrating the enantiomeric purity of Fmoc-D-β^3-Trp(Boc)-OH (**33**). Hence, no racemisation occurred during the optimised ARNDT-EISTERT homologation.

4.1.2 β-Peptides

β-Peptides, *i.e*. oligomers of β-amino acid residues are a unique class of peptides.[128] In contrast to their natural α-amino acid counterparts (usually about 15-20 amino acids are needed for a stable secondary structure), β-peptides are known to form conformational well-defined and stable secondary helix structures starting from sequences of six amino acid residues.[17,109] Structural studies on β-peptides like X-ray crystallography, molecular dynamic simulation studies as well as NMR- and CD-spectroscopy have shown that β-peptides adopt a various number of stable secondary structures.[9,103,116,129–132] So far, five different helical structures have been identified in the field of β-peptides that are defined by the size of 8-, 10-, 12, or 14-membered hydrogen bonded rings between an amide proton and a main chain carbonyl: the 8-helix, the 10-helix, the 10/12-helix, the 12-helix (2.5_{12}-helix) and the 14-helix (3_{14}-helix) (Figure 29A).[113,133]

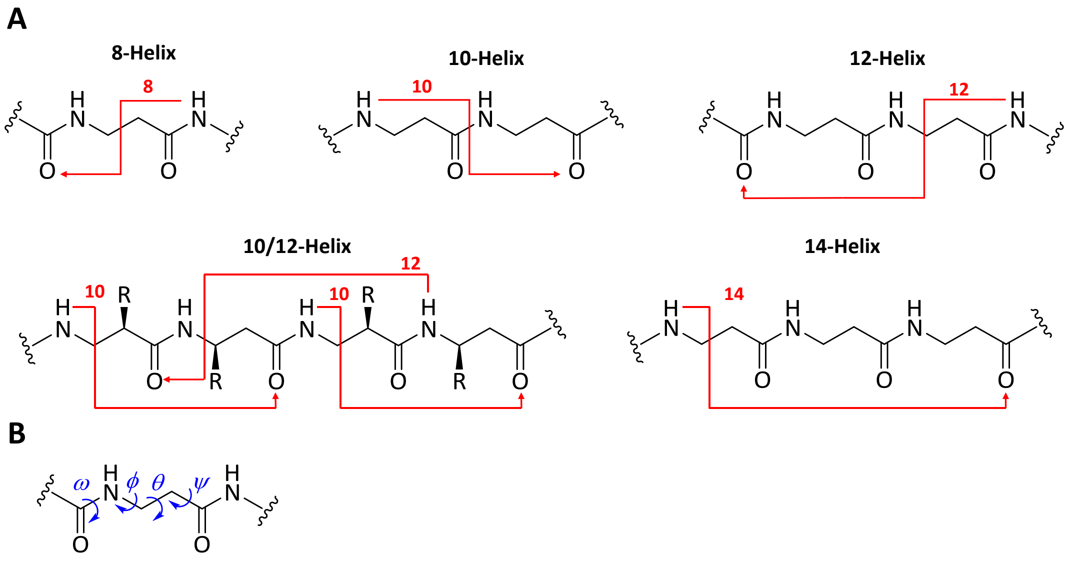

Figure 29: A: Schematic view of the nomenclature of β-peptide helices based on hydrogen-bonding pattern; B: Definition of torsion angles in β-peptides.[110]

Based on BALRAM *et al.*, the conformations of these secondary structures of the β-peptides are defined by the torsion angles ω, ϕ, θ and ψ where the torsion angle of the CO–N-bond is designated as ω, the HN–C$_\beta$-bond is assigned as ϕ, and the CO–C$_\alpha$-bond as ψ. The C$_\alpha$–C$_\beta$-bond describes the most important torsion angle θ for secondary structure formation (Figure 29B).[110,134] The conformation of the β-peptide secondary structure depends not only on the torsion angles but also on the substitution pattern (see 4.1.1).[110] The helix type is largely determined by the choice of the amino acid monomer.[135] As aliphatic and mono-substituted residues (β^2- or β^3- amino acids) prefer a *gauche* conformation with a torsion angle θ of 60°, they show the tendency to fold as 14-helices when arranged or as 10/12-helices if patterned as alternating β^2/β^3-amino acid residues.[134,136,137] As the most frequently documented secondary structure of folded β-peptides, the 14-helix consists of 14-membered hydrogen-bond rings between N–H (*i*) and C=O I (*i*+2) with a three-residue repeating arrangement of the side chains and a pitch of approximately 5.0 Å.[138] This uniform orientation of every third side chain allows an individual assignment of properties of the three helical faces.[4,17] Hence, this secondary structure is also designated as 3_{14}-helix. In contrast to the α-helix with 3.6 amino acids per turn, 13-membered hydrogen bonded rings and a radius of 4.3 Å, the 3_{14}-helix has a slightly larger radius (4.8 Å), which is the result of the different size of the hydrogen bonded rings.[109] In addition, the 3_{14}-helix has an inverted overall helical dipole compared to the α-helix as the amide carbonyl- and the NH-groups protrude towards the *N*- and *C*-terminus, respectively (Figure 30).[110]

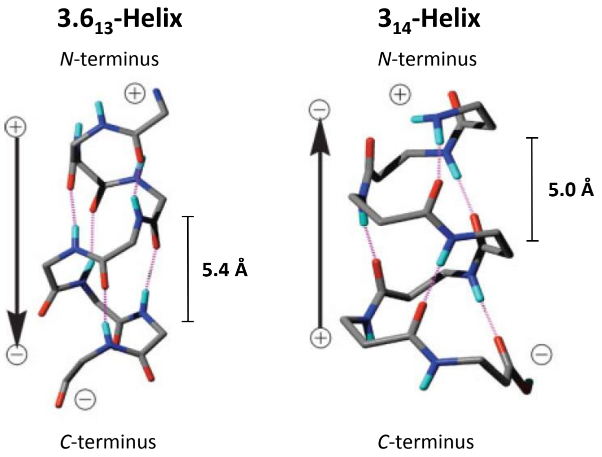

Figure 30: Crystal structures of the 3.6_{13}-helix (α-peptide, left) with a pitch (*p*) of 5.4 Å and the 3_{14}-helix (β-peptide, right) with a pitch of 5.0 Å and comparison of the stabilising interactions and the inverted dipole moment. (Structure based on SEEBACH *et al.*).[133]

Branched side chains adjacent to the C_β-atom (β^3-amino acid residues) are known to provide the 3_{14}-helical conformation of β-peptides.[139] Furthermore, GUNG *et al.* and HAMURO *et al*. have previously shown that the presence of valine side chains enhance the formation of the 3_{14}-helix of β-peptides.[140,141] In addition it should be mentioned that *e.g. trans*-2-aminocyclohexanecarboxlyic acid (achc) promotes the formation of the 3_{14}-helical structures.[142] Taking all these properties into account, the 3_{14}-helix seems to be a good choice for the design of transmembrane β-peptides.

4.2 Heavy-Atom Labelled Transmembrane β-Peptides

Membrane proteins and peptides play a vital role for many different cellular function.[143] Transmembrane (TM) β-peptides and their behaviour in lipid membranes are not fully understood yet. The conformation and distribution of transmembrane peptides within the lipid bilayer result from interactions with the membrane environment that are a necessity for many biological membrane functions.[6,67] These interactions affect the properties of both, peptides as well as lipids and consequently, the stability and function of transmembrane peptides can be highly influenced by membrane composition.[65,143] Therefore, transmembrane β-peptides should present relative structural simplicity as they will be frequently used to confirm experimental approaches, techniques and applications.[144–146] In the last three decades, the interest in design and analysis of synthetically modified β-peptides in membrane environment has grown continuously.[3,146]

In this work, novel β-peptides are introduced that are well suited as a model transmembrane domain system due to their conformational rigidity with stable helical structure formation. In order to establish these transmembrane β-peptides as a model system the proper formation and orientation of the helix has to be investigated within an appropriate membrane environment.[22] A better understanding of parameters like conformation, positioning and orientation of these β-peptides with respect to the lipid bilayer is achieved by new techniques and tools capable of probing these parameters.[13] From standard spectroscopy methods like fluorescence emission or circular dichroism (CD) qualitative information on the structure and localisation of the peptide species can be obtained.[104,147] More advanced applications, such as fluorescence resonance energy transfer analysis (FRET, parallax method), electron paramagnetic resonance techniques or solid state nuclear magnetic resonance (NMR) are used for quantitative views on lipid bilayers without the need for simulations or geometrical models. [23,146,148,149] As some of these techniques are limited by their sample preparation or their physiologically or biologically relevance, other techniques might be considered.[146] In order to pinpoint specific molecular moieties, heavy-atom labelling techniques of transmembrane β-peptides in combination with X-ray diffraction studies have been used to characterise β-peptide properties in lipid model systems, as it was already presented by SCHNEGGENBURGER *et al.* and KÜSEL *et al.* for transmembrane α-peptides.[13,14,146] Small angle X-ray diffraction studies on membrane surfaces are a powerful and highly appropriate method providing access to a variety of membrane parameters.[13] The heavy-atom label (**2**, Figure 31) provides strong electron density contrasts in the labelled region of the reconstructed electron density profiles (EDPs), revealing a certain group either from the lipid or the peptide.[22,150,151] Properties like the relative position of the β-peptide within the membrane, the tilting angle, β-peptide orientation, etc. can be derived from this electron density contrast.[22]

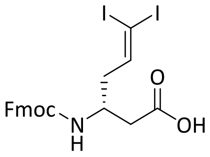

I
I
O
Fmoc
N
H
OH

2

Figure 31: Structural representation of Fmoc-D-β^3-6,6-diiodoallylhomoglycine (2).

4.2.1 Synthesis of the Iodine-labelled D-β^3-Amino Acid

The synthesis of a heavy-atom labelled α-peptide has previously been presented by SCHNEGGENBURGER *et al.*.[13] An amino acid side chain modification resulted in a doubly iodinated building block compatible with Fmoc-SPPS, which showed an increase in electron density profiles compared to non-iodinated analogues. For spectroscopic analysis, an attachment of the iodine atoms close to the peptide backbone was chosen, which did not affect the SPPS and the conformation of the synthesised peptides.[13]

Based on this knowledge, the synthesis of Fmoc-D-β^3-6,6-diiodo-allylhomoglycine (**2**) is presented, which is suitable for the synthesis of heavy-atom labelled transmembrane β-peptides using Fmoc-SPPS (Scheme 9). Starting point for the synthesis of iodine-labelled D-β^3-amino acid building block **2** was the commercially available amino acid Boc-L-Asp(OBzl)-OH, which was converted into Boc-D-β^3-Asp-OBzl (**35**) using an optimised ARNDT-EISTERT homologation method (see also 4.1.1.1).[104,109,122]

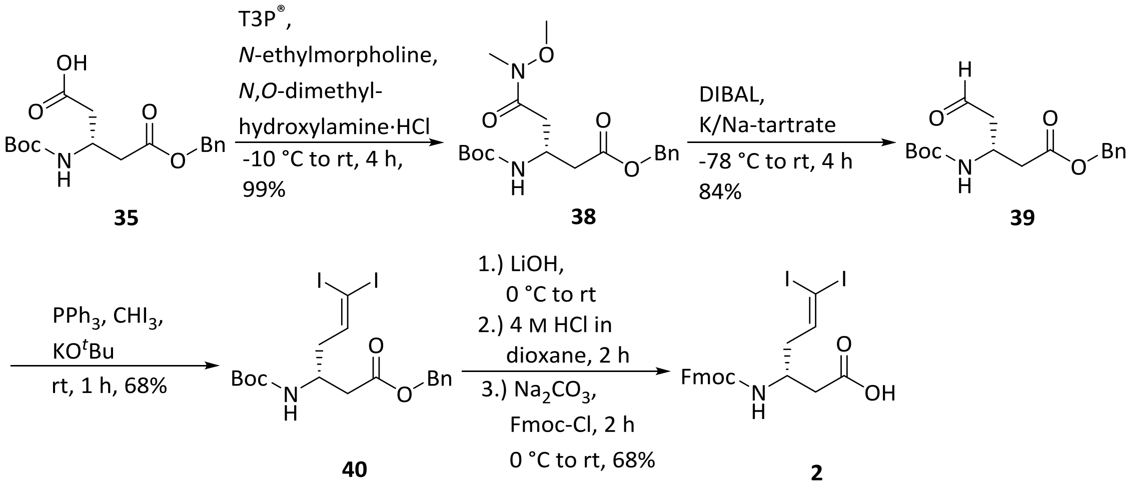

OH
O
O
Boc
N
H
O
Bn
35
T3P®,
N-ethylmorpholine,
N,O-dimethyl-
hydroxylamine·HCl
-10 °C to rt, 4 h,
99%
N
O
O
O
Boc
N
H
O
Bn
38
DIBAL,
K/Na-tartrate
-78 °C to rt, 4 h
84%
H
O
O
Boc
N
H
O
Bn
39
PPh3, CHI3,
KOtBu
rt, 1 h, 68%
I
I
O
Boc
N
H
O
Bn
40
1.) LiOH,
0 °C to rt
2.) 4 M HCl in
dioxane, 2 h
3.) Na2CO3,
Fmoc-Cl, 2 h
0 °C to rt, 68%
I
I
O
Fmoc
N
H
OH
2

Scheme 9: Synthesis of Fmoc-D-β^3-6,6-diiodoallylhomoglycine (2).

The conversion of the carboxylic acid side chain to the WEINREB amide **38** was performed using *N*-ethylmorpholine, *N*,*O*-dimethyl hydroxylamine hydrochloride and propylphosphonic anhydride solution (T3P®) to give 99% yield and no further purification was required.[152,153] The aldehyde **39** was obtained by dibutylaluminium hydride (DIBAL) reduction of the WEINREB amide **38** in 84% yield.[154–156] Then, the aldehyde **39** was treated with triiodomethane under WITTIG conditions to receive (*R*)-benzyl-3-*tert*-butoxycarbonylamino-6,6-diiodohex-5-enoate (**40**) in 68% yield.[13] Base hydrolysis of the benzyl ester using LiOH resulted in the free carboxylic acid. Subsequently, Boc-deprotection with 4 M HCl in dioxane was performed to get the unprotected iodine-labelled compound, which was finally Fmoc-protected using Fmoc–Cl in aqueous sodium carbonate/dioxane solution to obtain the final D-β^3-amino acid residue Fmoc-D-β^3-6,6-diiodo-allylhomoglycine (**2**) in 68% yield over three steps. This heavy-atom labelled D-β^3-amino acid building block (**2**) is suitable for Fmoc-SPPS and is incorporated in transmembrane β-peptides.

4.2.2 Design and Synthesis of Iodine-labelled Transmembrane β-Peptides

In order to synthesise transmembrane β-peptides that are able to form a 3_{14}-helix as their secondary structure element and to analyse their behaviour in membrane environment by X-ray diffraction studies, the β-peptide design should be considered thoroughly. To span the entire hydrophobic core of the membrane, the β-peptides are composed of 19 D-β^3-valines because β^3-valine is known to promote the formation of a stable 3_{14}-helical secondary structure.[113,136,157] Due to the unpolar nature of peptides containing multiple valines, polar amino acids moieties need to be integrated in order to gain water solubility. Lysine is known to facilitate the solubility in aqueous systems owing to its long and flexible side chains.[70] Thus, two D-β^3-lysine residues are attached at each side of the β-peptides. β-Peptide **41** function as reference where no heavy-atom label is inserted in its sequence. For an increase in electron density, the iodine-labelled amino acid residue **2** is incorporated close to the terminus (**42**) and in the centre (**43**) of the designed sequence by replacing one ^{h}Val (Figure 32, left). To compare the anchoring effect of D-β^3-lysine with that of D-β^3-tryptophan, a second set of β-peptides is synthesised. Herein, the β-peptides are flanked with two D-β^3-tryptophan residues at the *N*- and *C*-terminal end of the sequence as the aromatic indole moieties of these D-β^3-tryptophans are known to arrange in the polar/apolar interface of the lipid membrane.[70] The aromatic ring is preferentially orientated in the hydrophobic part of the membrane, whereas the indole NH-groups are contiguous to the lipid carbonyl moieties forming hydrogen bonds, which results in anchoring and stabilisation of the β-peptides within the lipid membrane.[65,71,158] Furthermore, two D-β^3-lysine residues are attached at each side of the β-peptide to again facilitate solubility in aqueous systems. The β-peptide **44** has no iodine-labelled amino acid residue in its sequence and functions as reference, whereas β-peptide **45** has the heavy-atom label close to the terminus and β-peptide **46** in the centre of the sequence (Figure 32, right).

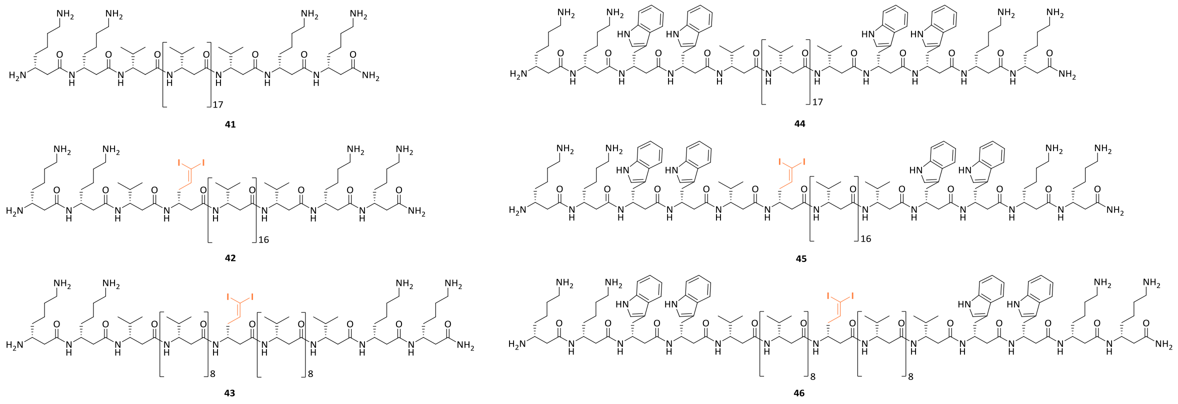
41
44
42
45
43
46

Figure 32: Synthesised transmembrane peptides 41-46. Left: β-Peptides 41-43 without ^{h}Trp. Right: β-Peptides 44-46 with ^{h}Trp. 41 and 44 have no heavy-atom label and function as reference. 42 and 45 have the iodine-label (highlighted in orange) near the end and 43 and 46 in the middle of the sequence to increase electron density at defined positions.

In total, six different transmembrane β-peptides were designed, one set (**41**-**43**) without ^{h}Trp and another set (**44**-**46**) with ^{h}Trp to investigate if ^{h}Trp could enhance the anchoring effect of ^{h}Lys.

The β-peptides **41**-**46** were synthesised using manual microwave assisted Fmoc-SPPS. Therefore, the D-β^{3}-amino acid **29**, **30** and **33** (see 4.1.1.1) and the heavy-atom label **2** (see 4.2.1) were synthesised and utilized for the β-peptide synthesis using the Fmoc-protocol (Scheme 10).[128,159] The synthesis was performed on a rink amide MBHA resin (0.57 mmol/g) in a 75.0 µmol scale and it resulted in β-peptides with a *C*-terminal amide, which is more active than the corresponding free carboxylic acid.[12]

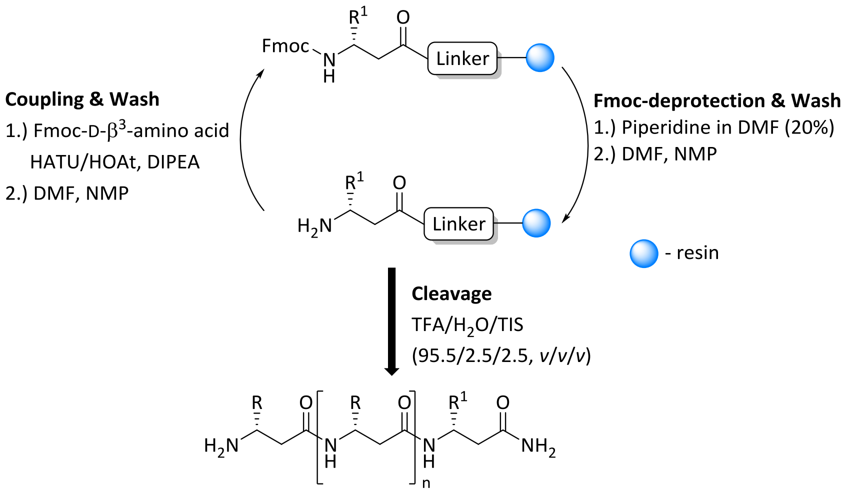
Fmoc
Linker
Coupling & Wash
1.) Fmoc-D-β³-amino acid
HATU/HOAt, DIPEA
2.) DMF, NMP
Fmoc-deprotection & Wash
1.) Piperidine in DMF (20%)
2.) DMF, NMP
- resin
Cleavage
TFA/H₂O/TIS
(95.5/2.5/2.5, v/v/v)
n

Scheme 10: Synthesis of β-peptides using Fmoc-SPPS.

The resin was preloaded manually using Fmoc-D-β^3-Lys(Boc)-OH (**31**). The *N*-terminal Fmoc-protecting group was removed with piperidine in DMF (20%) using a microwave. Each coupling step (single coupling) was performed utilizing the respective D-β^3-amino acid (4.00 eq) activated by HATU (4.90 eq), HOAt (5.00 eq) and DIPEA (10.0 eq) under microwave irradiation. Cleavage from the solid support and simultaneous removal of the protecting groups were carried out using TFA/H_2O/TIS (95.5/2.5/2.5, *v*/*v*/*v*) followed by HPLC purification (Scheme 10).

4.2.3 CD-Spectroscopic Analysis of the Synthesised β-Peptides

CD spectroscopy is a well-established and common method to analyse secondary structure elements of peptides and proteins.[116,160] Previously performed structural investigations in the field of β-peptides (see 4.1.2) have shown that β-peptides adopt very stable secondary structures in solution.[9,103,116,129–132] Here, the synthesised transmembrane β-peptides **41**-**43** (Figure 33, left) and **44**-**46** (Figure 33, right) were analysed in a membrane environment, *i.e.* large unilamellar vesicles (LUVs) composed of DOPC at a P/L-ratio of 1/20 (TRIS® buffer) and a peptide concentration of 38 µM using CD spectroscopy. The CD-spectra of the β-peptides (**41**-**46**) show a pattern with a minimum at 189 nm, a zero crossing at 198 nm and a maximum at 205 nm.[130]

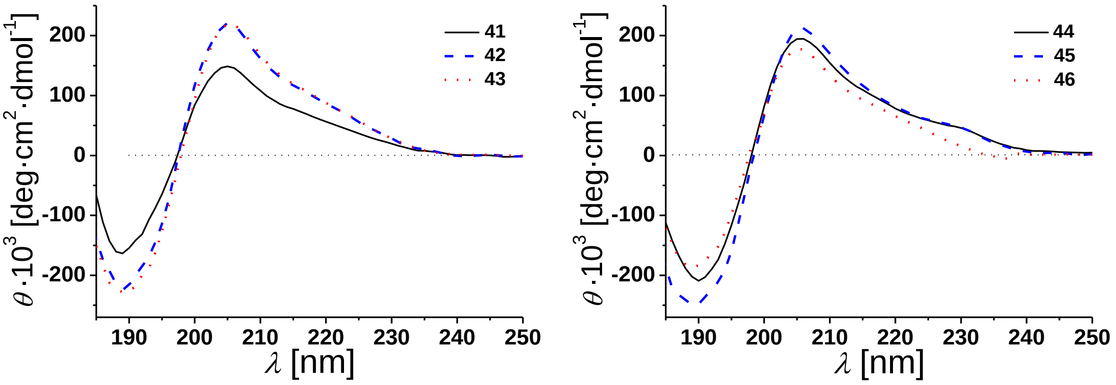

Figure 33: CD-spectra of the transmembrane β-peptides 41-46 in DOPC LUVs (P/L-ratio = 1/20, β-peptide concentration: 38 µM, TRIS® buffer, 25 °C). Left: β-Peptides 41-43. Right: β-Peptides 44-45.

SEEBACH and co-workers already performed structural analysis of the 3_{14}-helix by a combination of X-ray crystallography, molecular dynamic simulation studies and CD- and NMR-spectroscopy which show that the characteristic CD bands are a result of a left-handed 3_{14}-helix.[9,103,116,131,132] The CD-spectra of the membrane reconstituted β-peptides (**41**-**46**) show a similar yet mirrored CD-pattern indicative of folding of the β-peptides (**41**-**46**) into right-handed 3_{14}-helices. HAMURO *et al.* have shown that the mean residue ellipticity increases in a length-dependent manner. Furthermore, they found out that the presence of micelles strongly stabilises the 3_{14}-helical conformation of amphiphilic β-peptides which is in good consistency with the presented results.[110,138,141] In addition, the CD-spectra of the β-peptides (**41**-**46**) are slightly shifted compared to the presented results by SEEBACH and co-workers.[116,161] These shifts of the maxima and minima are a consequence of the differences in the dielectric constants of the used solvents.[52] CD-spectroscopic pattern are dependent on backbone as well as side chain conformation.[162] Thus, aromatic side chains like the indole ring of tryptophan, show characteristic CD values in the 225 nm-region, even though they are positioned close to the end of the helical peptide.[163–165] Indeed, in addition to the characteristic CD-pattern of a right-handed 3_{14}-helix, the presented CD-spectra of the β-peptides **45** and **46** show a weak shoulder at 230 nm due to the four D-β^3-tryptophans (two at each side), which were attached to the β-peptide sequences. Beside the mere determination of the secondary structure, the CD-spectra also demonstrate no influence of the iodine-label on the secondary structure, as expected.

4.2.4 X-ray Diffraction Analyses in Model Lipid Multilayer

In order to analyse parameters like orientation and membrane-insertion of these transmembrane β-peptides, X-ray diffraction studies were performed. This also comprises, where possible, quantification of lipid chain ordering, analysis of the helix tilt as well as bilayer thickness or summarised in a more general way, its electron density distribution.[22] Furthermore, β-peptides with additional D-β^3-tryptophan residues were analysed and compared with β-peptides containing only D-β^3-lysine residues to answer the question if ^{h}Trp could enhance the anchoring effect of ^{h}Lys. The labelled and the non-labelled transmembrane β-peptides were investigated and evaluated by Y. XU from the SALDITT research group. As these multilamellar membranes with well-defined equilibrium periodicity *d* provide high increase in diffraction signal, they also show, in case of orientated membranes, a precise separation between scattering vector component parallel to the membrane plane $q_{\parallel}$ and perpendicular to the membrane q_z.[22,166–171] For studying peptide-lipid interaction this means that structural signals can be clearly assigned to correlations in the lateral membrane plane or the vertical direction *z* along the membrane normal.[22]

A simple sketch of the experimental setup of X-ray reflectivity measurements is shown in Figure 34a, where the incident angle α_i always equals the exit angle α_f.[22] In principle, small-angle X-ray diffraction studies regarding the distribution, concentration and structural integrity of the β-peptides can give several structural parameters (Figure 34b):[146,171,172] (1) By recording a reflectivity scan, sharp BRAGG peaks can be obtained, from which the one-dimensional electron density profile (EDP) $\rho(z)$ along the membrane normal is determined. The EDP provides information about the distance between the head group density maxima associated with the phosphate groups which is defined as the bilayer thickness d_{hh} and it provides information about the water layer thickness

d_w.[22,94] (2) The lateral ordering of lipids and peptides in the membrane plane is analysed by scanning q_{II}, which results in the correlation peak corresponding to the short range of acyl chain correlation.[173] When using a 2D-detector positioned in GID geometry, more information can be collected by probing the correlation peak and the complete scattering intensity distribution in the q_{II}/q_z plan. (3) After incorporation of β-peptides into lipid bilayers the entire effect on both perpendicular and lateral membrane structures can be analysed in the same way as in pure lipid systems.[22]

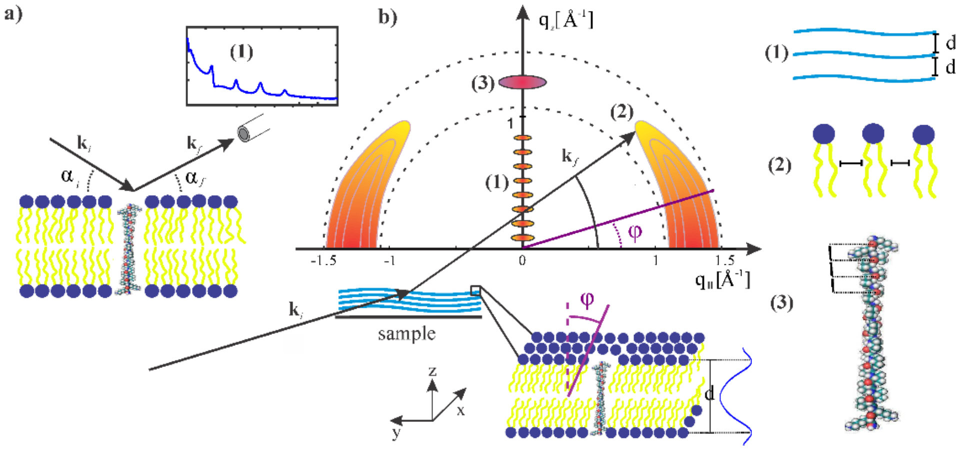

Figure 34: (a) Simple sketch of the experimental setup of X-ray reflectivity measurements. The incident angle α_i always equals the exit angle α_f; (b) Schematic view of the X-ray diffraction experiment with three different kinds of observed peaks on the detector plane: (1) BRAGG peaks which indicate the multilayer order in *z* direction, (2) chain correlation peaks that designate the lateral acyl chain order, and (3) helical peaks that comes from the secondary structure of the β-peptides. Figure 34 was kindly provided by Y. XU.[22]

4.2.4.1 Analysis of the electron density profile

The reflectivity mode deals with the momentum transfer perpendicular to the membrane. Hence, the electron density profile (EDP) can be calculated on relative scale in direction of the membrane normal (*z*-direction) by FOURIER synthesis method of the measured BRAGG peaks.[174] The reflectivity curves of the multilamellar peptide-lipid complexes (P/L-ratio = 1/10) of the β-peptides **41**-**46** embedded in DOPC-stacks are shown in Figure 35 (left), where the β-peptides **41**-**43** (without ^{h}Trp) have four BRAGG peaks while five BRAGG peaks (the fifth is extremely weak) can be detected for the peptides **44**-**46** (with ^{h}Trp). These results indicate an increased lamellar disorder as they are in sharp contrast to the eight orders observed for pure DOPC (not shown) under the same conditions ($T \simeq 20$ °C and $RH \simeq 95\%$), which is well-known from other membrane peptides.[175] The electron density profile (Figure 35, right) show the typical and renowned pattern with its two head group maxima, and a decrease in the density in the acyl chain region, which can be described more precisely as the methyl group minimum in the bilayer midplane.[176] In order to illustrate the orientation of the lipids Y. XU placed DOPC molecular models above the EDPs (Figure 35, right).

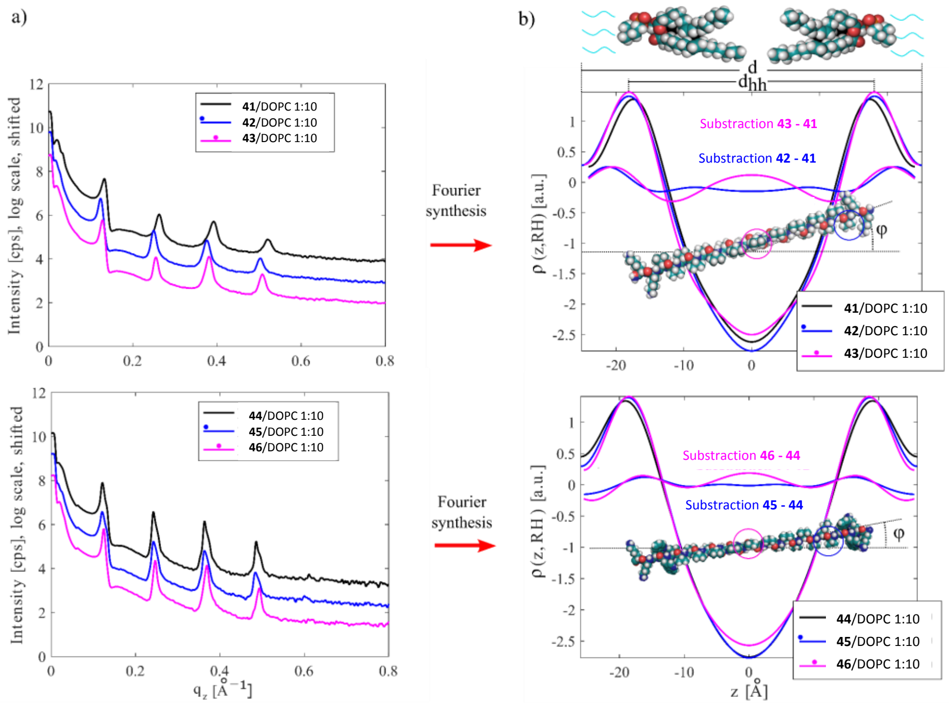

Figure 35: Left: Reflectivity curves of β-peptides (41-46)/DOPC mixtures (P/L = 1/10) recorded at *T* ≃ 20 °C and *RH* ≃ 95%. The reflectivity curves are shifted for clarity. Right: The respective EDPs, where the EDPs of the labelled β-peptides are subtracted by the non-labelled ones and presented in the middle. Possible β-peptide orientations are shown by placing the molecular drawing against the EDPs. The labelling conditions are sketched in the legends. Information provided by Y. XU.

In order to compare the relative shape function of the EDPs, the EDPs of the non-labelled β-peptides were subtracted from the iodine-labelled β-peptides (curves in the middle of the EDPs in Figure 35, right).[177] In case of the centre-labelled β-peptides (**43** and **46**) a significant contrast is clearly observed in the centre region of the EDP which confirms the full insertion of the β-peptides in a transmembrane fashion. Hence, the β-peptides always position themselves in the bilayer midplane. The β-peptides labelled near the end of the terminus (**42** and **45**) do not show a similar contrast compared with the centre-labelled ones since the iodine-label could be 'shielded' by the head group region. Assuming that the small peaks in the EDPs of **42** represent the iodine-label at the terminal end of the sequence, the β-peptides have to adopt a tilted conformation.

In Figure 36 d_{hh} and d_w are shown, which have been received from the EDPs in Figure 35. Herein, d_{hh} is defined as the distance between the phosphate groups and d_w as the water layer thickness ($d_w = d - d_{hh}$). A decrease of d_{hh} with respect to the P/L-ratio is shown for both types of β-peptides (with and without ^{h}Trp anchors). Due to the insertion of the β-peptides in a transmembrane helical conformation, the observed decrease seems to be a result of a membrane thinning effect, which could be caused by a positive hydrophobic mismatch (see also 3.4.1). Therefore, the β-peptides and the lipids have to adjust their hydrophobic part to achieve a match.[74]

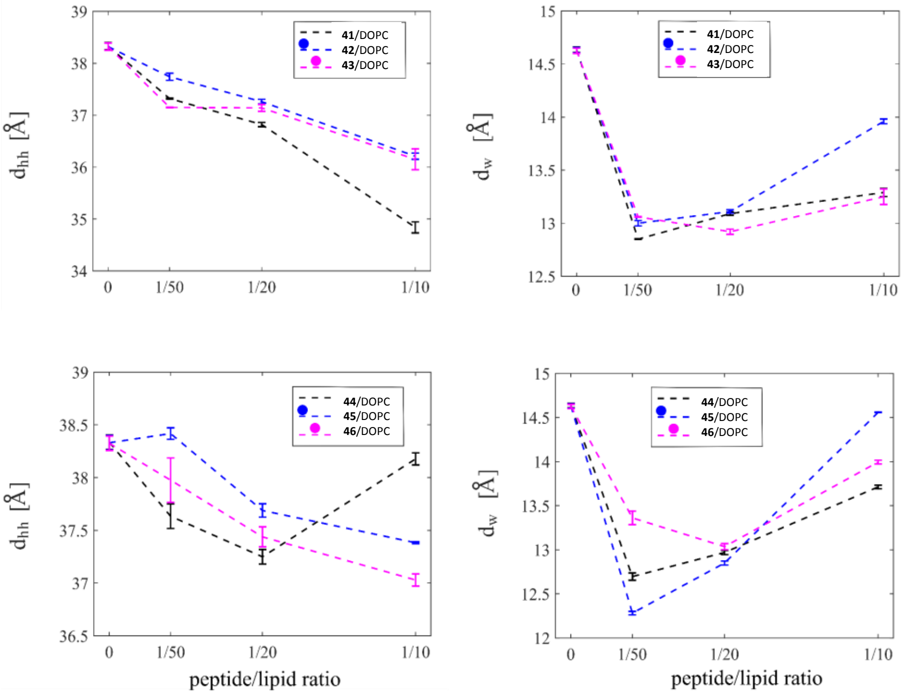

Figure 36: The bilayer thickness d_{hh} and the water layer thickness d_w of the β-peptides 41-46 at different P/L-ratios. Top: 41, 42 and 43. Bottom: 44, 45 and 46. The labelled conditions are sketched in the legends. Information provided by Y. XU.

The acyl chain length of DOPC (d_c ~ 30.0 Å at *RH* ~ 95%) is slightly shorter than the hydrophobic part of the β-peptides (d_c ~ 31.17 Å) and a match of the β-peptides within the lipid bilayer can be accomplished either by β-peptides shrinking or by β-peptides tilting.[178] In the first case, a membrane thickening effect instead of a membrane thinning effect is expected. Thus, the positive hydrophobic mismatch is equalised only by a tilt of the helical transmembrane β-peptide reducing its exposure to polar groups, with an estimated tilt angle of 16°.[69] As a result of the tilted transmembrane β-peptide, the acyl chains in its neighbourhood are tilted, too, which would explain the observed thinning effect. This thinning effect is more significant for the β-peptides **41**-**43** (without ^{h}Trp) than for **44**-**46** (with ^{h}Trp), which means that additional ^{h}Trp-anchors may reduce the tendency of incorporated β-peptides to tilt themselves to compensate hydrophobic mismatch. It also explains the small contrast of the end-labelled β-peptides, as the distribution function of tilted transmembrane domain tends to smear out the already small contribution to the total electron density.[22] In addition, by comparison of labelled with non-labelled β-peptides, d_{hh} and d_w behave similar, indicating that the heavy-atom label does not induce significant structural changes in the lipid bilayer.

4.2.4.2 Analysis of the chain-correlation peak

In order to confirm the explanation of the monitored thinning effect by a higher proportion of tilted acyl chains, X-ray grazing incidence diffraction (GID) around the chain correlation peak was used for the β-peptides **41**-**43** (without ^{h}Trp). The diffraction pattern of pure DOPC and mixtures of DOPC with the β-peptides **44**-**46** at a P/L-ratio = 1/10 are demonstrated in Figure 37a and the typical broad and bent line shape of the chain correlation are found for pure DOPC.[179]

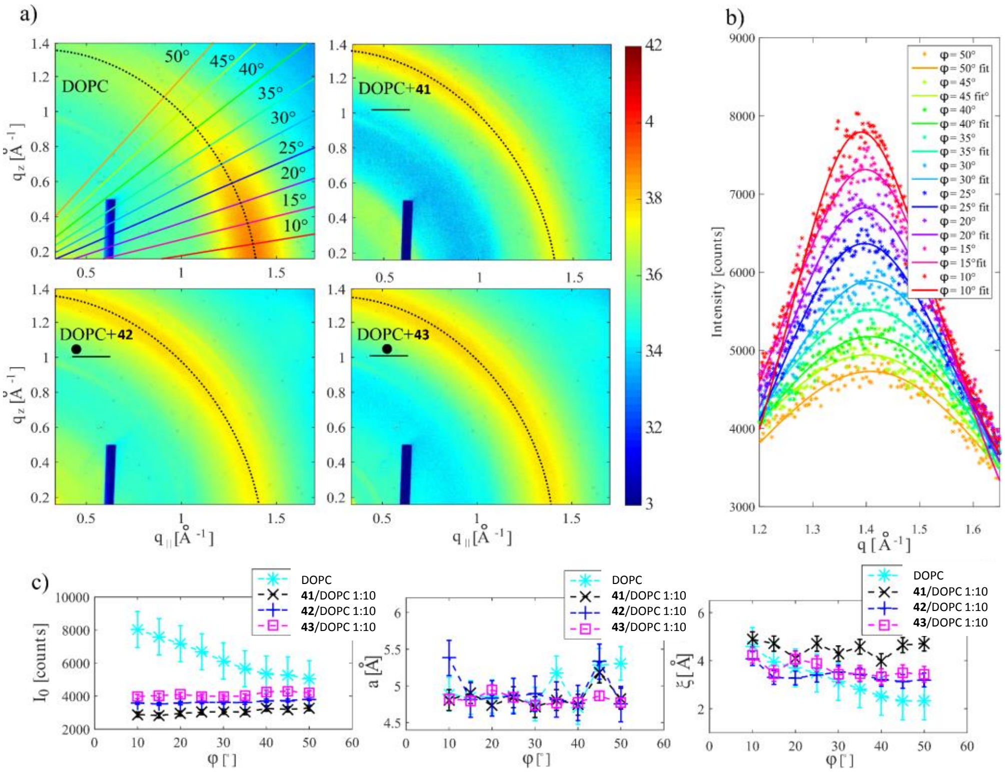

Figure 37: (a) Diffraction pattern of pure DOPC and mixtures of DOPC with the β-peptides without ^{h}Trp (41-43) in logarithmic scale. The labelling conditions are sketched under the sample names and the primary beam is depicted in the lower left of the diffraction pattern. Lines with different colours in DOPC denote different tilting angles φ and the dashed lines denote the profile maximum intensities I_0 and the dark blue bar is the unremoved beam-stop. (b) Fittings along different tilting angles φ together with the intensity profiles result in the diffraction pattern of pure DOPC. (c) Lateral membrane ordering parameters deduced from the fittings: maximum intensity I_0 of each φ, chain-chain distance a, and chain correlation length ζ as a function of φ. Information provided by Y. XU.

A decrease in the chain correlation signal for the β-peptide containing samples indicates a higher disorder in the chain packing as expected for transmembrane peptides and can be considered as a further strong evidence for β-peptides insertion in a transmembrane fashion. In addition, the curved chain peak intensity does not decrease towards higher tilting angles φ and can be explained as a result of a broad distribution function for the chain tilt probability. This observation is perfectly in line with the already mentioned explanation of the membrane thinning. The structural peak of the 3_{14}-helix itself is expected to have a maximum centred near $q_z \sim 1.35$ Å, assuming a helical pitch of $p = 4.7$ Å for the observed β-peptides **41**-**43**, which is in good accordance with the literature known value of $p = 5.0$ Å for a 3_{14}-helix.[21,109,180] However, this structural peak could also be smeared out on an arc and passed into the chain correlation peak without clear separation. Hence, this contribution seems to be a reason for the ring-shaped signal at high q_z, which would also confirm the successful incorporation of the β-peptides **41**-**46** into lipid bilayers (DOPC). SPAAR *et al*. and HUB *et al*. have previously shown that this liquid-like order peaks can be qualitatively analysed in terms of a liquid structure factor, which was reproduced by molecular dynamic simulations. [180,181] In addition, WEINHAUSEN *et al*. presented the least-square fitting tools, which were used to analyse the obtained data.[179] First of all, the intensity profiles at different tilting angles φ are plotted (Figure 37b, for pure DOPC as an example) and fitted resulting in the lateral membrane ordering parameters, *i.e*. the maximum intensities I_0 of each φ, the chain-chain distance a, and the chain correlation length ζ (Figure 37c).The analysis of the parameters I_0, a and ζ is premised on a decay of chain populations as a function of the angle φ of tilted chain segments.[179] As already mentioned in literature, the intensity I_0 of pure DOPC decreases with increasing φ with the maximum in the $\varphi \leq 10°$ region reflecting that the majority of chain segments is untilted (Figure 37c).[179] However, the β-peptides containing samples show a flat I_0 (φ) curve, indicative of a broad distribution of chain tilts induced by tilted transmembrane β-peptides. Furthermore, the chain-chain distance a (φ) of β-peptide free and β-peptide containing membranes remains almost constant. In the small φ region where helical contributions can be excluded, the chain-chain distance a vary between 4.82 Å and 5.38 Å and the chain correlation length ζ between 4.23 Å and 4.88 Å. A β-peptide associated effect results in a sharper peak of the chain correlation length ζ at higher φ, which is a direct signal of the 3_{14}-helix. Thus, a substantial distribution of helical tilt angles must exist with an averaged tilt angle of 16° and perfect vertical orientated transmembrane β-peptides can be ruled out.

4.2.5 Conclusion

A new heavy-atom labelled D-β^3-amino acid residue has been synthesised and incorporated into different transmembrane β-peptides to increase the difference of electron density profiles in lipid membranes and therefore, to answer the question if additional ^{h}Trp anchors could enhance the anchoring effect of ^{h}Lys. First of all, the CD-spectra of the designed β-peptides reconstituted into unilamellar vesicles (DOPC) show a characteristic pattern indicative of a right-handed 3_{14}-helical secondary structure. Furthermore, X-ray diffraction studies performed by Y. XU from the SALDITT research group provide information about β-peptides properties in model lipid multilayer. The results demonstrate that all β-peptides (**41**-**46**) are inserted into the model membrane stacks and form helical transmembrane domains with the central D-β^3-amino acid residue positioned at the bilayer midplane. As the hydrophobic part of the β-peptides is slightly longer than the one of the lipids, both have to adjust their hydrophobic part to attain a match. In order to relieve the so called positive hydrophobic mismatch, a helical tilt is observed that induces an increase in chains with corresponding tilt angles. Consequently, a thinning of the membrane and a perturbation of the acyl chain packing did occur, but the ^{h}Trp anchor can partially suppress this elastic response and stabilise the vertical insertion of the β-peptides. Hence, the β-peptide H-^{h}Lys$_2$-^{h}Trp$_2$-^{h}Val$_{19}$-^{h}Trp$_2$-^{h}Lys$_2$-NH$_2$ (**47**) seems to be a suitable model transmembrane domain system for further investigations in the field of β-peptides.

4.3 Self-Association of Transmembrane β-Peptides within Lipid Bilayers via Hydrogen-Bond Formation of β-Glutamine

During the last three decades, the design and synthesis of artificial β-peptide oligomers in solutions, became of great interest. These β-peptide oligomers should be able to form well-defined and stable secondary structures and they should be resistant to proteolytic degradation by proteases and peptidases.[9,21] These folding processes take an important part in protein/peptide architecture as well as in recognition processes between peptides.[17] The complexity of protein structures often limit the detailed analysis of biological functions, mechanisms and activities on a molecular level.[4] Therefore, integral membrane proteins were investigated as they are involved in many kinds of cellular processes and represent almost 30% of the human proteome.[5,15] To fulfil their biological role, membrane proteins may function as monomers or need to assemble into oligomeric structures. Studies on membrane protein oligomerisation, have been done intensively using model systems of transmembrane α-peptide helices.[5,15,16,87,182] These transmembrane α-peptide helices and their organisation and assembly are influenced by the lipid environment and the interacting molecular species themselves, which are still not fully understood.[22] Hence, synthetically easily accessible transmembrane peptide models are a fundamental tool to analyse peptide-peptide and peptide-lipid interactions that are a result of membrane associated processes.[3,15] However, the field of transmembrane β-peptide helices and their association within a lipid membrane is still largely unresearched. It has been previously demonstrated by APPELLA *et al.*, that small 10-residue amphiphilic β-peptides are able to form aggregates, which are soluble in water.[142,183] In addition, BRÜCKNER *et al.* and CHAKRABORTY *et al.* presented specific β-peptide helix interactions in solution. These β-peptide helix associations were initiated by the attachment of nucleobases that function as recognition units.[4,17] Another possibility for self-association of a model transmembrane α-helix by means of the recognition potential of hydrogen bonding was generated by the incorporation of asparagine.[16,23] In the present study, transmembrane β-peptides were designed to allow for peptide oligomerisation based on hydrogen bond formation within a lipid bilayer. Therefore, D-β^3-glutamine residues (Figure 38) were placed at defined positions within the β-peptides due to their structural and chemical similarity to asparagine.

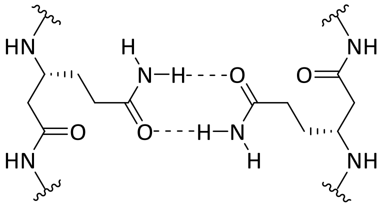

Figure 38: Schematic view of hydrogen bond formation of D-β^3-glutamine residues.

4.3.1 Design and Synthesis of ^{h}Gln-functionalised Transmembrane β-Peptides

Investigations of heavy-atom labelled transmembrane β-peptides have revealed that the centre of the synthesised β-peptide is located in the middle of the membrane (see 4.2).[22] Thus, the core unit of the designed β-peptides consists of 19 D-β^3-valines, which span the entire hydrophobic inner membrane part.[136,157] Furthermore, the β-peptides are flanked with two D-β^3-tryptophan residues at the *N*- and *C*-terminal end of the sequence to stabilise and anchor the transmembrane β-peptides in the lipid membrane.[65,70,71,158] Previous investigations have shown that ^{h}Trp anchors stabilise vertical insertion of the transmembrane β-peptides.[22] In addition, four D-β^3-lysine residues (two at each side) are attached to the β-peptides as lysine is known to facilitate the solubility in aqueous systems.[70] In total, the transmembrane β-peptide H-^{h}Lys$_2$-^{h}Trp$_2$-^{h}Val$_{19}$-^{h}Trp$_2$-^{h}Lys$_2$-NH$_2$ (**47**) will be used as a basic structure for studies on self-assembly of transmembrane β-peptides within lipid bilayers.

The basic structure of this transmembrane β-peptide is known to form a 3_{14}-helix as its secondary structure element and it is inserted into lipid bilayers in a transmembrane fashion.[22] As previously described, in a 3_{14}-helix three β^3-amino acids form one helix turn in which every third amino acid side chain is oriented on the same face of the helix (see 4.1.2).[64,170] Thus, the basic structure of the β-peptide seems to be a great model system to analyse transmembrane β-peptides and their association in lipid membranes. Here, D-β^3-glutamine (**3**) is introduced as the recognition unit to control transmembrane β-peptide helix aggregation by means of hydrogen bond formation. Due to the additional CH$_2$-group at the side chain, D-β^3-glutamine (**3**) is more flexible compared to asparagine. D-β^3-Valine residues are replaced by two or three D-β^3-glutamines, respectively. BRÜCKNER *et al*. and CHAKRABORTY *et al*. have already shown that nucleobase functionalised β-peptides favour an antiparallel strand orientation in aqueous solutions.[4,17] Assuming an antiparallel formation of the transmembrane β-peptides, the D-β^3-glutamine residues were placed accordingly (Figure 39 and Table 5). To perform FRET experiments (see also 3.7), the fluorophores (NBD (**8**), TAMRA (**9**)), were attached to the β-peptides. Thus, one additional D-β^3-lysine was added either to the *C*-terminal or the *N*-terminal end of the β-peptide sequence. To avoid any conformational restriction by labelling with fluorophores, they were attached to the side chain of the additional D-β^3-lysine. Furthermore, free peptide termini enable a better membrane insertion.[15] The transmembrane β-peptides **48**-**56** were synthesised using manual microwave assisted Fmoc-SPPS, as previously described (see 4.2.2 and Scheme 10).[128,159] Therefore, the side chains of the D-β^3-amino acid residues ^{h}Lys, ^{h}Trp and ^{h}Gln were orthogonally protected to avoid side reactions. Three differently protected ^{h}Lys were needed for attaching the fluorophores NBD (**8**) and 5(6)-TAMRA (**9**) to the respective β-peptide.

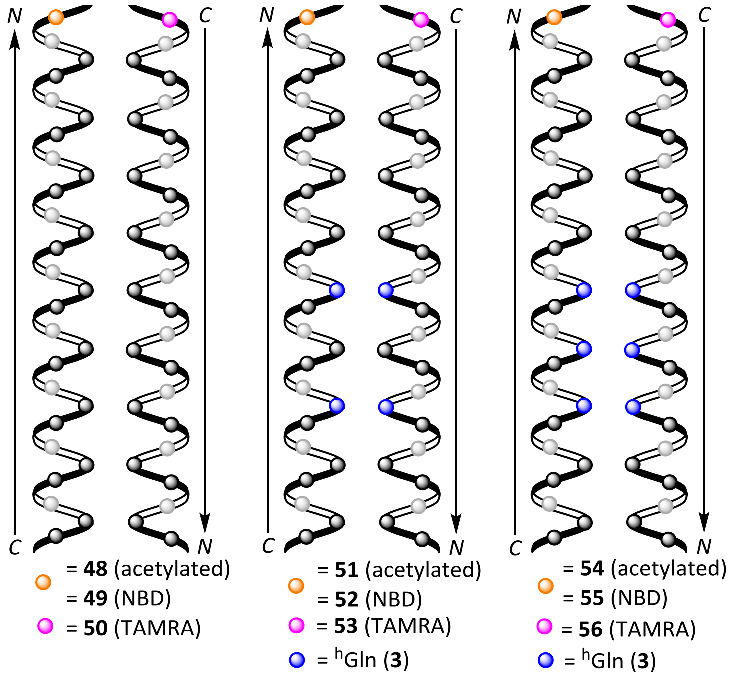

Figure 39: Schematic view on the antiparallel 3_{14}-helical β-peptides where three amino acid residues form one turn. Left: zero ^{h}Gln (48/49/50); Middle: two ^{h}Gln (51/52/53); Right: three ^{h}Gln (54/55/56). The β-peptides were acetylated or labelled with NBD and TAMRA for FRET-analysis and synthesised from *N*- to *C*-terminus.[3]

Boc-D-β^3-Lys(Fmoc)-OH (**31**) was coupled as final D-β^3-amino acid to the *N*-terminal end of the β-peptide and after Fmoc-deprotection with piperidine in DMF (20%), NBD was labelled to the deprotected side chain. Therefore, NBD–Cl (3.00 eq) in DMF was activated by DIPEA (20.0 eq) and allowed to react at rt overnight. Alternatively, the free side chain amino functionality of the *N*-terminal ^{h}Lys was acetylated with DMF/Ac_2O/DIPEA (18:1:1, *v*/*v*/*v*) at rt for 10 min, as during FRET-experiments the total peptide concentration has been kept constant by using the acetylated β-peptides **48**, **51** or **54**. Fmoc-D-β^3-Lys(Alloc)-OH (**32**) was introduced at the *C*-terminal end of the sequence providing orthogonality to the Boc-protecting group. However, during Alloc-deprotection using $Me_2NH{\cdot}BH_3$ (40.0 eq) and $Pd(PPh_3)_4$ (0.10 eq) in dry DMF, the *N*-terminal Fmoc-group was deprotected as well. To prevent a free *N*-terminus in this step Boc-D-β^3-Lys(Boc)-OH (**57**) was coupled as the final D-β^3-amino acid to the *N*-terminal end of the sequence. After successful Alloc-deprotection, TAMRA was labelled at the β-peptide sequence. Therefore, 5(6)-TAMRA (**9**) (5.00 eq) in DMF was activated by PyBop® (4.70 eq) and DIPEA (9.80 eq) and allowed to react at rt overnight. After successful fluorophore-labelling cleavage from the solid support and simultaneous removal of the protecting groups was carried out using TFA/H_2O/TIS (95.5/2.5/2.5, *v*/*v*/*v*) followed by HPLC purification. In total three different kinds of transmembrane β-peptides were synthesised for analysing β-peptide helix association: *i*) **48**/**49**/**50** with zero ^{h}Gln, *ii*) **51**/**52**/**53** with two ^{h}Gln and *iii*) **54**/**55**/**56** with three ^{h}Gln as recognition units (Table 5).

Table 5: Synthesised transmembrane β-peptides with zero, two or three D-β^3-glutamine recognition units.

No.	Synthesised Transmembrane β-Peptides
	Zero recognition units
48	H-^{h}Lys(acetyl)-^{h}Lys$_2$-^{h}Trp$_2$-^{h}Val$_{19}$-^{h}Trp$_2$-^{h}Lys$_2$-NH$_2$
49	H-^{h}Lys(NBD)-^{h}Lys$_2$-^{h}Trp$_2$-^{h}Val$_{19}$-^{h}Trp$_2$-^{h}Lys$_2$-NH$_2$
50	H-^{h}Lys$_2$-^{h}Trp$_2$-^{h}Val$_{19}$-^{h}Trp$_2$-^{h}Lys$_2$- ^{h}Lys(TAMRA)-NH$_2$
	Two ^{h}Gln recognition units
51	H-^{h}Lys(acetyl)-^{h}Lys$_2$-^{h}Trp$_2$-^{h}Val$_9$-^{h}Gln-^{h}Val$_5$-^{h}Gln-^{h}Val$_3$-^{h}Trp$_2$-^{h}Lys$_2$-NH$_2$
52	H-^{h}Lys(NBD)-^{h}Lys$_2$-^{h}Trp$_2$-^{h}Val$_9$-^{h}Gln-^{h}Val$_5$-^{h}Gln-^{h}Val$_3$-^{h}Trp$_2$-^{h}Lys$_2$-NH$_2$
53	H- ^{h}Lys$_2$-^{h}Trp$_2$-^{h}Val$_3$-^{h}Gln-^{h}Val$_5$-^{h}Gln-^{h}Val$_9$-^{h}Trp$_2$-^{h}Lys$_2$-^{h}Lys(TAMRA)-NH$_2$
	Three ^{h}Gln recognition units
54	H-^{h}Lys(acetyl)-^{h}Lys$_2$-^{h}Trp$_2$-^{h}Val$_9$-^{h}Gln-^{h}Val$_2$-^{h}Gln-^{h}Val$_2$-^{h}Gln-^{h}Val$_3$-^{h}Trp$_2$-^{h}Lys$_2$-NH$_2$
55	H-^{h}Lys(NBD)-^{h}Lys$_2$-^{h}Trp$_2$-^{h}Val$_9$-^{h}Gln-^{h}Val$_2$-^{h}Gln-^{h}Val$_2$-^{h}Gln-^{h}Val$_3$-^{h}Trp$_2$-^{h}Lys$_2$-NH$_2$
56	H-^{h}Lys$_2$-^{h}Trp$_2$-^{h}Val$_3$-^{h}Gln-^{h}Val$_2$-^{h}Gln-^{h}Val$_2$-^{h}Gln-^{h}Val$_9$-^{h}Trp$_2$-^{h}Lys$_2$-^{h}Lys(TAMRA)-NH$_2$

4.3.2 CD-Spectroscopic Analysis of the Synthesised β-Peptides

CD spectroscopy was performed to analyse the secondary structure of the synthesised transmembrane β-peptides **48**, **51** and **54** reconstituted in large unilamellar vesicles (LUVs) composed of DOPC at a P/L-ratio of 1/20 (TRIS® buffer) and a peptide concentration of 38 µM (Figure 40). The CD-spectra of all three β-peptides (**48**, **51** and **54**) show a pattern indicative of a right-handed 3$_{14}$-helix with a minimum at 196 nm, a zero crossing near 199 nm and a maximum at 206 nm, which are again mirrored and slightly shifted compared to the left-handed 3$_{14}$-helical structure in solutions (see 4.2.3).[52,116,130,161]

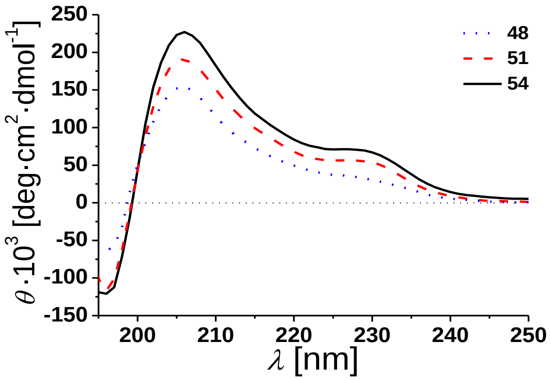

Figure 40: CD-spectra of the transmembrane β-peptides 48, 51 and 54 in DOPC LUVs (P/L-ratio = 1/20, TRIS® buffer, β-peptide concentration: 38 µM, 25 °C).

As already mentioned, CD spectroscopy depends on both, backbone and side chain conformation.[22,162] As a results of the aromatic side chains of the four D-β^{3}-tryptophan residues (two at each side of the sequence), which are known to have typical CD values in the 225 nm-region, the depicted CD-spectra of the β-peptides (**48**, **51** and **54**) have a weak maximum at 229 nm.[162–164] The secondary structures of the β-peptides is expected to be very stable, in particular if embedded in a lipid bilayer. Herein, the thermal stability of the secondary structure of the β-peptides **51** and **54** was investigated using of CD spectroscopy.[141] Therefore, CD-spectra of the β-peptides **51** and **54** reconstituted in DOPC (LUVs, P/L-ratio = 1/20, peptide concentration: 38 µM, TRIS® buffer) were recorded at 25 °C and at 60 °C (Figure 41). Results show that the secondary structure of the β-peptides is almost unaffected by the increase in temperature, which confirms the thermal stability of the β-peptide secondary structures. Apart from the secondary structure determination and the thermal stability of the β-peptide secondary structures, the CD-spectra also demonstrate that neither the recognition units nor the acetylated side chain influence the secondary structure.

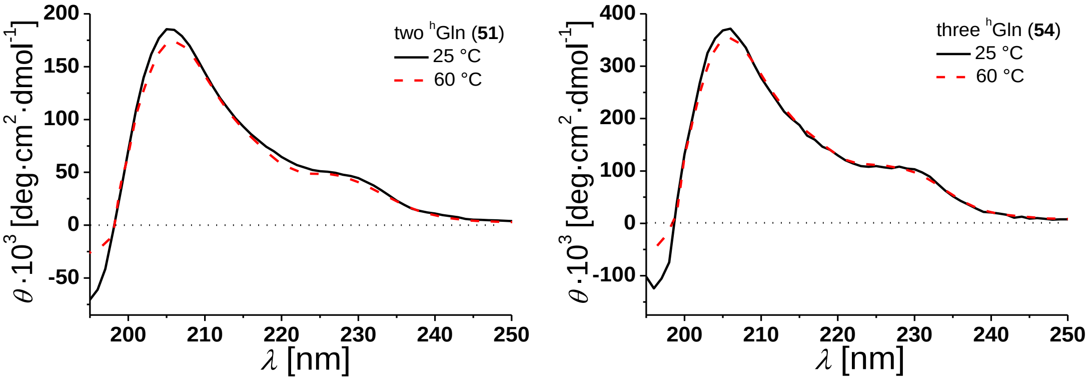

Figure 41: CD-spectra of the transmembrane β-peptides 51 (left) and 54 (right) in DOPC LUVs (P/L-ratio = 1/20, β-peptide concentration: 38 µM, TRIS® buffer) at 25 °C and at 60 °C.

4.3.3 Fluorescence Spectroscopic Analysis of the Synthesised β-Peptides

From X-ray reflectivity analyses it has been proofed that the selected transmembrane peptide should be inserted into the model membrane with the central D-β^{3}-amino acid residue located in the bilayer midplane (see 4.2). Here, a successful membrane insertion was analysed by fluorescence spectroscopy detecting the intrinsic tryptophan fluorescence, as tryptophan fluorescence is sensitive towards the polarity of its local environment.[12,184,185] If tryptophan residues are positioned in a hydrophobic area like the inner membrane part, the emission maximum (λ_{max}) of Trp would be expected to be < 330 nm due to interaction of the indole ring with the adjacent acyl chains of surrounding lipids.[184,186,187] If the tryptophan residues are oriented in a more polar environment, the tryptophan emission is however red-shifted (λ_{max} > 330 nm) and water exposure to the indole-ring results in a fluorescence maximum at 350 nm.[184,188] Herein, two tryptophan residues were placed at each, the *N*- and *C*-terminal part of the β-peptide sequences and the β-peptides were positioned in a transmembrane fashion where the tryptophan residues are located at the polar/apolar interface of the lipid membrane. In order to analyse β-peptides' positions inside the lipid bilayer tryptophan fluorescence spectroscopy was performed to determine the tryptophan emission maximum λ_{max} (Figure 42).

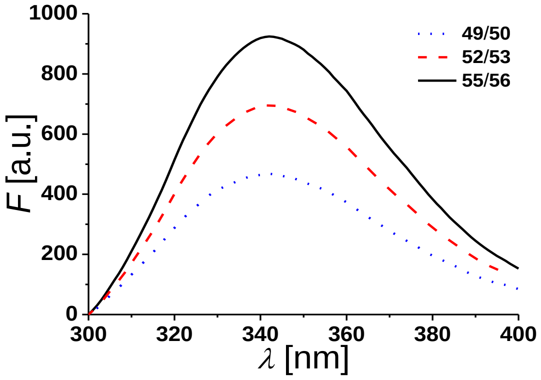

Figure 42: Fluorescence emission spectra of equimolar mixtures of the transmembrane β-peptides 49/50, 52/53 and 55/56 in DOPC (LUVs) (P/L-ratio = 1/500, β-peptide concentration: 12 µM, TRIS® buffer, 25 °C).

The fluorescence emission spectra of equimolar mixtures of the β-peptides **49**/**50**, **52**/**53** and **55**/**56** reconstituted in DOPC (LUVs) at a P/L-ratio of 1/500 (TRIS® buffer) and a β-peptide concentration of 12 µM are presented in Figure 42. In all cases, the fluorescence emission λ_{max} of the tryptophan residues was detected to be 342 nm. These results demonstrate the localization of the tryptophan residues in a more polar environment like the polar/apolar interface of the lipid bilayer. These results confirm a transmembrane orientation of the β-peptides within the DOPC bilayer.

4.3.4 Determination of Peptide Aggregation State of Transmembrane β-Peptides using FRET

The association state of the transmembrane β-peptides reconstituted into DOPC vesicles by using D-β^3-glutamine as a potential recognition unit was investigated by fluorescence resonance energy transfer (FRET) experiments. Therefore, a donor- (NBD, **8**) acceptor (TAMRA, **9**) pair was attached to β-peptides.[78,93] As an example, the fluorescence emission spectra of the β-peptides **51**/**52**/**53** (two ^{h}Gln, Figure 43, left) and **54**/**55**/**56** (three ^{h}Gln, Figure 43, right) at a P/L-ratio of 1/500 at 25 °C are presented (see 7.3 and 7.4 for all fluorescence emission spectra at different P/L-ratios). The degree of β-peptide aggregation becomes accessible by measuring the ratio of NBD fluorescence intensity F at 530 nm in the presence of TAMRA-labelled β-peptides and F_0, NBD fluorescence intensity at 530 nm in its absence as a function of the TAMRA-labelled β-peptides concentration. The total peptide/lipid-ration was kept constant by adding the respective acetylated and non-labelled β-peptides (Figure 43).[23]

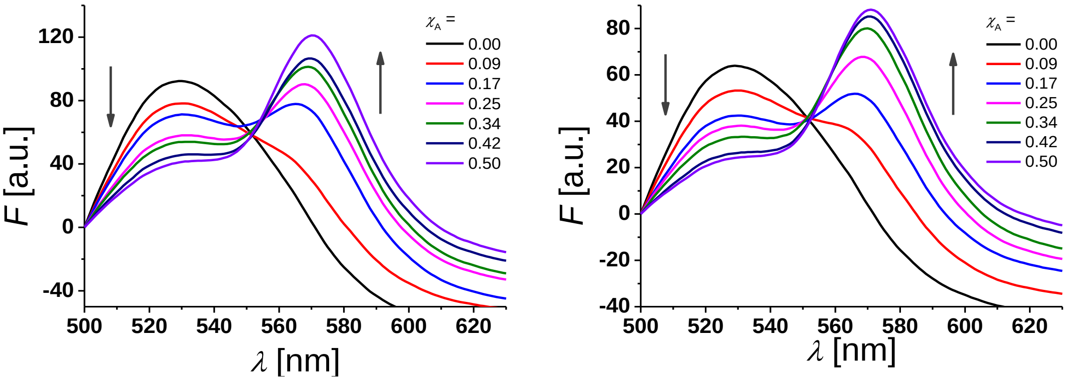

Figure 43: Fluorescence emission spectra of 51/52/53 with two ^{h}Gln (left) and 54/55/56 with three ^{h}Gln (right). The spectra show NBD-labelled β-peptides (donor, 6.0 µM) with varying amounts of TAMRA-labelled species from 0-0.5 determined at 25 °C. The non-labelled compound was added to keep the total β-peptide concentration constant (12 µM) and the P/L-ratio at 1/500 (DOPC).

β-Peptides lacking ^{h}Gln are expected to remain monomeric in the membrane, whereas the β-peptides with two ^{h}Gln or three ^{h}Gln residues should associate due to hydrogen bond formation in lipid vesicles.[3] Figure 44 shows the ratio F/F_0 for all three cases (zero ^{h}Gln, two ^{h}Gln and three ^{h}Gln) as a function of the mole fraction (χ_A) of the acceptor of the β-peptides at 25 °C and a P/L-ratio of 1/500. The spectra show a decrease in the ratio F/F_0 with increasing mole fraction (χ_A) of the acceptor of the β-peptides. For the β-peptides with ^{h}Gln as recognition units, this decrease is significantly enhanced compared to that without ^{h}Gln. Hence, the three types of synthesised β-peptides associate in a different way.

Supposing that the β-peptides without recognition unit (**48**/**49**/**50**) are monomeric in the vesicles, the statistically occurring FRET in the vesicles was calculated following WOLBER *et al.*, which was performed by C. STEINEM as described previously (see 3.7).[15,23,78,83,85,88,91] Based on WOLBER *et al.*, the statistically occurring FRET was calculated by taking the area of 0.7 nm^2 for a DOPC lipid, vesicle diameter of 100 nm and a P/L-ratio of 1/500 into account and the grey solid line (Figure 44) is the result of a fitting routine, from which the FÖRSTER radius of $R_0 = 5.1 \pm 0.1$ nm was determined.[15,83] For β-peptides lacking ^{h}Gln (**48**/**49**/**50**), the calculated plot (Figure 44, grey solid line) is in a very good accordance with the data points and the value of the determined FÖRSTER radius is in perfect agreement with previous acquired FÖRSTER radii.[15] These results confirm the anticipated monomeric state for the β-peptides without ^{h}Gln (**48**/**49**/**50**) as a recognition unit. An oligomerisation of the two other β-peptide cases are expected, as their observed FRET is more pronounced compared to the FRET of the β-peptides without ^{h}Gln.

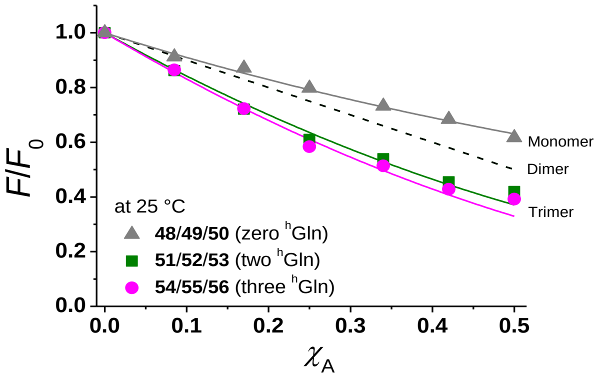

Figure 44: The plots show the relative changes in NBD-fluorescence emission (*F*/*F*$_0$) as a function of increasing acceptor concentration (χ_A) for all three cases at 25 °C. Grey: 48/49/50 (with zero ^{h}Gln). Green: 51/52/53 (with two ^{h}Gln). Pink: 54/55/56 (with three ^{h}Gln). The grey solid line is the result of a modelling according to WOLBER *et al.*, by taking only statistical occurrence of FRET in vesicles into account without the formation of aggregates.[15,83] A monomer-dimer equilibrium cannot clarify the data and even the assumption of a pure dimer (dashed black lines) does not explain the observed plots. The global fit analysis taking a monomer-trimer equilibrium into account results into the solid lines with $K_D = (17.2 \pm 7.0)\cdot10^{-8}$ MF^2 (two ^{h}Gln, green) and $K_D = (4.4 \pm 4.3)\cdot10^{-8}$ MF^2 (three ^{h}Gln, pink).

The data sets obtained for different P/L-ratios (1/500, 1/750 and 1/1000, see 7.3, 7.4, and 7.5) were also analysed by C. STEINEM assuming a monomer-dimer and a monomer-trimer equilibrium (Figure 44).[15,23,83,88] Results show no agreement between the data and the plots for a monomer-dimer equilibrium and even the assumption of a pure dimer (Figure 44, dashed black line) cannot explain the detected plots. However, the global fit analysis taking a monomer-trimer equilibrium into account results in an agreement between the data and the plots with dissociation constants

K_D = (17.2 ± 7.0)·10^{-8} MF^2 for the β-peptides with two ^{h}Gln (**51/52/53**) and K_D = (4.4 ± 4.3)·10^{-8} MF^2 for the β-peptides with three ^{h}Gln (**54/55/56**) (Figure 44, solid lines). The outcomes clearly demonstrate that the β-peptides **51/52/53** (two ^{h}Gln) and **54/55/56** (three ^{h}Gln) form aggregates due to hydrogen bond formation of the ^{h}Gln residues.[3]

To analyse the influence of hydrogen bond formation on the association properties more precisely, the temperature was increased. It is known that hydrogen bonds are weaker at higher temperatures.[99,100] Already performed CD-spectroscopic analyses of the β-peptides **51** and **54** at 25 °C and at 60 °C confirmed a very stable secondary structures of the synthesised β-peptides, even at higher temperatures. Hence, if hydrogen bonds are responsible for aggregate formation, an increase in temperature should influence the aggregation state of the β-peptides.[3] Fluorescence emission spectra of the β-peptides **48/49/50** (zero ^{h}Gln), **51/52/53** (two ^{h}Gln) and **54/55/56** (three ^{h}Gln) reconstituted in a lipid membrane (DOPC, P/L-ratio = 1/500) were recorded at 25 °C and 60 °C (see 7.3). In order to avoid any temperature effects, such as the temperature dependency of the extinction coefficients of the fluorophore NBD and TAMRA, the relative changes in fluorescence intensity F/F_0 are considered.[15]

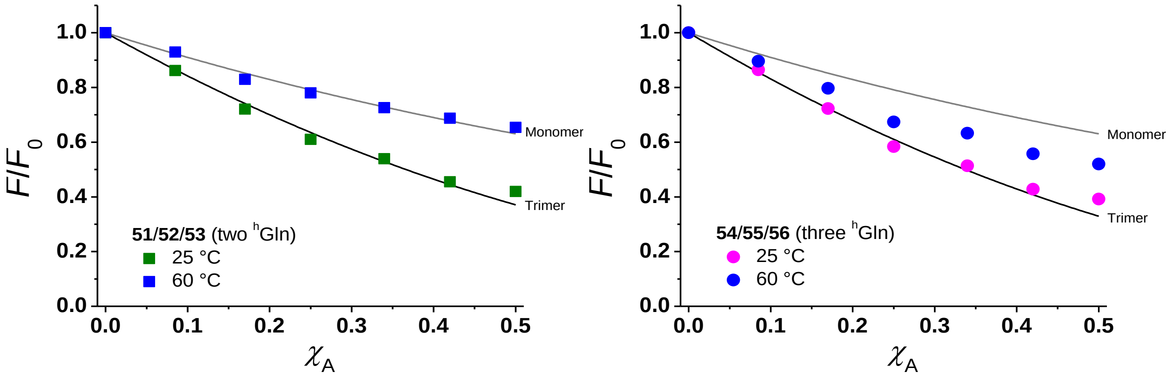

Figure 45: The plots show the relative changes in NBD-fluorescence emission (*F*/*F*₀) as a function of increasing acceptor concentration (χ_A) for 51/52/53 (with two ^{h}Gln, left) and 54/55/56 (with three ^{h}Gln, right) at 25 °C and 60 °C. The grey solid line is the result of a modelling according to WOLBER *et al.*, by taking only statistical occurrence of FRET in vesicles into account without the formation of aggregates.[15,83] The global fit analysis taking a monomer-trimer equilibrium into account results into the black solid lines with K_D = (17.2 ± 7.0)·10^{-8} MF^2 (two ^{h}Gln) and K_D = (4.4 ± 4.3)·10^{-8} MF^2 (three ^{h}Gln).

The results obtained at 25 °C and 60 °C for the β-peptides **51/52/53** (two ^{h}Gln, left) and **54/55/56** (three ^{h}Gln, right) are shown in Figure 45 together with the expected F/F_0 (χ_A) for monomeric β-peptides (grey solid lines) and the result of the global fit analysis taking a monomer-trimer equilibrium into account (black solid lines). The spectra clearly demonstrate that for both β-peptide cases (Figure 45, left and right) the detected FRET effect is reduced at 60 °C compared to that at 25 °C. The β-peptides **51/52/53** (two ^{h}Gln) seem to be in the monomeric state at 60 °C (Figure 45, left), whereas β-peptides **54/55/56** (three ^{h}Gln) do not fully dissociate into monomers at 60 °C, but still show an amended monomer-trimer equilibrium (Figure 45, right). The absence of a full dissociation of the β-peptides **54/55/56** even at 60 °C seems to be owed to a higher number of hydrogen bonds in the aggregates due to the additional recognition unit, which makes them more thermally stable than the β-peptides **51/52/53** with two recognition units. These results confirm the presumption that hydrogen bond formation via the D-β^{3}-glutamine residues allows to control the aggregation state of the β-peptides in a membrane environment.

Beside the state of aggregation and the associated hydrophobic interactions, the strength of these hydrophobic interactions was analysed. Thus, the relative changes in NBD-fluorescence emission (F/F_0) as a function of increasing acceptor concentration (χ_A) at different P/L-ratios (1/500, 1/750 and 1/1000) at 25 °C for the β-peptides with two ^{h}Gln (**51/52/53**, left) and with three ^{h}Gln (**54/55/56**, right) are shown in Figure 46 (for the fluorescence emission spectra see 7.3 and 7.4).

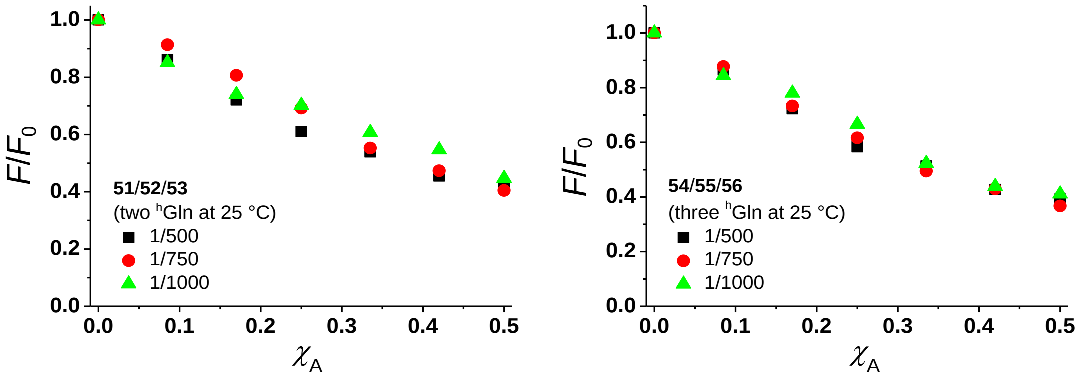

Figure 46: The plots show the relative changes in NBD-fluorescence emission (F/F_0) as a function of increasing acceptor concentration (χ_A) at different P/L-ratios (1/500, 1/750 and 1/1000) at 25 °C for the β-peptides with two ^{h}Gln (51/52/53, left) and with three ^{h}Gln (54/55/56, right).

In both cases, two ^{h}Gln and three ^{h}Gln, the spectra clearly demonstrated no concentration-dependency of the aggregation state, as all data points are almost on top of each other. These characteristics let to the assumption that the hydrogen bond formations are very stable, even at a P/L-ratio of 1/1000.

4.3.5 Conclusion

Several transmembrane β-peptides harbouring different numbers of D-β^3-glutamine residues were designed and synthesised (SPPS) to analyse β-peptide helix-helix interaction and their association state in membrane environment. D-β^3-Glutamine residues were used as specific recognition units to reveal the impact of hydrogen bond formation within the membrane on the recognition and assembly processes. First, the secondary structure of the β-peptides reconstituted into unilamellar vesicles (LUVs, DOPC) was analysed by means of CD-spectroscopy. Results show that the secondary structure of the transmembrane β-peptides is similar to a right-handed 3_{14}-helix, which is almost unaffected by an increase in temperature. As already mentioned (see 4.2.5), the β-peptides were inserted in an transmembrane fashion with the centre D-β^3-amino acid residue located at the bilayer midplane. Here, the membrane insertion was verified by fluorescence spectroscopy detecting the intrinsic tryptophan fluorescence. The association state of the β-peptides as a function of the number of D-β^3-glutamine residues became accessible by FRET measurements. The β-peptides with ^{h}Gln as recognition units associated into oligomers, likely trimers, whereas the β-peptides without recognition unit were monomeric. Furthermore, temperature dependent FRET analysis have shown that the stability of the β-peptide helix-helix association depends on the number of ^{h}Gln residues in the helix.

SUMMARY

A various number of cellular key functions such as signalling and transport are mediated by membrane proteins, which are either adhesively bound to the membrane surface or exhibit transmembrane domains.[4,23,189] Many transmembrane peptides accomplish their full function by interacting with each other. Hence, an increasing amount of studies on the fundamental molecular aspects of protein association have been done intensively using model systems of transmembrane α-peptide helices. The assembly and organisation of these transmembrane peptide helices depend on the lipid environment and/or the interacting species themselves but the processes behind these interactions still need to be fully clarified.[3,8,157,190] In order to apprehend the essentials and molecular details of transmembrane peptides within the lipid bilayer, simple model systems in combination with specific recognition units became of great interest.[4,12,72]

In the first part of this thesis, the design, synthesis and investigation of a novel 7-azaindole based recognition unit **11** were presented. The fluorescence emission and intensity of the 7-AI chromophore are known to be sensitive to their local environment.[18–20] The 7-AI building block **11** was further incorporated in a transmembrane model system, *i.e*. KALP, which was previously presented by KILLIAN and co-workers.[66,72] The secondary structure of the peptides reconstituted into unilamellar vesicles was determined to be an α-helix at 25 °C and 60 °C by means of CD spectroscopy. KALP **17** was analysed by fluorescence spectroscopy detecting the intrinsic 7-AI fluorescence.[66] The results clearly demonstrate the dependence of KALP **17** on its local environment and they present a suitable application of the new 7-azaindole building block **11** in the field of peptide research as it can be used to verify a successful incorporation of a transmembrane peptide (Figure 47).

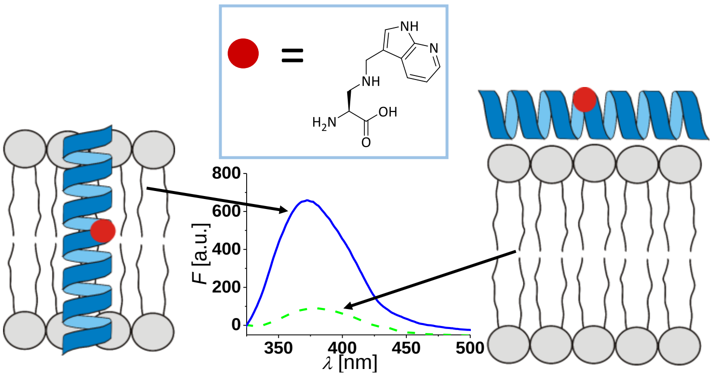

Figure 47: Schematic view of KALP 17 within the lipid bilayer (left) and outside the lipid bilayer (right).

Even though no tautomeric fluorescence band was measureable an association of the 7-AI building block **11** inside lipid bilayers cannot be completely excluded and hence, FRET measurements in collaboration with C. STEINEM were performed to investigate a possible association state inside the lipid membrane. Therefore, two fluorophores (NBD, TAMRA) were covalently attached to the side chain of the KALPs. The results show that peptides without recognition unit already assemble into dimers. Due to a negative hydrophobic mismatch lysine flanked peptides are known to dimerise to compensate this mismatch.[67] Peptides with recognition unit tend to form more complex oligomers than the presented dimers of peptides without recognition unit indicating an association of the 7-azaindole building block **11** inside the peptides. With increased temperature peptides with recognition unit dissociate into dimers. As no tautomeric fluorescence band was detected during fluorescence spectroscopy of KALP **17**, it can be assumed that the observed association could be due to π-stacking of the aromatic system of the 7-AI building block **11**. Unfortunately, it cannot be verified what kind of association occurs. In addition, it also cannot be excluded that the negative hydrophobic mismatch as well as the 7-AI building block **11** itself can have any impact on the results of the FRET experiments. Thus, the design of the 7-AI building block **11** should be reconsidered as it might not be flexible enough for a dimerisation process. Broadening the field of interest to β-peptides it seems to be beneficial to choose a different transmembrane model system. Therefore, the synthesis of D-β^3-7-azaindole building block **24** is presented, which in the future can be integrated into transmembrane β-peptides.

As previously mentioned, transmembrane model systems have been used in many different ways to analyse basic principles of protein-lipid and protein-protein interactions. However, the influences on transmembrane β-peptide helices, which have the advantage of high structural stability and are not easily degraded, are still widely unexplored. Thus, a suitable model system would decisively advance β-peptide research.[9,21]

In the second part of the presented thesis, artificial transmembrane β-peptides were introduced, which might be a suitable model transmembrane domain system. In order to establish these transmembrane β-peptides as model system structural parameters such as conformation, orientation and penetration depth of the β-peptide helices were investigated within an appropriate membrane environment by X-ray diffraction studies. Therefore, a novel heavy-atom labelled D-β^3-amino acid residue was synthesised and incorporated into different transmembrane β-peptides to increase the difference of electron density profiles in lipid membranes. Six different transmembrane β-peptides were designed, one set without ^{h}Trp and another set with ^{h}Trp to investigate if ^{h}Trp could enhance the anchoring effect of ^{h}Lys. CD spectroscopic measurements of all β-peptides reconstituted into unilamellar vesicles (DOPC) show a characteristic pattern indicative of a 3_{14}-helical secondary structure.

Further X-ray diffraction studies and X-ray grazing incidence diffraction (GID) analysis performed by Y. XU from the SALDITT research group provide information about β-peptide`s properties in model lipid multilayer. Results demonstrate that all β-peptides are inserted into the model membrane stacks and form helical transmembrane domains with the central D-β^3-amino acid residue placed at the bilayer midplane. Hence, the β-peptides position themselves in the bilayer midplane. As the hydrophobic part of the β-peptides is slightly longer than the one of the lipids, both have to adjust their hydrophobic part to attain a match, which can be reached by β-peptides tilting with an estimated tilt angle of 16° (Figure 48).[69]

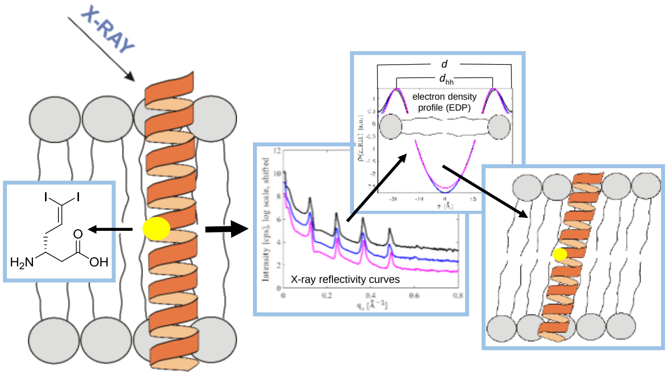

Figure 48: Overview of the results of the X-ray diffraction studies on β-peptides using 6,6-diiodo-allylhomoglycine as the recognition unit.[22]

Consequently, a membrane thinning effect and a perturbation of the acyl chain packing did occur, which were further confirmed by X-ray GID analysis for the β-peptides without ^{h}Trp. The β-peptides with ^{h}Trp anchor can partially suppress this elastic response and stabilise the vertical insertion of the β-peptides. Hence, the β-peptide H-^{h}Lys$_2$-^{h}Trp$_2$-^{h}Val$_{19}$-^{h}Trp$_2$-^{h}Lys$_2$-NH$_2$ (**47**) seems to be a suitable model transmembrane domain system for further investigations in the field of β-peptides (Figure 49).

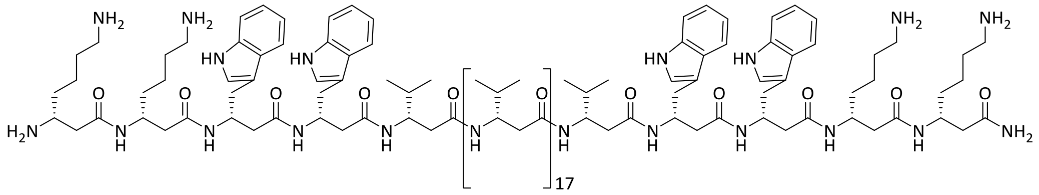

47

Figure 49: Structure of the designed and synthesized model transmembrane β-peptide (47).

This model transmembrane β-peptide (**47**) was then used to analyse the organisation and assembly of transmembrane β-peptide helices in membrane environment utilizing D-β^3-gluatmine as the association unit. Therefore, several β-peptides harbouring different numbers of D-β^3-glutamine residues (^{h}Gln) were designed and synthesised using Fmoc-SPPS. Three sets of transmembrane β-peptides were preserved for analysing β-peptide helix association: *i*) with zero ^{h}Gln, *ii*) with two ^{h}Gln and *iii*) with three ^{h}Gln as recognition units. D-β^{3}-Glutamine residues were used as specific recognition units to reveal the impact of hydrogen bond formation within the membrane on the recognition and assembly processes. The secondary structure of the β-peptides reconstituted into unilamellar vesicles (LUVs, DOPC) was analysed to be similar to a right-handed 3_{14}-helix, which is almost unaffected by an increase in temperature and hence, no unfolding does appear. The association state of the β-peptides as a function of the number of D-β^{3}-glutamine residues became accessible by FRET measurements in collaboration with C. STEINEM. Therefore, the fluorophores NBD and TAMRA were covalently attached to the side chain of the transmembrane β-peptide helices. The results clearly show that the β-peptides with ^{h}Gln as recognition units associated into oligomers, likely trimers, whereas the β-peptides without recognition unit were monomeric. Furthermore, temperature-dependent FRET analysis were performed to study the influence of hydrogen bond formation on the association properties more precisely, because hydrogen bonds become weaker at higher temperatures.[99,100] Indeed, an increase in temperature influence the aggregation state of both β-peptide species. The β-peptides with two ^{h}Gln residues seem to be monomeric at higher temperature, whereas the β-peptides with three ^{h}Gln residues do not fully dissociate into monomers due to a higher number of hydrogen bonds in the aggregates. In addition, the association state is not concentration-dependent, which leads to the assumption that the hydrogen bond formations are very stable. Hence, it has been shown that the strength of the β-peptide helix-helix association depends on the number of ^{h}Gln residues in the helix and that it is possible to adjust the aggregation state (monomeric or oligomeric, Figure 50).

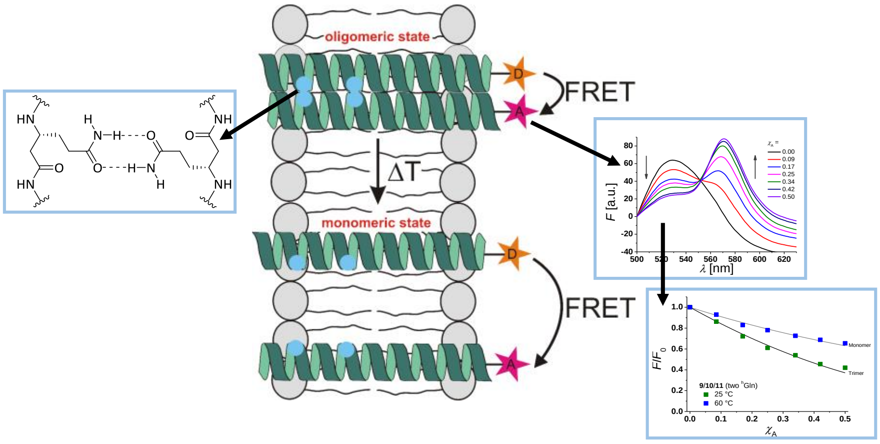

Figure 50: Overview of the results of the association studies using D-β^{3}-glutamine as the recognition unit inside β-peptides.

Combining the results, a novel transmembrane β-peptide (**47**) has been developed, that can function as transmembrane model system. This model system is inserted into lipid bilayers in a transmembrane fashion with the central amino acids located at the bilayer midplane.[22] D-β^3-Glutamine-mediated association of these transmembrane β-peptides was successfully performed and controlled by temperature and number of ^{h}Gln residues. Due to the well-defined 3_{14}-helix in which every third amino acid residue is located on the same face of the helix, a specific labelling of the transmembrane β-peptide (**47**) renders it possible to precisely position different recognition units like the D-β^3-7-azaindole building block **24**. Hence, it seems to be feasible to control the aggregation state and the strength of the interactions between transmembrane β-peptides, which will open up new opportunities to rationally design various peptide assemblies with different functionalities.

EXPERIMENTAL PART

6.1 General

Solvents

Dry solvents like DMF, THF, DCM and MeOH were purchased from ACROS ORGANICS (Geel, Belgium) and SIGMA-ALDRICH (Taufkirchen, Germany) and stored over molecular sieves (4 Å). Technical solvents were purified prior to use. Solvents of analytical or HPLC grade were used as supplied from FLUKA (Taufkirchen, Germany), VWR INTERNATIONAL (Fontenay-sous-Bois, France), ACROS ORGANICS (Geel, Belgium) and SIGMA-ALDRICH (Taufkirchen, Germany). Ultra-pure water was obtained by using the water purification unit SIMPLICITY (MILLIPORE, Bredford, UK).

Reagents

All reagents were of highest grade available and used as supplied. All amino acid derivatives as well as coupling reagents and the resin for solid phase peptide synthesis were obtained from NOVABIOCHEM (Darmstadt, Germany), BACHEM (Bubendorf, Switzerland), GL BIOCHEM (Shanghai, China), IRIS BIOTECH (Marktredwitz, Germany) and VWR INTERNATIONAL (Fontenay-sous-Bois, France). All other chemicals were purchased from FLUKA (Taufkirchen, Germany), VWR INTERNATIONAL (Fontenay-sous-Bois, France), ACROS ORGANICS (Geel, Belgium), SIGMA-ALDRICH (Taufkirchen, Germany), ALFAR AESAR (Karlsruhe, Germany), APPLICHEM (Darmstadt, Germany), TCI (Zwijndrecht, Belgium), ABCR (Karlsruhe, Germany), FLUOROCHEM (Hadfield, UK), CARL ROTH GMBH (Karlsruhe, Germany), GRÜSSING GMBH (Filsum, Germany), MERCK (Darmstadt, Germany) and RIEDEL-DE HAËN (Seelze, Germany). Lipids were purchased from AVANTI POLAR LIPIDS (Alabama, USA).

Reaction

Air and/or water sensitive reactions were carried out under argon atmosphere using standard SCHLENK-technique. The glass apparatus was heated with a heat gun under reduced pressure and flushed with argon (3 x).

Freeze-drying

Freeze-drying (lyophilisation) of building blocks and peptides from aqueous solutions and mixtures containing minor amounts of acetonitrile or dioxane was performed using Christ Alpha-2-4 lyophilizer (Osterode am Harz, Germany) equipped with a high-vacuum pump. For small amounts, an evacuable Christ RVC 2-18 CD plus or Christ RVC 2-18 centrifuge, that was connected to the lyophilisation device, was applied.

Thin layer chromatography (TLC)

Analytical TLC was carried out using Merck (Darmstadt, Germany) coated aluminium sheets of silica gel 60 F_{254} (layer thickness 0.25 mm). Substances were visualized under UV fluorescence at 254 nm and/or by treatment with ninhydrin (3% in EtOH) followed by heating to detect amines.

Flash column chromatography

Flash column chromatography was performed using Merck (Darmstadt, Germany) silica gel 60 F_{254} (40-63 µm) at 0.5-1.0 bar. Columns were packed with wet silica gel (50-100-fold weight excess) and the sample was loaded onto silica gel or as a concentrated solution.

High performance liquid chromatography (HPLC)

Reversed phase (RP)-HPLC analyses were performed using a system (Äkta Basic 900, pump type P 900, variable wavelength detector UV-900) from Amersham Pharmacia Biotech (Freiburg, Germany). The UV-absorption was detected at 215 nm, 254 nm and 280 nm for non-labelled peptides. If the derivatives were labelled with NBD or TAMRA, the UV-absorptions were recorded at 464 nm or 540 nm instead of the detection at 254 nm. Following C-18 columns were utilized using a linear gradient of A (water + 0.1% TFA) to B (MeOH + 0.1% TFA):

Analytical: MN Nucleodur® 100-5-C18, 250 mm × 4.6 mm, 5 µm, flow rate: 1 mL/min.
Semi-preparative: MN Nucleodur® 100-5-C18, 250 mm × 10 mm, 5 µm, flow rate: 3 mL/min.
Preparative: MN Nucleodur® 100-5-C18, 250 mm × 21 mm, 5 µm, flow rate: 10 mL/min.

6.2 Characterisation

Nuclear magnetic resonance spectroscopy (NMR)

NMR spectra were recorded on a VARIAN spectrometer (Unity 300, Mercury-Vx 300, VNMRS-300 and Inova 500). The sample temperature was 308.1 K ([D6]-DMSO) or ambient temperature (CD_3OD). The chemical shifts (δ) were denoted in parts per million (ppm) downfield of TMS. As internal standards the resonances of the residual protons of the deuterated solvents were used. Following abbreviations for the multiplets are used: s (singlet), d (doublet), t (triplet), q (quartet), m (multiplet), br (broad). Coupling constants are $^{n}J_{X,Y}$ in Hertz (Hz) where n is the order of coupling and X and Y the coupling partners.

Mass spectrometry

Electrospray-ionisation (ESI) and high resolution ESI (HR-MS (ESI)) spectra were obtained with BRUKER devices (maXis or MicrOTOF).

Circular dichroism spectroscopy (CD)

CD spectroscopy was performed on a JASCO-810 spectropolarimeter (Groß-Umstadt, Germany) equipped with a JASCO PTC-423S temperature control or on a JASCO-1500 spectropolarimeter (Groß-Umstadt, Germany) equipped with a JULABO F250 (Seelbach, Germany) temperature control. The sample cell was flushed with nitrogen and a quartz glass precision cell Suprasil® (type: 110-QS, 1 mm) was used. The spectra were recorded at 20 °C or 30 °C in a wavelength range of 260-180 nm with 1.0 nm bandwidth, using the ´continuous mode´, a data pitch of 1.0 nm, a response time of 1.0 s, a scanning speed of 20 nm/min and an average of five spectra. The spectra were background-corrected against pure vesicle suspension without incorporated peptides, smoothed (SAVITZKY-GOLAY) and expressed as molar ellipticity θ ($\mathrm{deg} \cdot \mathrm{cm}^2 \cdot \mathrm{dmol}^{-1}$) according to GREENFIELD, with the following equation:[191]

$$\theta\ \left[\mathrm{deg{\cdot}cm^2{\cdot}dmol^{-1}}\right] = \frac{\mathrm{CD}}{c \cdot d \cdot N_{AA}} \qquad (5.1)$$

CD: ellipticity [mdeg]

c: concentration of the peptide [$\mathrm{mol{\cdot}L^{-1}}$]

d: length of the cuvette [mm]

N_{AA}: number of residues

UV/Vis spectroscopy

UV spectra for estimation of occupancy or peptide concentration were measured using the JASCO UV/Vis spectrophotometer V550 or the THERMO SCIENTIFIC nanodrop ND-2000c spectrophotometer. Peptide concentration was calculated by using LAMBERT-BEER's law (for extinction coefficients see Table 6). The molecular absorption coefficients were calculated by summation of the single coefficients at a set wavelength. For labelled molecules the absorption was measured for the maximum absorption of the labels (NBD, TAMRA).

Table 6: Extinction coefficients for tryptophan (Trp), 7-azatryptophan, NBD and TAMRA.[35,87,192]

	Absorption Maximum [nm]	Extinction Coefficient [$cm^{-1}M^{-1}$]
Tryptophan	280	5690
7-Azatryptophan	288	6200
NBD	466	22000
TAMRA	565	91000

Fluorescence spectroscopy

Fluorescence spectra were measured at a Jasco FP 6200 (Groß-Umstadt, Germany) under temperature control using a JASCO thermostat (model ETC-272T, Groß-Umstadt, Germany).

For analysing of the tryptophan fluorescence emission excitation was performed at 280 nm and the fluorescence emission was detected between 290-420 nm using a micro quartz glass precision cell Suprasil® (type: 115F-QS, 10 mm). The excitation- and emission-bandwidths were set to 5.0 nm, the data pitch was 1.0 nm, the response was ˈfastˈ, the sensitivity was ˈhighˈ and the scanning speed was set to 125 nm/min.

In case of the concentration-dependent FRET analysis, the concentration of the respective NBD-labelled peptide (6.0 µM) as well as the total peptide concentration (12 µM) were kept constant using the corresponding non-labelled peptide and the mole fraction (χ_A) of the respective TAMRA-labelled peptide was varied from 0.0-0.5. The fluorescence emission was detected between 500-650 nm at 25 °C and 60 °C (β-peptides) or at 30 °C (α-peptides) for the whole sample set using a micro quartz glass precision cell Suprasil® (type: 115F-QS, 10 mm) and the fluorescence emission excitation was performed at 464 nm. The excitation- and emission-bandwidth was set to 5.0 nm, the data pitch was 1.0 nm, the response was ˈfastˈ, the sensitivity was ˈhighˈ or ˈmediumˈ and the scanning speed was set to 125 nm/min.

6.3 Standard Operating Procedures (SOPs)

6.3.1 SOPs for the Syntheses of the β^3-Amino Acids

6.3.1.1 SOP1: Synthesis of the diazo ketone[103,104]

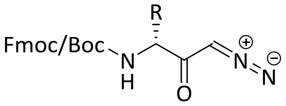

According to the procedure of GUICHARD *et al.*, the *N*-Boc/Fmoc-protected amino acid (12.4 mmol, 1.00 eq) was dissolved in dry THF (58 mL) under an argon atmosphere and cooled to 0 °C, followed by addition of triethylamine (1.10 eq) and isobutylchloroformate (1.10 eq). After stirring at 0 °C for 30 min, under exclusion of light diazomethane in diethyl ether (0.6-0.7 M, 2.00 eq) was added to the solution and the mixture was stirred at rt for 5 h. Afterwards, the excess of diazomethane was quenched by addition of glacial acetic acid (1.4 mL) and the mixture was taken up in 6% $NaHCO_3$ (aq, 100 mL) and extracted with EtOAc (3 × 100 mL). The combined organic phases were washed with saturated NH_4Cl (aq, 3 × 60 mL), saturated NaCl (aq, 3 × 60 mL), dried over $MgSO_4$ and the solvent was removed under reduced pressure. The product (yellow oil/solid) was obtained in quantitative yield and used without further purification.

6.3.1.2 SOP2: Synthesis of the D-β^3-amino acid

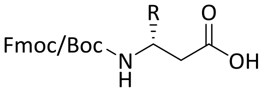

SOP2.1[103,104]

Based on a procedure of GUICHARD *et al.*, the diazo ketone (12.4 mmol, 1.00 eq) was dissolved in THF/H_2O (9:1, *v*/*v*, 75 mL) and under exclusion of light silver benzoate (0.10 eq) was added. The reaction was carried out by sonication for 2 h. Afterwards, the mixture was diluted with H_2O (50 mL), adjusted to pH = 2-3 with 1.0 M HCl (aq) and extracted with EtOAc (3 × 100 mL). The combined organic phases were dried over $MgSO_4$ and the solvent was removed under reduced pressure. The crude product was taken up in DCM and added dropwise to cold pentane (-22 °C). The obtained precipitate was filtered off, washed with cold pentane (2 ×) and dried overnight under reduced pressure.

SOP2.2[122]

Based on a procedure of PATIL *et al.*, silver benzoate was added (0.10 eq) to a solution of the diazo ketone (14.7 mmol, 1.00 eq) in 1,4-dioxane/H_2O (2:1, *v*/*v*, 150 mL) and the reaction was performed under microwave irradiation in a domestic microwave oven (55 s, 460 W). The solvent was removed under reduced pressure, the resulting residue was diluted with H_2O (50 mL), adjusted to pH = 2-3 with 1.0 M HCl (aq) and extracted with EtOAc (3 × 100 mL). The combined organic phases were dried over $MgSO_4$ and the solvent was removed under reduced pressure. The crude product was taken up in DCM and added dropwise to cold pentane (-22 °C). The obtained precipitate was filtered off, washed with cold pentane (2 ×) and dried overnight under reduced pressure.

6.3.2 SOPs for the Syntheses of α- and β-Peptides

6.3.2.1 SOP3: Loading resin with first amino acid[193]

The rink amide MBHA resin (132 mg, 75.0 µmol, 1.00 eq) was swollen in a PE-frit equipped BECTON-DICKINSON (BD) discardit II syringe (Heidelberg, Germany) in DMF (2.0 mL) for 2 h. The Fmoc-protecting group was cleaved microwave assisted (25 W, 50 °C, 30 s) using piperidine in DMF (20%, 1.5 mL). Afterwards, the resin was washed with DMF (10 × 2.0 mL) and the second cleavage (20% piperidine in DMF) was performed under microwave irradiation (35 W, 60 °C, 3.0 min). After washing with DMF (10 × 2.0 mL), the required amino acid building block (5.00 eq) and HOBt (5.00 eq) were dissolved in DMF (1.5 mL). After addition of DIC (5.00 eq) the coupling was achieved microwave assisted (35 W, 65 °C, 15 min). The resin was washed with DMF (10 × 2.0 mL), MeOH (10 × 2.0 mL) and DCM (5 × 2.0 mL) and dried under reduced pressure overnight. The estimation of the level of the first residue attachment was performed using SOP4. After resin loading the remaining free amine functions were capped applying DMF/Ac_2O/DIPEA (18:1:1, *v*/*v*/*v*) for 10 min at room temperature, followed by washing with DMF (10 × 2.0 mL), MeOH (10 × 2.0 mL) and DCM (5 × 2.0 mL) and drying under reduced pressure overnight.

6.3.2.2 SOP4: Determination of the occupancy[194]

According to the procedure of GUDE *et al.*, estimation of the occupancy of the first residue attachment was performed via UV-absorption spectroscopy. Therefore, a small amount of resin (5.0-10 mg) was placed in a graduated flask (10 mL) and DBU (2 % in DMF, 2.0 mL) was added. After gentle agitation for 1 h, the solution was diluted with MeCN (to 10 mL). The reaction mixture was further diluted with MeCN (1/12.5) and transferred to an UV precision cuvette. The absorption of the cleaved Fmoc-dibenzofulven species was detected at 304 nm (ε_{304} = 7624 L · mol^{-1} · cm^{-1}) and corrected by the reference. The reference solution was prepared in the same manner but without addition of the resin. Fmoc loading was calculated using following equation.

$$\rho_{\text{resin}}\left[\frac{\text{mmol}}{\text{g}}\right] = \frac{1}{m_{\text{resin}}\ [\text{g}]} \cdot \left(\frac{\Delta abs \cdot V[\text{L}] \cdot f}{\varepsilon[\text{L mol}^{-1}\ \text{cm}^{-1}] \cdot d[\text{cm}]} \cdot 10^6\right) \qquad (5.2)$$

Thereby, ρ_{resin} is the loading density of the resin, Δabs = (abs_{sample}-abs_{ref}), V the volume of the graduated flask (here 0.01 L), f the thinning factor (here f = 12.5), ε the absorption coefficient of dibenzofulven, d the path length of the cuvette (here 1.0 cm) and m_{resin} the mass of the analysed resin. Thus, following equation is given.

$$\rho_{\text{resin}}\left[\frac{\text{mmol}}{\text{g}}\right] = \frac{\Delta abs \cdot 16.4}{m_{\text{resin}}[\text{mg}]} \qquad (5.3)$$

6.3.2.3 SOP5: KAISER-Test[195]

For checking the completeness of amino acid coupling or successful deprotection during SPPS, the KAISER-test was performed. Based on a procedure of KAISER *et al.*, a small amount of resin was placed in a glass tube and 2-3 drops of each of the three reagents were added. The tube was kept on a heating plate at 100 °C for 3.0 min with occasional swirling. Upon observation the solution could remain yellow (negative test), indicating a complete reaction or could turn into deep blue (positive test), which indicates an incomplete reaction (free amino groups). In utilizing the reagent following three solutions were prepared:

KAISER-test reagent 1:	1.0 g Ninhydrin in 20 mL ethanol.
KAISER-test reagent 2:	16 mg Phenol in 4 mL ethanol.
KAISER-test reagent 3:	0.5 mL Solution of KCN (1mM) diluted to 25 mL with pyridine.

6.3.2.4 SOP6: Automated SPPS

General automated SPPS was realized with different peptide synthesizers. Firstly, the LIBERTY™ automated synthesizer from CEM (Kamp-Lintfort, Germany), equipped with a DISCOVER microwave (MW) reaction cavity (CEM) was used for automated peptides synthesis. The resin was swollen in DMF for 2 h prior usage. The standard Fmoc-protocol was selected using 0.10-SCALE and NMP was used as solvent. The Fmoc-protecting group was removed by treatment with piperidine (20% in NMP, *v*/*v*, 2 × 2.5 mL; D1: 25 W, 50 °C, 30 s; D2: 35 W, 50 °C, 3 min). Fmoc-protected amino acids and Fmoc-protected building blocks were used as a 0.2 M solution in NMP, activated by HBTU/HOBt in NMP (0.49 M/0.5 M) and DIPEA in NMP (2.0 M) and double coupling was conducted microwave assisted (35 W, 55 °C, 7 min). Alternatively, the LIBERTY BLUE™ automated synthesizer from CEM

(Kamp-Lintfort, Germany), equipped with a DISCOVER microwave (MW) reaction cavity (CEM) was used for automated peptides synthesis. Here, the standard Fmoc-protocol was selected using 0.10-SCALE too, but DMF was used as solvent. The Fmoc-protecting group was removed by treatment with piperidine (20% in DMF, *v/v*; 155 W, 75 °C, 15 s → 30 W, 90 °C, 50 s). Fmoc-protected amino acids and Fmoc-protected building blocks were used as a 0.2 M solution in DMF, activated by DIC in DMF (0.5 M) and Oxyma® in DMF (1.0 M) and single coupling was conducted microwave assisted (170 W, 90 °C, 15 s → 30 W, 90 °C, 110 s). After the peptide synthesis was completed, the resin was transferred into a PE-frit equipped BECTON-DICKINSON (BD) discardit II syringe (Heidelberg, Germany), washed with DMF (10 x 5.0 mL), MeOH (10 x 5.0 mL) and DCM (10 x 5.0 mL) and dried under reduced pressure.

6.3.2.5 SOP7: Manual SPPS[104,196]

General manual SPPS was carried out in a PE-frit equipped BECTON-DICKINSON (BD) discardit II syringe (Heidelberg, Germany) in a 75.0 µmol scale using a DISCOVER microwave (MW) reaction cavity (CEM) (Kamp-Lintfort, Germany). The pre-loaded resin was initially swollen in DMF for 2 h. The Fmoc-protecting group was cleaved microwave assisted (25 W, 50 °C, 30 s) using piperidine in DMF (20%, 1.5 mL). Afterwards, the resin was washed with DMF (10 × 2.0 mL) and the second cleavage (20% piperidine in DMF) was performed (35 W, 60 °C, 3 min). After washing with DMF (10 × 2.0 mL), the required amino acid building block in DMF (0.2 M, 0.5 mL) was activated with HATU/HOAt in DMF (0.46 M/0.5 M, 0.5 mL) and DIPEA in NMP (2.0 M, 0.25 mL) and single coupling was performed (35 W, 65 °C, 15 min) followed by washing with DMF (10 × 2.0 mL). If mentioned, the coupling was repeated or the free amino groups were capped with Ac_2O (10% in DMF, 1.5 mL). After completion of the peptide sequence the final wash was performed with DMF (10 x 2.0 mL), MeOH (10 x 2.0 mL) and DCM (10 x 2.0 mL) and the resin was dried under reduced pressure.

6.3.2.6 SOP8: Alloc-Deprotection[197]

Based on a procedure of WU *et al.*, under an argon atmosphere $Me_2NH{\cdot}BH_3$ (180 mg, 3.00 mmol, 40.0 eq) and $Pd(PPh_3)_4$ (8.63 mg, 7.50 µmol, 0.10 eq) were added to the resin (75.0 µmol, 1.00 eq) in dry DMF (3.0 mL) and argon was bubbled through the mixture for 4 h. Afterwards, the mixture was transferred to a PE-frit equipped BECTON-DICKINSON (BD) discardit II syringe (Heidelberg, Germany) and washed with DMF (10 × 2.0 mL), MeOH (10 × 2.0 mL) and DCM (5 × 2.0 mL).

6.3.2.7 SOP9: Cleavage[193,198,199]

Cleavage from the dry resin and simultaneous removal of the protecting groups was performed in a PE-frit equipped BECTON-DICKINSON (BD) discardit II syringe (Heidelberg, Germany) using

TFA/H_2O/Tis (95/2.5/2.5, *v*/*v*/*v*) under vigorous shaking for 2 h. The reaction mixture was concentrated under a nitrogen stream and the crude peptide was precipitated from -20 °C cold diethyl ether. The crude product was isolated by centrifugation (9000 rpm, 20 min, -15 °C), washed five times with cold diethyl ether followed by centrifugation and drying under reduced pressure overnight.

6.3.3 SOPs for the Preparation of Peptide/Lipid Complexes

6.3.3.1 SOP10: Small unilamellar vesicles (SUVs)[66]

According to the procedure of DE PLANQUE *et al.*, lipids dissolved in $CHCl_3$ and alcoholic stock solutions (MeOH) were mixed yielding a solution of $CHCl_3$/MeOH (1/1, *v*/*v*) at defined P/L-ratio. Removing the solvent at a nitrogen stream produced an almost clear peptide/lipid film at the test tube walls. After adding TFE for providing the formation of the secondary structure, the solvent was removed at a nitrogen stream and the resulting peptide/lipid film was dried under reduced pressure at 40 °C overnight. Afterwards, the peptide/lipid film was hydrated in buffer (100 mM NaCl, 25 mM TRIS®, pH 7.1) yielding the desired peptide concentration. After 2 h incubation at 40 °C the hydrated peptide/lipid film was vortexed (30 s) and incubated (5.0 min) in five cycles. The sample was then sonicated for 20 min at 48 W, using a BANDELIN Sonoplus UW 2070 (Berlin, Germany) sonicator.

6.3.3.2 SOP11: Large unilamellar vesicles (LUVs)[200]

According to the procedure of MACDONALD *et al.*, lipids dissolved in $CHCl_3$ and alcoholic stock solutions (MeOH) of the peptides were mixed yielding a solution of $CHCl_3$/MeOH (1/1, *v*/*v*) at defined P/L-ratio. Removing the solvent at a nitrogen stream produced an almost clear peptide/lipid film at the test tube walls. After adding TFE for providing the formation of the secondary structure, the solvent was removed at a nitrogen stream and the resulting peptide/lipid film was dried under reduced pressure at 40 °C overnight. Afterwards, the peptide/lipid film was hydrated in ultra-pure water or in buffer (100 mM NaCl, 25 mM TRIS®, pH 7.1) yielding the desired peptide concentration. After 2 h incubation at 40 °C the hydrated peptide/lipid film was vortexed (30 s) and incubated (5 min) in five cycles. The milky suspension was extruded 31 times through a polycarbonate membrane (100 nm nominal pore size) using an AVESATIN Liposofast mini extruder (Ottawa, Canada) to produce a clear vesicle suspension containing vesicles of 100 nm size providing a rather small polydiversity.

6.3.4 SOP12: Enantiomeric purity (MARFEY's reagent)[124–127]

The corresponding β^3-amino acid was treated with piperidine (20% in DMF, 5.0 mL) and stirred at rt for 15 min. After removal of the solvent under reduced pressure the residue was taken up in diethyl ether and the solid was isolated by centrifugation (9000 rpm, 10 min, 25 °C), washed five times with diethyl ether followed by centrifugation and drying under reduced pressure. According to the procedures of MAFREY *et al.* and BHUSHAN *et al.*, the resulting solid was diluted in acetone/H_2O (1/1, *v*/*v*, 400 µL). 100 µL of this mixture and 0.5 M Na_2CO_3 (aq, 40.0 µL) were added to a solution of MARFEY's reagent (**37**) in acetone (1.1 mM, 200 µL). The mixture was shaken for 1 h at 40 °C. Afterwards, it was cooled to 2 °C, 1.0 M HCl (aq, 20.0 µL) was added and the sample was centrifuged (15000 rpm, 5.0 min, 25 °C).

6.4 Syntheses

6.4.1 Synthesis of 1-Methyl-7-azaindole

1-Methyl-7-azaindole (10)[51]

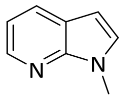

$C_8H_8N_2$
132.17 g/mol

10

According to the procedure of KRITSANIDA *et al.*, under an argon atmosphere 7-azaindole (**5**) (580 mg, 4.91 mmol, 1.00 eq) was dissolved in dry DMF (17 mL) and NaH (289 mg, 12.0 mmol, 2.44 eq) was added. After stirring at rt for 30 min, MeI (361 µL, 5.80 mmol, 1.18 eq) in dry DMF (3.0 mL) was added and it was allowed to stir at rt overnight. H_2O (35 mL) was added and the mixtures was extracted with DCM (3 × 50 mL). The combined organic phases were back extracted with H_2O (2 × 30 mL), dried over Na_2SO_4 and the solvent was removed under reduced pressure. The crude product was purified by flash column chromatography (DCM) to yield product **10** (328 mg, 2.48 mmol, 51%) as a yellow oil.

^{1}H-NMR (300 MHz, [D6]DMSO): δ (ppm) = 3.89 (s, 3 H, CH_3), 6.45 (d, 1 H, $^3J_{H,H}$ = 3.5 Hz, CH_{ar}), 7.05 (dd, 1 H, $^3J_{H,H}$ = 7.8, 4.7 Hz, CH_{ar}), 7.17 (d, 1 H, $^3J_{H,H}$ = 3.4 Hz, CH_{ar}), 7.90 (dd, 1 H, $^3J_{H,H}$ = 7.8 Hz, $^4J_{H,H}$ = 1.6 Hz, CH_{ar}), 8.34 (dd, 1 H, $^3J_{H,H}$ = 4.7 Hz, $^4J_{H,H}$ = 1.6 Hz, CH_{ar}).
ESI-MS (*m/z*): 133.1 $[M+H]^+$.
HR-MS (ESI): calc. for $[C_8H_9N_2]^+$ ($[M+H]^+$): 133.0760, found: 133.0764.

6.4.2 Synthesis of the 7-Azaindole Building Block

7-Azaindole-3-carboxaldehyde (12)[61]

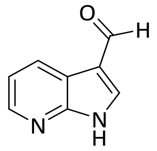

$C_8H_6N_2O$
146.15 g/mol

12

According to the procedure of SU *et al.*, hexamethylenetetramine (2.73 g, 18.7 mmol, 1.10 eq) was added to a solution of 7-azaindole (**5**) (2.00 g, 16.9 mmol, 1.00 eq) in H_2O/AcOH (2:1, *v*/*v*, 16.8 mL). The reaction mixture was stirred under reflux for 6 h. After cooling to 0 °C the resulting precipitate was filtered off and washed with cold H_2O (3 × 20 mL). The crude product was recrystallized from H_2O and dried under reduced pressure to yield product **12** (1.65 g, 11.3 mmol, 67%) as colourless needles.

^{1}H-NMR (300 MHz, [D6]DMSO): δ (ppm) = 7.20-7.30 (m, 1 H, CH_{ar}), 8.32-8.47 (m, 3 H, 3 × CH_{ar}), 9.93 (s, 1 H, CHO), 12.6 (s_{br}, 1 H, NH).
ESI-MS (*m*/*z*): 147.1 $[M+H]^+$, 145.0 $[M-H]^-$.
HR-MS (ESI): calc. for $[C_8H_7N_2O]^+$ ($[M+H]^+$): 147.0553, found: 147.0550; calc. for $[C_8H_5N_2O]^-$ ($[M-H]^-$): 145.0407, found: 145.0407.

1-*tert*-Butoxycarbonyl-7-azaindole-3-carboxaldehyde (13)[62]

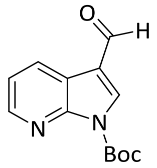

$C_{13}H_{14}N_2O_3$
246.27 g/mol

13

According to the procedure of SALMAN *et al.*, under an argon atmosphere 7-Azaindole-3-carboxaldehyde (**12**) (500 mg, 3.42 mmol, 1.00 eq) was dissolved in dry MeCN (8.5 mL) and cooled to 0 °C. DMAP (62.7 mg, 513 µmol, 0.15 eq) and Boc_2O (896 mg, 4.10 mmol, 1.20 eq) were added at 0 °C and the reaction mixture was stirred at rt for 4 h. The solvent was removed under reduced pressure and the crude product was purified by flash column chromatography (pentane/EtOAc = 2:1, *v*/*v*) to yield product **13** (764 mg, 3.10 mmol, 91%) as a colourless solid.

^{1}H-NMR (300 MHz, [D6]DMSO): δ (ppm) = 1.64 (s, 9 H, 3 × CH_3), 7.41 (dd, 1 H, $^3J_{H,H}$ = 7.9, 4.8 Hz, CH_{ar}), 8.40-8.52 (m, 2 H, 2 × CH_{ar}), 8.74 (s, 1 H, CH_{ar}), 10.0 (s, 1 H, CHO).
ESI-MS (*m/z*): 269.1 $[M+Na]^+$, 285.1 $[M+K]^+$ 245.1 $[M-H]^-$.
HR-MS (ESI): calc. for $[C_{13}H_{14}N_2O_3Na]^+$ ($[M+Na]^+$): 269.0897, found: 269.0895; calc. for $[C_{13}H_{13}N_2O_3]^-$ ($[M-H]^-$): 245.0932, found: 245.0933.

(*S*)-2-(9-Fluorenylmethyloxycarbonyl)-2,3-diaminopropionic acid (15)[63]

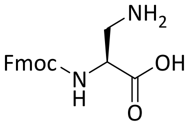

$C_{18}H_{18}N_2O_4$
326.35 g/mol

15

According to the procedure of ZHANG *et al.*, Fmoc-Asn-OH (**14**) (1.00 g, 2.82 mmol, 1.00 eq) was suspended in MeCN/EtOAc/H_2O (2:2:1, *v*/*v*/*v*, 25 mL) and cooled to 0 °C. PIDA (1.09 g, 3.38 mmol, 1.20 eq) was added at 0 °C and the mixture was stirred at 0 °C for 30 min and at rt for 4 h. The resulting precipitate was filtered off, washed with cold EtOAc (3 × 40 mL) and dried under reduced pressure to yield product **15** (603 mg, 1.85 mmol, 66%) as a colourless solid.

^{1}H-NMR (300 MHz, [D6]DMSO): δ (ppm) = 2.76-3.09 (m, 2 H, β-CH_2), 3.68-3.83 (m, 1 H, α-CH), 4.17-4.33 (m, 3 H, Fmoc-CH_2, Fmoc-CH), 6.81 (d, 1 H, $^3J_{H,H}$ = 6.4 Hz, NH), 7.26-7.46 (m, 4 H, 4 × Fmoc-CH_{ar}), 7.69 (d, 2 H, $^3J_{H,H}$ = 7.4 Hz, 2 × Fmoc-CH_{ar}), 7.85-7.89 (m, 2 H, 2 × Fmoc-CH_{ar}).
ESI-MS (*m/z*): 327.1 $[M+H]^+$, 349.1 $[M+Na]^+$, 653.1 $[2M+H]^+$, 675.2 $[2M+Na]^+$, 325.1 $[M-H]^-$, 651.2 $[2M-H]^-$.
HR-MS (ESI): calc. for $[C_{18}H_{19}N_2O_4]^+$ ($[M+H]^+$): 327.1339, found: 327.1337; calc. for $[C_{18}H_{18}N_2O_4Na]^+$ ($[M+Na]^+$): 349.1159, found: 349.1152; calc. for $[C_{18}H_{17}N_2O_4]^+$ ($[M-H]^-$): 325.1194, found: 325.1186.

(*S*)-2-(9-Fluorenylmethyloxycarbonyl)-amino-3-*tert*-butoxycarbonyl-(1'-*tert*-butoxycarbonyl-7'-azaindole)-3'-(methyl)amino-propionoic acid (11)

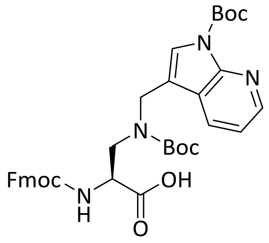

$C_{36}H_{40}N_4O_8$
656.74 g/mol

11

Fmoc-Dap-OH (**15**) (500 mg, 1.53 mmol, 1.00 eq) and 1-*tert*-butoxycarbonyl-7-azaindole-3-carboxaldehyde (**13**) (566 mg, 2.30 mmol, 1.50 eq) were dissolved in dry MeOH (7.20 mL). DIPEA (64.5 µL, 3.83 mmol, 2.50 eq) were added and the mixture was stirred at 50 °C for 4 h. After cooling to 0 °C $NaBH_4$ (116 mg, 3.06 mmol, 2.00 eq) was added in portions. Further stirring rt for 1 h was followed by removing MeOH under reduced pressure. Afterwards, H_2O (7.20 mL) was added and it was extracted with Et_2O (3 × 15.0 mL). The aqueous phase was cooled to 0 °C and Boc_2O (333 mg, 1.53 mmol, 1.00 eq) dissolved in dioxane (4.00 mL) was added and the mixture was allowed to stir at rt overnight. After removing dioxane under reduced pressure, H_2O (10.0 mL) was added and the mixture was adjusted to pH = 2-3 with 1.0 M HCl (aq) and extracted with EtOAc (3 × 50.0 mL). The combined organic phases were dried over $MgSO_4$ and the solvent was removed under reduced pressure. The resulting orange oil was purified by flash column chromatography (EtOAc/MeOH: 4:1, *v*/*v*) to yield product **11** (563 mg, 857 µmol, 56%) as a yellow solid.

^{1}H-NMR (300 MHz, CD_3OD): δ (ppm) = 1.47 (s, 9 H, 3 × CH_3), 1.61 (s, 9 H, 3 × CH_3), 3.60-3.73 (m, 1 H, α-CH), 4.08-4.17 (m, 1 H, β-CH), 4.19-4.32 (m, 2 H, CH_2), 4.40-4.66 (m, 4 H, Fmoc-CH_2, Fmoc-CH, β-CH), 7.18-7.38 (m, 5 H, 4 × Fmoc-CH_{ar}, CH_{ar}), 7.60 (t, 2 H, $^3J_{H,H}$ = 7.1 Hz, 2 × Fmoc-CH_{ar}), 7.67 (s, 1 H, CH_{ar}), 7.74 (d, 2 H, $^3J_{H,H}$ = 7.6 Hz, 2 × Fmoc-CH_{ar}), 7.99-8.10 (m, 1 H, CH_{ar}), 8.31-8.37 (m, 1 H, CH_{ar}).
ESI-MS (*m*/*z*): 657.3 $[M+H]^+$, 679.3 $[M+Na]^+$, 653.1 $[2M+H]^+$, 655.3 $[M-H]^-$, 1311.6 $[2M-H]^-$.
HR-MS (ESI): calc. for $[C_{36}H_{41}N_4O_8]^+$ ($[M+H]^+$): 657.2919, found: 657.2918; calc. for $[C_{36}H_{40}N_4O_8Na]^+$ ($[M+Na]^+$): 679.2738, found: 679.2738; calc. for $[C_{36}H_{39}N_4O_8]^+$ ($[M-H]^-$): 655.2773, found: 655.2774.

6.4.3 Synthesis of the 7-Azaindole D-β³-Building Block

(*R*)-2-(9-Fluorenylmethyloxycarbonyl)-2,3-diamino-propionic acid (26)[63]

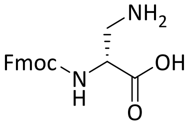

$C_{18}H_{18}N_2O_4$
326.35 g/mol

26

According to the procedure of ZHANG *et al.*, Fmoc-D-Asn-OH (**25**) (1.00 g, 2.82 mmol, 1.00 eq) was suspended in MeCN/EtOAc/H_2O (2:2:1, *v*/*v*/*v*, 25 mL) and cooled to 0 °C. PIDA (1.09 g, 3.38 mmol, 1.20 eq) was added at 0 °C and the mixture was stirred at 0 °C for 30 min and at rt for 4 h. The resulting precipitate was filtered off, washed with cold EtOAc (3 × 40 mL) and dried under reduced pressure to yield product **26** (603 mg, 1.85 mmol, 66%) as a colourless solid.

¹H-NMR (300 MHz, [D6]DMSO): *δ* (ppm) = 2.76-3.09 (m, 2 H, β-CH_2), 3.68-3.83 (m, 1 H, α-CH), 4.17-4.33 (m, 3 H, Fmoc-CH_2, Fmoc-CH), 6.81 (d, 1 H, $^3J_{H,H}$ = 6.4 Hz, NH), 7.26-7.46 (m, 4 H, 4 × Fmoc-CH_{ar}), 7.69 (d, 2 H, $^3J_{H,H}$ = 7.4 Hz, 2 × Fmoc-CH_{ar}), 7.85-7.89 (m, 2 H, 2 × Fmoc-CH_{ar}).
ESI-MS (*m*/*z*): 327.1 $[M+H]^+$, 349.1 $[M+Na]^+$, 653.1 $[2M+H]^+$, 675.2 $[2M+Na]^+$, 325.1 $[M-H]^-$, 651.2 $[2M-H]^-$.
HR-MS (ESI): calc. for $[C_{18}H_{19}N_2O_4]^+$ ($[M+H]^+$): 327.1339, found: 327.1337; calc. for $[C_{18}H_{18}N_2O_4Na]^+$ ($[M+Na]^+$): 349.1159, found: 349.1152; calc. for $[C_{18}H_{17}N_2O_4]^+$ ($[M-H]^-$): 325.1194, found: 325.1186.

(*R*)-2-(9-Fluorenylmethyloxycarbonyl)-amino-3-*tert*-butoxycarbonylamino-propionic acid (27)[102]

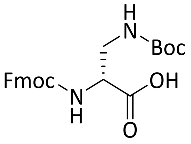

$C_{23}H_{26}N_2O_6$
426.47 g/mol

27

According to the procedure of MYERS *et al.*, Fmoc-D-Dap-OH (**26**) (1.01 g, 3.11 mmol, 1.00 eq) was dissolved in H_2O (20.0 mL) and $NaHCO_3$ (523 mg, 6.22 mmol, 2.00 eq) was added. The reaction mixture was cooled to 0 °C, Boc_2O (813 mg, 3.73 mmol, 1.20 eq) in 1,4-dioxane (9.00 mL) was added dropwise at 0 °C and it was stirred at rt overnight. H_2O (15.0 mL) was then added, the aqueous layer is extracted with EtOAc (2 × 30.0 mL). The combined organic layers are 'back' extracted with saturated $NaHCO_3$ (aq, 3 × 30.0 mL). The combined aqueous layers are adjusted to pH = 2-3 with 1.0 M HCl (aq) and extracted with EtOAc (3 × 50.0 mL). The combined organic phases were dried over $MgSO_4$ and the solvent was removed under reduced pressure to yield product **27** (1.47 g, 3.45 mmol, 92%) as a colourless oil.

^{1}H-NMR (300 MHz, [D6]DMSO): δ (ppm) = 1.38 (s, 9 H, 3 × CH_3), 3.25-3.37 (m, 2 H, β-CH_2), 4.05-4.16 (m, 1 H, α-CH), 4.18-4.35 (m, 3 H, Fmoc-CH_2, Fmoc-CH), 6.78 (m, 1 H, Fmoc-NH), 7.29-7.46 (m, 5 H, 4 × Fmoc-CH_{ar}, Boc-NH), 7.71 (d, 2 H, $^3J_{H,H}$ = 7.4 Hz, 2 × Fmoc-CH_{ar}), 7.83-7.92 (m, 2 H, 2 × Fmoc-CH_{ar}), 12.58 (s_{br}, 1 H, OH).
ESI-MS (*m/z*): 449.2 $[M+Na]^+$, 875.4 $[2M+Na]^+$, 1301.1 $[3M+Na]^+$.
HR-MS (ESI): calc. for $[C_{23}H_{26}N_2O_6Na]^+$ ($[M+Na]^+$): 449.1683, found: 449.1678.

(*S*)-3-(9-Fluorenylmethyloxycarbonyl)-3,4-diamino-butanoic acid (28)

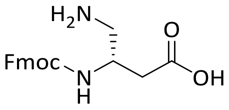

$C_{19}H_{20}N_2O_4$
340.38 g/mol

28

Starting with Fmoc-D-Dap(Boc)-OH (**27**) (2.34 g, 5.28 mmol, 1.00 eq), the synthesis was achieved following SOP1 and SOP2.1 to yield Fmoc-D-β^3-Dap(Boc)-OH as a colourless solid. Afterwards, Fmoc-D-β^3_Dap(Boc)-OH (4.27 mmol, 1.00 eq) was dissolved in dioxane (1.70 mL) and HCl (4 M in dioxane, 5.00 mL) was added. The mixture was stirred for 2 h at rt. The solvent was removed under reduced pressure and the crude product was extracted with Et_2O (3 × 30 mL). Freeze-drying of the aqueous phase has yielded the product **28** (1.22 g, 3.57 mmol, 68%) as a colourless solid.

^{1}H-NMR (300 MHz, [D6]DMSO): δ (ppm) = 2.82-3.05 (m, 2 H, γ-CH_2), 3.25-3.48 (m, 2 H, α-CH_2), 3.95-4.12 (m, 1 H, β-CH), 4.23-4.35 (m, 3 H, Fmoc-CH_2, Fmoc-CH), 7.28-7.52 (m, 5 H, 4 × Fmoc-CH_{ar}, Fmoc-NH), 7.72 (d, 2 H, $^3J_{H,H}$ = 7.3 Hz, 2 × Fmoc-CH_{ar}), 7.87-7.95 (m, 2 H, 2 × Fmoc-CH_{ar}).
ESI-MS (*m/z*): 341.2 $[M+H]^+$, 339.2 $[M-H]^-$, 375.1 $[M+Cl]^-$.
HR-MS (ESI): calc. for $[C_{19}H_{20}N_2O_4]^+$ ($[M+H]^+$): 341.1497, found: 341.1496; calc. for $[C_{19}H_{19}N_2O_4]^-$ ($[M-H]^-$): 339.1350, found: 339.1339.

(*S*)-3-(9-Fluorenylmethyloxycarbonyl)-amino-4-*tert*-butoxycarbonyl-(1'-*tert*-butoxycarbonyl-7'-azaindole)-3'-(methyl)amino-butanoic acid (24)

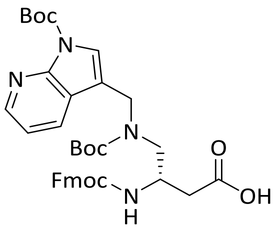

$C_{37}H_{42}N_4O_8$
670.76 g/mol

24

Fmoc-D-β³-Dap-OH (**28**) (200 mg, 589 µmol, 1.00 eq) and 1-*tert*-butoxycarbonyl-7-azaindole-3-carboxaldehyde (**13**) (219 mg, 884 µmol, 1.50 eq) were dissolved in dry MeOH (3.60 mL). DIPEA (37.2 µL, 2.21 mmol, 2.50 eq) was added and the mixture was stirred at 50 °C for 4 h. After cooling to 0 °C $NaBH_4$ (84.7 mg, 2.21 mmol, 2.50 eq) was added in small portions. Further stirring at rt for 1 h was followed by removing MeOH under reduced pressure. Afterwards, H_2O (4.00 mL) was added and it was extracted with Et_2O (3 × 15.0 mL). The aqueous phase was cooled to 0 °C and Boc_2O (128 mg, 589 µmol, 1.00 eq) dissolved in dioxane (1.70 mL) was added and it was allowed to stir at rt overnight. After removing dioxane under reduced pressure, H_2O (5.00 mL) was added and the mixture was adjusted to pH = 2-3 with 1.0 M HCl (aq) and extracted with EtOAc (3 × 50.0 mL). The combined organic phases were dried over $MgSO_4$ and the solvent was removed under reduced pressure. The resulting orange oil was purified by flash column chromatography (100% EtOAc) to yield product **24** (198 mg, 295 µmol, 50%) as a colourless solid.

^{1}H-NMR (300 MHz, [D6]DMSO): *δ* (ppm) = 1.24-1.65 (m, 18 H, 6 × CH_3), 2.37 (t, 2 H, $^3J_{H,H}$ = 6.86 Hz, α-CH_2), 2.95-3.13 (m, 2 H, γ-CH_2), 3.80-3.95 (m, 1 H, β-CH), 4.12-4.33 (m, 5 H, CH_2, Fmoc-CH_2, Fmoc-CH), 6.73-6.82 (m, 1 H, NH), 7.13 (d, 1 H, $^3J_{H,H}$ = 8.35 Hz, CH_{ar}), 7.24-7.45 (m, 6 H, 4 × Fmoc-CH_{ar}, 2 × CH_{ar}), 7.64-7.72 (m, 3 H, 2 × Fmoc-CH_{ar}, CH_{ar}), 7.85-7.90 (m, 2 H, 2 × Fmoc-CH_{ar}), 12.15 (s_{br}, 1 H, OH).

ESI-MS (*m/z*): 671.3 $[M+H]^+$, 693.3 $[M+Na]^+$, 1363.6 $[2M+Na]^+$.

HR-MS (ESI): calc. for $[C_{37}H_{43}N_4O_8]^+$ ($[M+H]^+$): 671.3075, found: 671.3076; calc. for $[C_{37}H_{42}N_4O_8Na]^+$ ($[M+Na]^+$): 693.2895, found: 693.2887.

6.4.4 Synthesis of the Diiodoallylhomoglycine Building Block

(*R*)-3-*tert*-Butoxycarbonylamino-4-carboxy-butanoic benzyl ester (35)

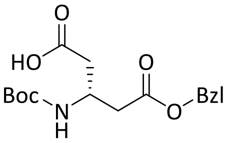

$C_{17}H_{23}NO_6$
337.37 g/mol

35

Starting with Boc-Asp(OBzl)-OH (4.00 g, 12.4 mmol, 1.00 eq), the synthesis was achieved following SOP1 and SOP2.2 to yield product **35** as a colourless solid (3.46 g, 10.3 mmol, 83%).

^{1}H-NMR (300 MHz, [D6]DMSO): δ (ppm) = 1.36 (s, 9 H, 3 × CH_3), 2.41 (dd, 2 H, $^3J_{H,H}$ = 6.8 Hz, $^4J_{H,H}$ = 1.9 Hz, γ-CH_2), 2.54 (dd, 2 H, $^3J_{H,H}$ = 6.8 Hz, $^4J_{H,H}$ = 2.4 Hz, α-CH_2), 4.06-4.20 (m, 1 H, β-CH), 5.07 (s, 2 H, Bzl-CH_2), 6.82 (d, 1 H, $^3J_{H,H}$ = 8.5 Hz, NH), 7.25-7.41 (m, 5 H, 5 × CH_{ar}).
ESI-MS (*m/z*): 338.2 $[M+H]^+$, 360.2 $[M+Na]^+$, 697.3 $[2M+Na]^+$, 336.1 $[M-H]^-$.
HR-MS (ESI): calc. for $[C_{17}H_{24}NO_6]^+$ ($[M+H]^+$): 338.1598, found: 338.1598; calc. for $[C_{17}H_{23}NO_6Na]^+$ ($[M+Na]^+$): 360.1418, found: 360.1421; calc. for $[C_{17}H_{22}NO_6]^+$ ($[M-H]^-$): 336.1453, found: 336.1452.

(*R*)-3-*tert*-Butoxycarbonylamino-5-(methoxy(methyl)amino)-5-oxopentanoic benzyl ester (38)

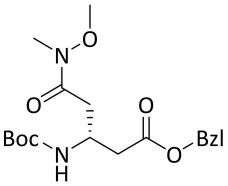

$C_{19}H_{28}N_2O_6$
380.44 g/mol

38

The D-β^3-amino acid **35** (3.34 g, 9.91 mmol, 1.00 eq), *N*,*O*-dimethylhydroxylamine hydrochloride (1.35 g, 13.9 mmol, 1.40 eq) and *N*-ethylmorpholine (8.44 mL, 65.4 mmol, 6.60 eq) were dissolved in dry DCM (15.0 mL), cooled to -10 °C and a propylphosphonic anhydride solution (T3P® 50% in DMF, 9.91 mL, 33.7 mmol, 1.70 eq) was added. The reaction mixture was stirred at -10 °C for 90 min and then at rt for 3 h. The solvent was removed under reduced pressure and the resulting residue was taken up in EtOAc (100 mL). The organic phase was washed with 5% $KHSO_4$ (aq, 3 × 60.0 mL), 2.5% $NaHCO_3$ (aq, 3 × 60.0 mL), saturated NaCl (aq, 3 × 60.0 mL) and water (3 × 60.0 mL) and dried over $MgSO_4$. Removal of the solvent yielded product **38** (3.73 g, 9.80 mmol, 99%) as a yellow oil.

^{1}H-NMR (300 MHz, [D6]DMSO): *δ* (ppm) = 1.36 (s, 9 H, 3 × CH_3), 2.46-2.67 (m, 4 H, α-CH_2, γ-CH_2), 3.06 (s, 3 H, NCH_3), 3.62 (s, 3 H, OCH_3), 4.12-4.25 (m, 1 H, β-CH_2), 5.07 (s, 2 H, Bzl-CH_2), 6.76 (d, 1 H, $^3J_{H,H}$ = 8.5 Hz, NH), 7.26-7.41 (m, 5 H, 5 × CH_{ar}).

ESI-MS (*m/z*): 381.2 $[M+H]^+$, 403.2 $[M+Na]^+$, 403.2 $[M+K]^+$, 783.4 $[2M+Na]^+$.

HR-MS (ESI): calc. for $[C_{19}H_{29}N_2O_6]^+$ ($[M+H]^+$): 381.2020, found: 381.2023; calc. for $[C_{19}H_{28}N_2O_6Na]^+$ ($[M+Na]^+$): 403.1840, found: 403.1843.

(*R*)-3-*tert*-Butoxycarbonylamino-5-oxopentanoic benzyl ester (39)

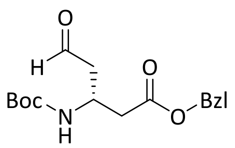

$C_{17}H_{23}NO_5$
321.37 g/mol

39

Fresh diisobutylaluminium hydride (1.00 M in THF, 20.6 mL, 20.7 mmol, 2.30 eq) was added dropwise at -78 °C within 90 min to (*R*)-3-*tert*-butoxycarbonylamino-5-(methoxy(methyl)amino)-5-oxopentanoic benzyl ester (**38**) (3.42 g, 8.99, 1.00 eq) dissolved in dry THF (51.0 mL). After stirring at -78 °C for 3 h a saturated K/Na-tartrate solution (aq, 6.50 mL) was added at this temperature. The reaction mixture was allowed to warm to rt and additional saturated K/Na-tartrate solution (aq, 32.3 mL) was added dropwise. After stirring at rt for 1 h the reaction mixture was extracted with Et_2O (3 × 40.0 mL) and the combined organic phases were dried over $MgSO_4$. The solvent was removed under reduced pressure and the crude product was purified by flash column chromatography (pentane/EtOAc: 3:2→1:1, *v*/*v*) to yield product **39** as a yellow oil (2.42 g, 7.53 mmol, 84%).

^{1}H-NMR (300 MHz, [D6]DMSO): *δ* (ppm) = 1.36 (s, 9 H, 3 × CH_3), 2.47-2.61 (m, 4 H, α-CH_2, γ-CH_2), 4.22-4.36 (m, 1 H, β-CH_2), 5.08 (s, 2 H, Bzl-CH_2), 6.94 (d, 1 H, $^3J_{H,H}$ = 8.4 Hz, NH), 7.28-7.39 (m, 5 H, 5 × CH_{ar}), 9.59 (s, 1 H, COH).

ESI-MS (*m/z*): 322.2 $[M+H]^+$, 344.2 $[M+Na]^+$, 320.1 $[M-H]^-$.

HR-MS (ESI): calc. for $[C_{17}H_{24}NO_5]^+$ ($[M+H]^+$): 322.1649, found: 322.1635; calc. for $[C_{17}H_{23}NO_5Na]^+$ ($[M+Na]^+$): 344.1468, found: 344.1459, calc. for $[C_{17}H_{22}NO_5]^+$ ($[M-H]^-$): 320.1503, found: 320.1500.

(*R*)-3-*tert*-Butoxycarbonylamino-6,6-diiodohex-5-enoic benzyl ester (40)

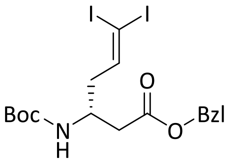

$C_{18}H_{23}I_2NO_4$
571.19 g/mol

40

PPh_3 (4.34 g, 16.5 mmol, 2.20 eq) and iodoform (6.19 g, 15.8 mmol, 2.10 eq) were dissolved in dry THF (70.0 mL) and KO^{t}Bu (1.69 g, 15.0 mmol, 2.00 eq) was added. After stirring at rt for 15 min aldehyde **39** (2.42 g, 7.53 mmol, 1.00 eq) in dry THF (38.0 mL) was added dropwise to the reaction mixture. Further stirring at rt for 1 h was followed by addition of brine (200 mL) and extraction with EtOAc (3 × 60.0 mL). The combined organic phases were dried over $MgSO_4$ and the solvent was removed under reduced pressure. The resulting brown oil was purified by flash column chromatography (pentane/EtOAc: 9:1, *v*/*v*) to yield product **40** (6.11 g, 10.7 mmol, 68%) as a yellow oil.

^{1}H-NMR (300 MHz, [D6]DMSO): δ (ppm) = 1.38 (s, 9 H, 3 × CH_3), 1.94-2.14 (m, 2 H, γ-CH_2), 2.51-2.55 (m, 2 H, α-CH_2), 3.87-4.04 (m, 1 H, β-CH_2), 5.08 (s, 2 H, Bzl-CH_2), 6.89 (d, 1 H, $^3J_{H,H}$ = 8.5 Hz, NH), 7.00 (t, 1 H, $^3J_{H,H}$ = 6.7 Hz, CH), 7.25-7.43 (m, 5 H, 5 × CH_{ar}).
ESI-MS (*m*/*z*): 572.0 $[M+H]^+$, 594.0 $[M+Na]^+$, 610.0 $[M+K]^+$, 1165.0 $[2M+Na]^+$.
HR-MS (ESI): calc. for $[C_{18}H_{24}I_2NO_4]^+$ ($[M+H]^+$): 571.9789, found: 571.9790; calc. for $[C_{18}H_{23}I_2NO_4Na]^+$ ($[M+Na]^+$): 593.9609, found: 593.9611.

(*R*)-3-(9-Fluorenylmethyloxycarbonyl)-amino-6,6-diiodohex-5-enoic acid (2)

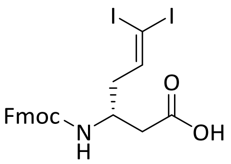

$C_{21}H_{19}I_2NO_4$
603.19 g/mol

2

(*R*)-Benzyl-3-*tert*-butoxycarbonylamino-6,6-diiodohex-5-enoate (**40**) (3.78 g, 6.09 mmol, 1.00 eq) was dissolved in 1,4-dioxane/H_2O/THF (2:1:1, *v*/*v*/*v*, 31.6 mL), cooled to 0 °C and LiOH·H_2O (2.47 g, 59.1 mmol, 9.70 eq) in H_2O (20.0 mL) was added dropwise. After stirring at rt for 1 h, the mixture was adjusted to pH = 5 with citric acid, extracted with EtOAc (3 × 50.0 mL) and the combined organic phases were evaporated under reduced pressure. The resulting brown oil was taken up in TFA/H_2O (95:5, *v*/*v*, 30.0 mL) and stirred at rt for 15 min. The solvent was co-evaporated with toluene (3 × 20.0 mL) and freeze-dried from aqueous solution. The resulting deprotected amino acid (6.09 mmol, 1.00 eq) was dissolved in 10% Na_2CO_3 (aq, 43.0 mL), cooled to 0 °C and Fmoc-Cl (2.05 g, 7.92 mmol, 1.3 eq) in 1,4-dioxane (28.0 mL) was added. The reaction was carried out by sonication for 30 min and then stirred at rt for 2 h. After removal of the solvent, the mixture was adjusted to pH = 2-3 with 1.0 M HCl (aq) and extracted with EtOAc (3 × 50.0 mL). The combined organic phases were dried over $MgSO_4$ and the solvent was removed under reduced pressure. The resulting brown oil was purified by flash column chromatography (pentane/EtOAc: 1:1 + 0.25% AcOH, *v*/*v*/*v*) to yield product **2** (1.98 g, 3.28 mmol, 54%) as a yellow solid.

^{1}H-NMR (300 MHz, [D6]DMSO): δ (ppm) = 1.99-2.17 (m, 2 H, γ-CH_2), 2.34-2.46 (m, 2 H, α-CH_2), 3.88-4.00 (m, 1 H, β-CH_2), 4.20-4.38 (m, 3 H, Fmoc-CH_2, Fmoc-CH), 7.02 (t, 1 H, $^3J_{H,H}$ = 6.6 Hz, CH), 7.28-7.46 (m, 4 H, 4 × Fmoc-CH_{ar}), 7.68 (d, 2 H, $^3J_{H,H}$ = 7.4 Hz, 2 × Fmoc-CH_{ar}), 7.88 (d, 2 H, $^3J_{H,H}$ = 7.5 Hz, 2 × Fmoc-CH_{ar}), 12.0 (s_{br}, 1 H, OH).

ESI-MS (*m*/*z*): 603.9 $[M+H]^+$, 625.9 $[M+Na]^+$, 1228.9 $[2M+Na]^+$, 601.9 $[M-H]^-$, 1204.9 $[2M-H]^-$.

HR-MS (ESI): calc. for $[C_{21}H_{20}I_2NO_4]^+$ ($[M+H]^+$): 603.9476, found: 603.9464; calc. for $[C_{21}H_{19}I_2NO_4Na]^+$ ($[M+Na]^+$): 625.9296, found: 625.9283; calc. for $[C_{21}H_{18}I_2NO_4]^+$ ($[M-H]^-$): 601.9331, found: 601.9317.

6.4.5 Syntheses of the β³-Amino Acids

(*R*)-3-(9-Fluorenylmethyloxycarbonyl)-amino-4-methyl-pentanoic acid (29)

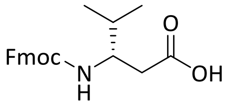

$C_{21}H_{23}NO_4$
353.42 g/mol

29

Starting with Fmoc-D-Val-OH (5.00 g, 14.7 mmol, 1.00 eq), the synthesis was achieved following SOP1 and SOP2.2 to yield product **29** (4.88 g, 13.8 mmol, 94%) as a colourless solid.

¹H-NMR (300 MHz, [D6]DMSO): *δ* (ppm) = 0.59-0.88 (m, 6 H, 2 × CH_3), 1.59-1.80 (m, 1 H, γ-CH), 2.21-2.46 (m, 2 H, α-CH_2), 3.56-3.83 (m, 1 H, β-CH), 4.07-4.38 (m, 3 H, Fmoc-CH_2, Fmoc-CH), 7.16 (d, 1 H, $^3J_{H,H}$ = 9.0 Hz, NH), 7.26-7.43 (m, 4 H, 4 × Fmoc-CH_{ar}), 7.64-7-71 (m, 2 H, 2 × Fmoc-CH_{ar}), 7.86 (d, 2 H, $^3J_{H,H}$ = 7.6 Hz, 2 × Fmoc-CH_{ar}), 12.0 (s_{br}, 1 H, OH).

ESI-MS (*m*/*z*): 354.2 $[M+H]^+$, 376.2 $[M+Na]^+$, 392.1 $[M+K]^+$, 707.4 $[2M+H]^+$, 729.3 $[2M+Na]^+$, 745.3 $[2M+K]^+$, 352.2 $[M-H]^-$, 705.3 $[2M-H]^-$.

HR-MS (ESI): calc. for $[C_{21}H_{24}NO_4]^+$ ($[M+H]^+$): 354.1700, found: 354.1698; calc. for $[C_{21}H_{23}NO_4Na]^+$ ($[M+Na]^+$): 376.1519, found: 376.1519; calc. for $[C_{21}H_{22}NO_4]^-$ ($[M-H]^-$): 352.1554, found: 352.1555.

(*R*)-7-*tert*-Butoxycarbonylamino-3-(9-fluorenylmethyloxycarbonyl)-amino-heptanoic acid (30)

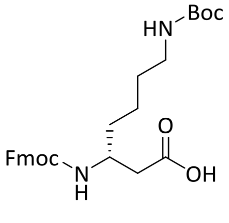

$C_{27}H_{34}N_2O_6$
482.58 g/mol

30

Starting with Fmoc-D-Lys(Boc)-OH (5.00 g, 10.7 mmol, 1.00 eq), the synthesis was achieved following SOP1 and SOP2.2 to yield product **30** (4.29 g, 8.89 mmol, 83%) as a colourless solid.

^{1}H-NMR (300 MHz, [D6]DMSO): *δ* (ppm) = 1.12-1.46 (m, 15 H, 3 × CH_3, γ-CH_2, δ-CH_2, ε-CH_2), 2.26-2.40 (m, 2 H, ζ-CH_2), 2.82-2.92 (m, 2 H, α-CH_2), 3.68-3.83 (m, 1 H, β-CH), 4.17-4.32 (m, 3 H, Fmoc-CH_2, Fmoc-CH), 6.69 (d, 1 H, $^3J_{H,H}$ = 5.9 Hz, NH), 7.15 (d, 1 H, $^3J_{H,H}$ = 8.6 Hz, NH), 7.28-7.45 (m, 4 H, 4 × Fmoc-CH_{ar}), 7.68 (d, 2 H, $^3J_{H,H}$ = 7.5 Hz, 2 × Fmoc-CH_{ar}), 7.88 (d, 2 H, $^3J_{H,H}$ = 7.5 Hz, 2 × Fmoc-CH_{ar}), 12.1 (s_{br}, 1 H, OH).

ESI-MS (*m/z*): 483.3 $[M+H]^+$, 505.3 $[M+Na]^+$, 521.2 $[M+K]^+$, 987.5 $[2M+Na]^+$, 1003.5 $[2M+K]^+$.

HR-MS (ESI): calc. for $[C_{27}H_{35}N_2O_6]^+$ ($[M+H]^+$): 483.2490, found: 483.2476; calc. for $[C_{27}H_{34}N_2O_6Na]^+$ ($[M+Na]^+$): 505.2309, found: 505.2309; calc. for $[C_{27}H_{34}N_2O_6K]^+$ ($[M+K]^+$): 521.2048, found: 521.2056.

(*R*)-3-*tert*-Butoxycarbonylamino-7-(9-fluorenylmethyloxycarbonyl)-amino-heptanoic acid (31)

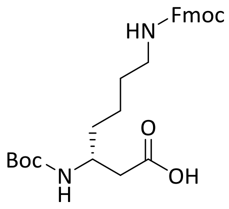

$C_{27}H_{34}N_2O_6$
482.58 g/mol

31

Starting with Boc-D-Lys(Fmoc)-OH (3.00 g, 6.40 mmol, 1.00 eq,) the synthesis was achieved following SOP1 and SOP2.1 to yield product **31** (2.23 g, 4.62 mmol, 72%) as a colourless solid.

^{1}H-NMR (300 MHz, [D6]DMSO): *δ* (ppm) = 1.17-1.47 (m, 15 H, 3 × CH_3, γ-CH_2, δ-CH_2, ε-CH_2), 2.24-2.37 (m, 2 H, ζ-CH_2), 2.91-3.02 (m, 2 H, α-CH_2), 3.66-3.77 (m, 1 H, β-CH), 4.15-4.36 (m, 3 H, Fmoc-CH_2, Fmoc-CH), 6.60 (d, 1 H, $^3J_{H,H}$ = 8.7 Hz, NH), 7.20 (t, 1 H, $^3J_{H,H}$ = 5.7 Hz, NH), 7.28-7.45 (m, 4 H, 4 × Fmoc-CH_{ar}), 7.68 (d, 2 H, $^3J_{H,H}$ = 7.4 Hz, 2 × Fmoc-CH_{ar}), 7.87 (d, 2 H, $^3J_{H,H}$ = 7.5 Hz, 2 × Fmoc-CH_{ar}), 12.1 (s_{br}, 1 H, OH).

ESI-MS (*m/z*): 483.3 $[M+H]^+$, 505.3 $[M+Na]^+$, 521.2 $[M+K]^+$, 987.5 $[2M+Na]^+$.

HR-MS (ESI): calc. for $[C_{27}H_{34}N_2O_6Na]^+$ ($[M+Na]^+$): 505.2309, found: 505.2309.

(*R*)-7-Allyloxycarbonylamino-3-(9-fluorenylmethyloxycarbonyl)-amino-heptanoic acid (32)

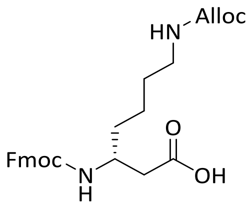

$C_{26}H_{30}N_2O_6$
466.53 g/mol

32

Starting with Fmoc-D-Lys(Alloc)-OH (3.00 g, 6.63 mmol, 1.00 eq), the synthesis was achieved following SOP1 and SOP2.1 to yield product **32** (2.15 g, 4.61 mmol, 70%) as a colourless solid.

^{1}H-NMR (300 MHz, [D6]DMSO): δ (ppm) = 1.11-1.52 (m, 6 H, γ-CH_2, δ-CH_2, ε-CH_2), 2.21-2.44 (m, 1 H, ζ-CH_2), 2.87-3.03 (m, 2 H, α-CH_2), 3.69-3.85 (m, 1 H, β-CH), 4.14-4.36 (m, 3 H, Fmoc-CH_2, Fmoc-CH), 4.37-4.54 (m, 2 H, Alloc-CH_2), 5.09-5.32 (m, 2 H, Alloc-CH_{2allyl}), 5.89 (ddt, 1 H, $^3J_{HH}$ = 17.3, 10.6, 5.3 Hz, Alloc-CH_{allyl}), 7.05-7.20 (m, 2 H, 2 × NH), 7.27-7.45 (m, 4 H, 4 × Fmoc-CH_{ar}), 7.68 (d, 2 H, $^3J_{H,H}$ = 7.4 Hz, 2 × Fmoc-CH_{ar}), 7.88 (d, 2 H, $^3J_{H,H}$ = 7.4 Hz, 2 × Fmoc-CH_{ar}), 12.1 (s_{br}, 1 H, OH).
ESI-MS (*m/z*): 467.2 $[M+H]^+$, 489.2 $[M+Na]^+$, 955.4 $[2M+Na]^+$.
HR-MS (ESI): calc. for $[C_{26}H_{31}N_2O_6]^+$ ($[M+H]^+$): 467.2177, found: 467.2170; calc. for $[C_{26}H_{30}N_2O_6Na]^+$ ($[M+Na]^+$): 489.1996, found: 489.2003.

(*R*)-3-*tert*-Butoxycarbonylamino-7-*tert*-butoxycarbonylamino-heptanoic acid (57)[102]

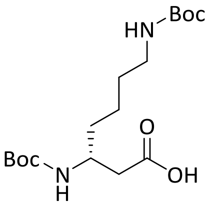

$C_{17}H_{32}N_2O_6$
360.45 g/mol

57

According to the procedure of MYERS *et al.*, to Fmoc-D-β^3-Lys(Boc)-OH (**30**) (1.50 g, 3.11 mmol, 1.00 eq) piperidine (20% in DMF, 10.0 mL) was added and stirred at rt for 15 min. After removal of the solvent under reduced pressure the residue was taken up in diethyl ether and the solid was isolated by centrifugation (9000 rpm, 10 min, -15 °C), washed five times with diethyl ether followed by centrifugation and drying under reduced pressure. The Fmoc-deprotected residue (3.11 mmol, 1.00 eq) was dissolved in H_2O (20.0 mL) and $NaHCO_3$ (523 mg, 6.22 mmol, 2.00 eq) was added. The reaction mixture was cooled to 0 °C, Boc_2O (813 mg, 3.73 mmol, 1.20 eq) in 1,4-dioxane (9.00 mL) was added dropwise at 0 °C and it was stirred at rt overnight. H_2O (15.0 mL) is then added, the aqueous layer is extracted with EtOAc (2 × 30.0 mL). The organic layers are back extracted with saturated $NaHCO_3$ (aq, 3 × 30.0 mL). The combined aqueous layers are adjusted to pH = 2-3 with 1.00 M HCl and extracted with EtOAc (3 × 50.0 mL). The combined organic phases were dried over $MgSO_4$ and the solvent was removed under reduced pressure to yield product **57** (1.03 g, 2.86 mmol, 92%) as a colourless oil.

^{1}H-NMR (300 MHz, [D6]DMSO): *δ* (ppm) = 1.20-1.43 (m, 24 H, 3 × CH_3, γ-CH_2, δ-CH_2, ε-CH_2), 2.21-2.35 (m, 2 H, ζ-CH_2), 2.82-2.93 (m, 2 H, α-CH_2), 3.61-3.76 (m, 1 H, β-CH), 6.58 (d, 1 H, $^3J_{H,H}$ = 8.7 Hz, NH), 6.65 (d, 1 H, $^3J_{H,H}$ = 6.4 Hz, NH), 12.1 (s_{br}, 1 H, OH).

ESI-MS (*m/z*): 383.2 $[M+Na]^+$, 399.2 $[M+K]^+$, 359.2 $[M-H]^-$, 719.5 $[2M-H]^-$.

HR-MS (ESI): calc. for $[C_{17}H_{32}N_2O_6Na]^+$ ($[M+Na]^+$): 383.2153, found: 383.2151; calc. for $[C_{17}H_{32}N_2O_6K]^+$ ($[M+K]^+$): 399.1892, found: 399.1892; calc. for $[C_{17}H_{31}N_2O_6]^-$ ($[M-H]^-$): 359.2188, found: 359.2190.

(*R*)-4-(1'-*tert*-Butoxycarbonyl-indo-3'-yl)-3-(9-fluorenylmethyloxycarbonyl)-amino-butanoic acid (33)

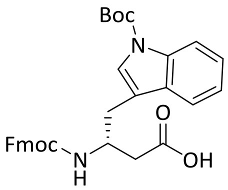

$C_{32}H_{32}N_2O_6$
540.62 g/mol

33

Starting with Fmoc-D-Trp(Boc)-OH (5.00 g, 9.50 mmol, 1.00 eq), the synthesis was achieved following SOP1 and SOP2.1 to yield product **33** (3.84 g, 7.11 mmol, 75%) as a yellowish solid.

^{1}H-NMR (300 MHz, [D6]DMSO): *δ* (ppm) = 1.55 (s, 9 H, 3 × CH_3), 2.44-2.51 (m, 2 H, γ-CH_2), 2.87 (d, 2 H, $^3J_{H,H}$ = 6.7 Hz, α-CH_2), 4.07-4.28 (m, 4 H, β-CH, Fmoc-CH_2, Fmoc-CH), 7.19-7.44 (m, 7 H, NH, 4 × Fmoc-CH_{ar}, 2 × CH_{ar}), 7.51 (s, 1 H, CH_{ar}), 7.54-7.72 (m, 2 H, 2 × Fmoc-CH_{ar}), 7.70 (d, 1 H, $^3J_{H,H}$ = 7.7 Hz, CH_{ar}), 7.86 (d, 2 H, $^3J_{H,H}$ = 7.6 Hz, 2 × Fmoc-CH_{ar}), 8.03 (d, 1 H, $^3J_{H,H}$ = 8.1 Hz, CH_{ar}), 12.2 (s_{br}, 1 H, OH).

ESI-MS (*m/z*): 541.3 $[M+H]^+$, 558.3 $[M+NH_4]^+$, 563.2 $[M+Na]^+$, 1103.5 $[2M+Na]^+$, 539.2 $[M-H]^-$, 1079.4 $[2M-H]^-$.

HR-MS (ESI): calc. for $[C_{32}H_{33}N_2O_6]^+$ ($[M+H]^+$): 541.2333, found: 541.2327; calc. for $[C_{32}H_{32}N_2O_6Na]^+$ ($[M+Na]^+$): 563.2153, found: 563.2148; calc. for $[C_{32}H_{31}N_2O_4]^-$ ($[M-H]^-$): 539.2188, found: 539.2188.

(*R*)-3-(9-Fluorenylmethyloxycarbonyl)-amino-6-oxo-6-tritylamino-hexanoic acid (34)

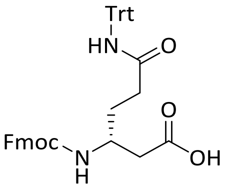

$C_{40}H_{36}N_2O_5$
624.74 g/mol

34

Starting with Fmoc-D-Gln(Trt)-OH (3.00 g, 4.91 mmol, 1.00 eq), the synthesis was achieved following SOP1 and SOP2.1 to yield product **34** (2.94 g, 4.71 mmol, 72%) as a colourless solid.

^{1}H-NMR (300 MHz, [D6]DMSO): *δ* (ppm) = 1.51-1.75 (m, 2 H, γ-CH_2), 2.21-2.42 (m, 4 H, α-CH_2, δ-CH_2), 3.77-3.92 (m, 1 H, β-CH), 4.18-4.35 (m, 3 H, Fmoc-CH_2, Fmoc-CH), 7.13-7.45 (m, 20 H, 3 × C_5H_5, NH, 4 × Fmoc-CH_{ar}), 7.69 (d, 2 H, $^3J_{H,H}$ = 7.4 Hz, 2 × Fmoc-CH_{ar}), 7.88 (d, 2 H, $^3J_{H,H}$ = 7.4 Hz, 2 × Fmoc-CH_{ar}), 8.49 (s, 1 H, NH), 12.1 (s_{br}, 1 H, OH).

ESI-MS (*m/z*): 625.3 $[M+H]^+$, 647.3 $[M+Na]^+$, 1271.5 $[2M+Na]^+$, 623.3 $[M-H]^-$.

HR-MS (ESI): calc. for $[C_{40}H_{37}N_2O_5]^+$ ($[M+H]^+$): 625.2701, found: 625.2697; calc. for $[C_{40}H_{36}N_2O_5Na]^+$ ($[M+Na]^+$): 647.2516, found: 647.2517; calc. for $[C_{40}H_{35}N_2O_5]^-$ ($[M-H]^-$): 623.2551, found: 623.2530.

4-(1'-*tert*-Butoxycarbonyl-indol-3'-yl)-3-(9-fluorenylmethyloxycarbonyl)-amino-butanoic acid (36)

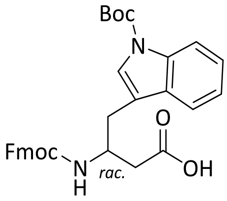

$C_{32}H_{32}N_2O_6$
540.62 g/mol

36

Starting with Fmoc-D-Trp(Boc)-OH (500 mg, 800 µmol, 0.50 eq) and Fmoc-L-Trp(Boc)-OH (500 mg, 800 µmol, 0.50 eq) the synthesis was achieved following SOP1 and SOP2.1 to yield product **36** (703 mg, 1.30 mmol, 68%) as a colourless solid.

For checking the enantiomeric purity of Fmoc-D-β^3-Trp(Boc)-OH (**33**) and Fmoc-D/L-β^3-Trp(Boc)-OH (**36**), the corresponding β^3-amino acid was treated according to SOP 12. HPLC analysis was performed with a linear gradient of A (water + 0.1% TFA) to B (MeCN + 0.1% TFA).

HPLC (MN Nucleodur® 100-5-C18, 250 mm × 4.6 mm, 5 µm, flow rate: 1.0 mL/min, gradient: 25-70% B in 60 min, λ in nm: 280, 340): D/L-β^3-mixture: t_{R1} = 46.7 min and t_{R2} = 48.6 min; D-amino acid: t_R = 48.7 min.

ESI-MS (*m/z*): 541.3 $[M+H]^+$, 558.3 $[M+NH_4]^+$, 563.2 $[M+Na]^+$, 1103.5 $[2M+Na]^+$, 539.2 $[M-H]^-$, 1079.4 $[2M-H]^-$.

HR-MS (ESI): calc. for $[C_{32}H_{33}N_2O_6]^+$ ($[M+H]^+$): 541.2333, found: 541.2327; calc. for $[C_{32}H_{32}N_2O_6Na]^+$ ($[M+Na]^+$): 563.2153, found: 563.2148; calc. for $[C_{32}H_{31}N_2O_4]^-$ ($[M-H]^-$): 539.2188, found: 539.2188.

6.4.6 Syntheses of functionalised KALPs and their non-functionalised Analogues

For all functionalised KALPs and their non-functionalised analogues the respective rink amide MBHA resin (176 mg, 100 µmol, 570 µmol/g, 1.00 eq) was preloaded with Fmoc-Ala-OH (58.3 mg, 500 µmol, 5.00 eq) following SOP3. The occupancy was tested following SOP4 and determined to be 460-520 µmol/g. The peptides **17** was synthesised using the LIBERTY™ automated synthesizer from CEM (Kamp-Lintfort, Germany). In the case of peptide **18**-**23** the peptide synthesis was performed with one third of the preloaded rink amid MBHA resin (59.0 mg, 33.3 mmol, 1.00 eq) and with the LIBERTY BLUE™ automated synthesizer from CEM (Kamp-Lintfort, Germany).

H-GKKLALALALA(11)ALALALALKKA-NH₂ (17)

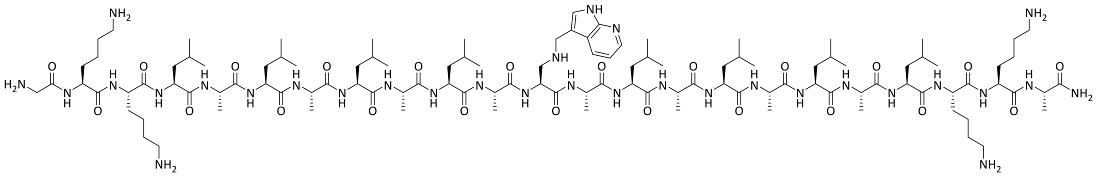

$C_{112}H_{199}N_{31}O_{23}$

2348.02 g/mol

17

The peptide was synthesised following SOP6 using Fmoc-Lys(Boc)-OH (234 mg, 500 µmol, 5.00 eq), Fmoc-Leu-OH (177 mg, 500 µmol, 5.00 eq), Fmoc-Ala-OH (156 mg, 500 µmol, 5.00 eq), Fmoc-Gly-OH (149 mg, 500 µmol, 5.00 eq) and the synthesised building block (**11**) (328 mg, 500 µmol, 5.00 eq). The cleavage was performed using SOP9 to obtain the crude peptide as a colourless solid which was purified by preparative HPLC to yield product **17** (12.2 mg, 5.20 µmol) as a colourless solid.

HPLC (preparative, gradient: 50-85% B in 30 min, λ in nm: 215, 254, 288): t_R = 19.34 min.
ESI-MS (*m/z*): 587.90 $[M+4H]^{4+}$, 783.54 $[M+3H]^{3+}$, 1174.81 $[M+2H]^{2+}$, 2346.59 $[M+H]^{+}$.
HR-MS (ESI): calc. for $[C_{112}H_{201}N_{31}O_{23}]^{2+}$ ($[M+2H]^{2+}$): 1174.7765, found: 1174.7774; calc. for $[C_{112}H_{202}N_{31}O_{23}]^{3+}$ ($[M+3H]^{3+}$): 783.5201, found: 783.5198; calc. for $[C_{112}H_{203}N_{31}O_{23}]^{4+}$ ($[M+4H]^{4+}$): 587.8919, found: 587.8920.

H-GK(acetyl)KKLALALALALALALALALKKA-NH2 (18)

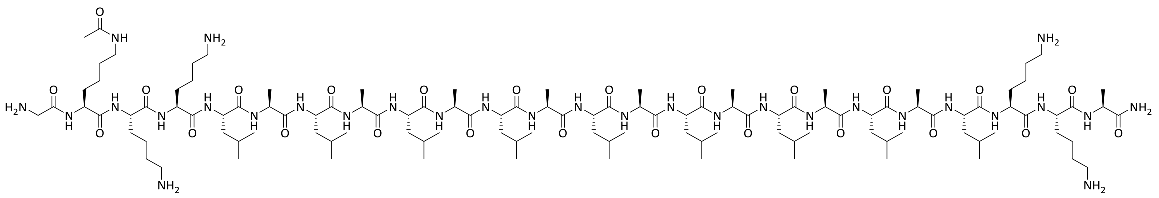

$C_{115}H_{212}N_{30}O_{25}$

2415.15 g/mol

18

The peptide was synthesised following SOP6 using Fmoc-Lys(Boc)-OH (77.9 mg, 167 µmol, 5.00 eq), Fmoc-Ala-OH (52.1 mg, 167 µmol, 5.00 eq), Fmoc-Leu-OH (177 mg, 167 µmol, 5.00 eq), Boc-Gly-OH (49.8 mg, 167 µmol, 5.00 eq) and Fmoc-Lys(Alloc)-OH (75.5 mg, 167 µmol, 5.00 eq). After Alloc-deprotection following SOP8 the free *N*-terminus at the side chain was acetylated with DMF/Ac_2O/DIPEA (18:1:1, *v*/*v*/*v*, 1.50 mL) at rt for 10 min and afterwards, the resin was washed with DMF (10 × 2.00 mL), MeOH (10 × 2.00 mL) and DCM (5 × 2.00 mL) and dried overnight under reduced pressure. The cleavage was performed using SOP9 to obtain the crude peptide as a colourless solid which was purified by preparative HPLC to yield product **18** (11.3 mg, 4.68 µmol) as a colourless solid.

HPLC (preparative, gradient: 70-100% B in 30 min, λ in nm: 215, 254): t_R = 18.52 min.
ESI-MS (*m*/*z*): 604.7 $[M+4H]^{4+}$, 805.9 $[M+3H]^{3+}$, 1208.3 $[M+2H]^{2+}$, 2413.6 $[M+H]^{+}$.
HR-MS (ESI): calc. for $[C_{115}H_{214}N_{30}O_{25}]^{2+}$ ($[M+2H]^{2+}$): 1208.3207, found: 1208.3205; calc. for $[C_{115}H_{215}N_{30}O_{25}]^{3+}$ ($[M+3H]^{3+}$): 805.8829, found: 805.8832; calc. for $[C_{115}H_{216}N_{30}O_{25}]^{4+}$ ($[M+4H]^{4+}$): 604.6640, found: 604.6647, calc. for $[C_{115}H_{217}N_{30}O_{25}]^{5+}$ ($[M+5H]^{5+}$): 483.9327, found: 483.9321.

H-GK(NBD)KKLALALALALALALALALKKA-NH₂ (19)

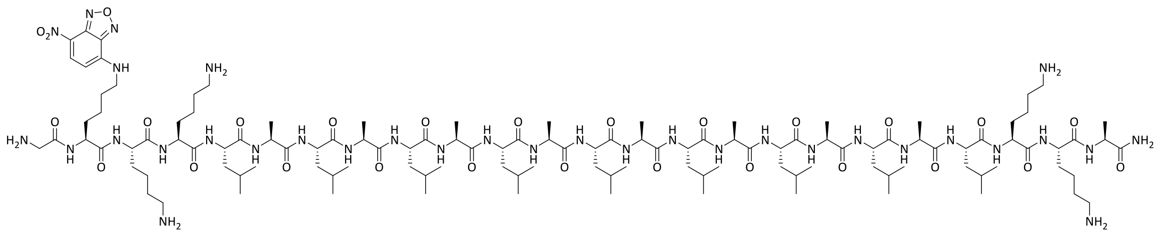

$C_{119}H_{211}N_{33}O_{27}$

2536.20 g/mol

19

The peptide was synthesised following SOP6 using Fmoc-Lys(Boc)-OH (77.9 mg, 167 µmol, 5.00 eq), Fmoc-Ala-OH (52.1 mg, 167 µmol, 5.00 eq), Fmoc-Leu-OH (177 mg, 167 µmol, 5.00 eq), Boc-Gly-OH (49.8 mg, 167 µmol, 5.00 eq) and Fmoc-Lys(Alloc)-OH (75.5 mg, 167 µmol, 5.00 eq). After Alloc-deprotection following SOP8 the free *N*-terminus at the side chain was labelled with NBD–Cl (20.0 mg, 100 µmol, 3.00 eq) in DMF (460 µL), which was activated with DIPEA (111 µL, 666 µmol, 20.0 eq). The reaction mixture was allowed to react at rt overnight. Afterwards, the resin was washed with DMF (10 × 2.00 mL), MeOH (10 × 2.00 mL) and DCM (5 × 2.00 mL) and dried overnight under reduced pressure. The cleavage was performed using SOP9 to obtain the crude peptide as a brown solid which was purified by preparative HPLC to yield product **19** (4.36 mg, 1.72 µmol) as an orange solid.

HPLC (preparative, gradient: 80-100% B in 30 min, *λ* in nm: 215, 464, 254): t_R = 12.43 min.
ESI-MS (*m/z*): 634.9 $[M+4H]^{4+}$, 846.2 $[M+3H]^{3+}$, 1268.8 $[M+2H]^{2+}$, 2534.6 $[M+H]^{+}$.
HR-MS (ESI): calc. for $[C_{119}H_{213}N_{33}O_{27}]^{2+}$ ($[M+2H]^{2+}$): 1268.8163, found: 1268.8169; calc. for $[C_{119}H_{214}N_{33}O_{27}]^{3+}$ ($[M+3H]^{3+}$): 846.2133, found: 846.2135; calc. for $[C_{119}H_{215}N_{33}O_{27}]^{4+}$ ($[M+4H]^{4+}$): 634.9118, found: 634.9124.

H-GKKLALALALALALALALALKKK(TAMRA)A-NH₂ (20)

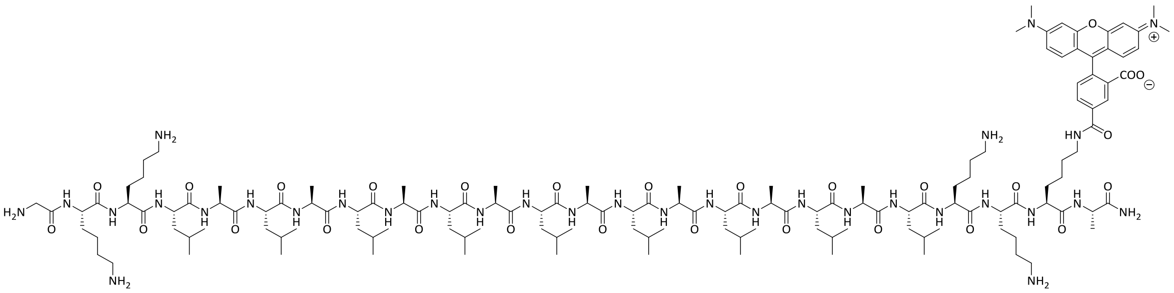

$C_{138}H_{230}N_{32}O_{28}$

2785.55 g/mol

20

The peptide was synthesised following SOP6 using Fmoc-Lys(Boc)-OH (77.9 mg, 167 µmol, 5.00 eq), Fmoc-Ala-OH (52.1 mg, 167 µmol, 5.00 eq), Fmoc-Leu-OH (177 mg, 167 µmol, 5.00 eq), Boc-Gly-OH (49.8 mg, 167 µmol, 5.00 eq) and Fmoc-Lys(Alloc)-OH (75.5 mg, 167 µmol, 5.00 eq). After Alloc-deprotection following SOP8 the free *N*-terminus at the side chain was labelled with TAMRA (71.3 mg, 167 µmol, 5.00 eq) in DMF (450 µL), which was activated with PyBOP® (81.8 mg, 157 µmol, 4.70 eq) and DIPEA (55.5 µL, 326 µmol, 9.80 eq) and allowed to react at rt overnight. Afterwards, the resin was washed with DMF (10 × 2.00 mL), MeOH (10 × 2.00 mL) and DCM (5 × 2.00 mL) and dried overnight under reduced pressure. The cleavage was performed using SOP9 to obtain the crude peptide as a pink solid which was purified by preparative HPLC to yield product **20** (3.38 mg, 1.21 µmol) as a pink solid.

HPLC (preparative, gradient: 80-95% B in 30 min, λ in nm: 215, 540, 254): t_R = 10.78 min.
ESI-MS (*m/z*): 558.0 $[M+5H]^{5+}$, 697.2 $[M+4H]^{4+}$, 929.3 $[M+3H]^{3+}$, 1393.4 $[M+2H]^{2+}$, 2783.8 $[M+H]^{+}$.
HR-MS (ESI): calc. for $[C_{138}H_{232}N_{32}O_{28}]^{2+}$ ($[M+2H]^{2+}$): 1393.3866, found: 1393.3870; calc. for $[C_{138}H_{233}N_{32}O_{28}]^{3+}$ ($[M+3H]^{3+}$): 929.2602, found: 929.2603; calc. for $[C_{138}H_{234}N_{32}O_{28}]^{4+}$ ($[M+4H]^{4+}$): 697.1969, found: 697.1973, calc. for $[C_{138}H_{235}N_{32}O_{28}]^{5+}$ ($[M+5H]^{5+}$): 557.9590, found: 557.9593.

H-GK(acetyl)KKLALALALALALA(11)ALALKKA-NH$_2$ (21)

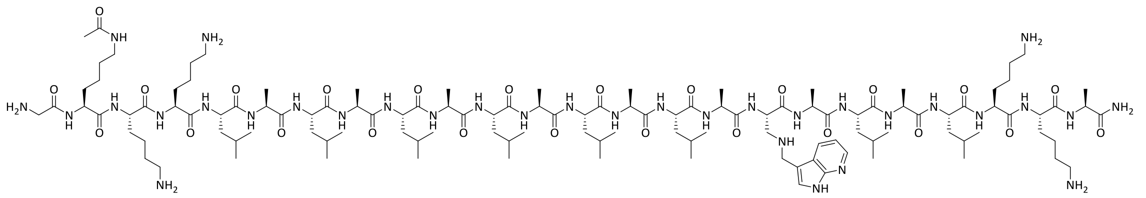

$C_{120}H_{213}N_{33}O_{25}$

2518.23 g/mol

21

The peptide was synthesised following SOP6 using Fmoc-Lys(Boc)-OH (77.9 mg, 167 µmol, 5.00 eq), Fmoc-Ala-OH (52.1 mg, 167 µmol, 5.00 eq), Fmoc-Leu-OH (177 mg, 167 µmol, 5.00 eq), Boc-Gly-OH (49.8 mg, 167 µmol, 5.00 eq), Fmoc-Lys(Alloc)-OH (75.5 mg, 167 µmol, 5.00 eq) and the synthesised building block (**11**) (328 mg, 167 µmol, 5.00 eq). After Alloc-deprotection following SOP8 the free *N*-terminus at the side chain was acetylated with DMF/Ac$_2$O/DIPEA (18:1:1, *v*/*v*/*v*, 1.50 mL) at rt for 10 min and afterwards, the resin was washed with DMF (10 × 2.00 mL), MeOH (10 × 2.00 mL) and DCM (5 × 2.00 mL) and dried overnight under reduced pressure. The cleavage was performed using SOP9 to obtain the crude peptide as a colourless solid which was purified by preparative HPLC to yield product **21** (2.62 mg, 1.04 µmol) as a colourless solid.

HPLC (semi-preparative, gradient: 55-85% B in 30 min, λ in nm: 215, 254, 288): t_R = 25.85 min.
ESI-MS (*m*/*z*): 597.9 $[M+4H]^{4+}$, 840.2 $[M+3H]^{3+}$, 1259.8 $[M+2H]^{2+}$, 2516.6 $[M+H]^{+}$.
HR-MS (ESI): calc. for $[C_{120}H_{215}N_{33}O_{25}]^{2+}$ ($[M+2H]^{2+}$): 1259.8292, found: 1259.8288; calc. for $[C_{120}H_{216}N_{33}O_{25}]^{3+}$ ($[M+3H]^{3+}$): 840.2219, found: 840.2225; calc. for $[C_{120}H_{27}N_{33}O_{25}]^{4+}$ ($[M+4H]^{4+}$): 630.4183, found: 640.4195.

H-GK(NBD)KKLALALALALALA(11)ALALKKA-NH$_2$ (22)

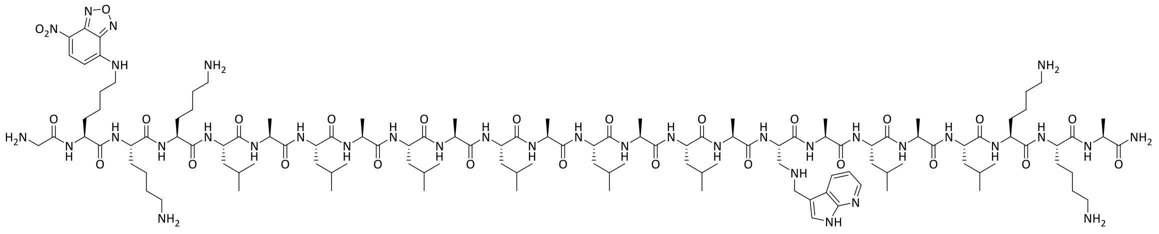

$C_{124}H_{212}N_{36}O_{27}$

2639.29 g/mol

22

The peptide was synthesised following SOP6 using Fmoc-Lys(Boc)-OH (77.9 mg, 167 µmol, 5.00 eq), Fmoc-Ala-OH (52.1 mg, 167 µmol, 5.00 eq), Fmoc-Leu-OH (177 mg, 167 µmol, 5.00 eq), Boc-Gly-OH (49.8 mg, 167 µmol, 5.00 eq), Fmoc-Lys(Alloc)-OH (75.5 mg, 167 µmol, 5.00 eq) and the synthesised building block (**11**) (328 mg, 167 µmol, 5.00 eq). After Alloc-deprotection following SOP8 the free *N*-terminus at the side chain was labelled with NBD–Cl (20.0 mg, 100 µmol, 3.00 eq) in DMF (460 µL), which was activated with DIPEA (111 µL, 666 µmol, 20.0 eq). The reaction mixture was allowed to react at rt overnight. Afterwards, the resin was washed with DMF (10 × 2.00 mL), MeOH (10 × 2.00 mL) and DCM (5 × 2.00 mL) and dried overnight under reduced pressure. The cleavage was performed using SOP9 to obtain the crude peptide as a brown solid which was purified by preparative HPLC to yield product **22** (3.23 mg, 1.23 µmol) as an orange solid.

HPLC (semi-preparative, gradient: 85-100% B in 35 min, λ in nm: 215, 254, 288): t_R = 30.37 min.
ESI-MS (*m/z*): 660.7 $[M+4H]^{4+}$, 880.6 $[M+3H]^{3+}$, 1320.3 $[M+2H]^{2+}$, 2637.6 $[M+H]^{+}$.
HR-MS (ESI): calc. for $[C_{124}H_{214}N_{36}O_{27}]^{2+}$ ($[M+2H]^{2+}$): 1320.3248, found: 13203238; calc. for $[C_{124}H_{215}N_{36}O_{27}]^{3+}$ ($[M+3H]^{3+}$): 880.5523, found: 880.5521; calc. for $[C_{124}H_{216}N_{36}O_{27}]^{4+}$ ($[M+4H]^{4+}$): 660.6661, found: 660.6664.

H-GKKLALA(11)ALALALALALALKKK(TAMRA)A-NH₂ (23)

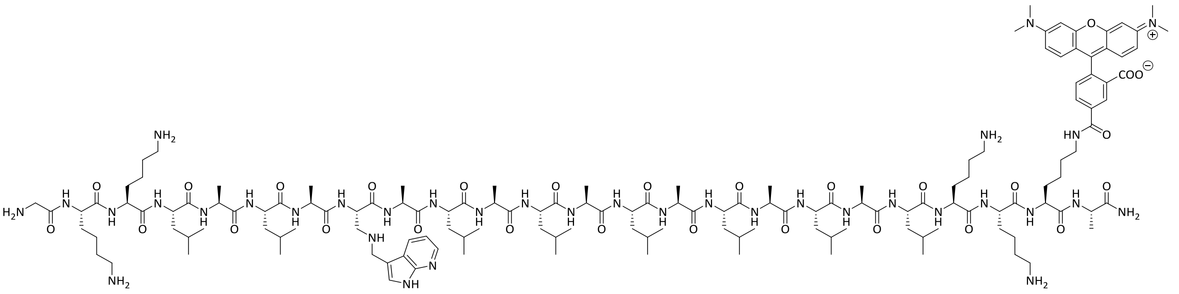

$C_{143}H_{231}N_{35}O_{28}$

2888.64 g/mol

23

The peptide was synthesised following SOP6 using Fmoc-Lys(Boc)-OH (77.9 mg, 167 µmol, 5.00 eq), Fmoc-Ala-OH (52.1 mg, 167 µmol, 5.00 eq), Fmoc-Leu-OH (177 mg, 167 µmol, 5.00 eq), Boc-Gly-OH (49.8 mg, 167 µmol, 5.00 eq), Fmoc-Lys(Alloc)-OH (75.5 mg, 167 µmol, 5.00 eq) and the synthesised building block (**11**) (328 mg, 167 µmol, 5.00 eq). After Alloc-deprotection following SOP8 the free *N*-terminus at the side chain was labelled with TAMRA (71.3 mg, 167 µmol, 5.00 eq) in DMF (450 µL), which was activated with PyBOP® (81.8 mg, 157 µmol, 4.70 eq) and DIPEA (55.5 µL, 326 µmol, 9.80 eq) and allowed to react at rt overnight. Afterwards, the resin was washed with DMF (10 × 2.00 mL), MeOH (10 × 2.00 mL) and DCM (5 × 2.00 mL) and dried overnight under reduced pressure. The cleavage was performed using SOP9 to obtain the crude peptide as a pink solid which was purified by preparative HPLC to yield product **23** (600 µg, 207 nmol) as a pink solid.

HPLC (preparative, gradient: 70-90% B in 35 min, *λ* in nm: 215, 254, 288): t_R = 22.83 min.
ESI-MS (*m/z*): 578.6 $[M+5H]^{5+}$, 723.0 $[M+4H]^{4+}$, 963.6 $[M+3H]^{3+}$, 2886.8 $[M+H]^{+}$.
HR-MS (ESI): calc. for $[C_{143}H_{234}N_{35}O_{28}]^{3+}$ ($[M+3H]^{3+}$): 963.5992, found: 963.5995; calc. for $[C_{143}H_{235}N_{35}O_{28}]^{4+}$ ($[M+4H]^{4+}$): 722.9512, found: 722.9512; calc. for $[C_{143}H_{236}N_{35}O_{28}]^{5+}$ ($[M+5H]^{5+}$): 578.5624, found: 578.5627.

6.4.7 Syntheses of the β-Peptides

6.4.7.1 Diiodoallylhomoglycine functionalised β-peptides and their non-functionalised analogues

For all diiodoallylhomoglycine functionalised β-peptides and their non-functionalised analogues the respective rink amide MBHA resin (132 mg, 75.0 µmol, 0.57 mmol/g, 1.00 eq) was preloaded with Fmoc-D-β^3-Lys(Boc)-OH (**30**) (181 mg, 375 µmol, 5.00 eq) following SOP3. The occupancy was tested following SOP4 and determined to be 0.49-0.53 mmol/g.

H-^{h}Lys$_2$-^{h}Val$_{19}$-^{h}Lys$_2$-NH$_2$ (41)

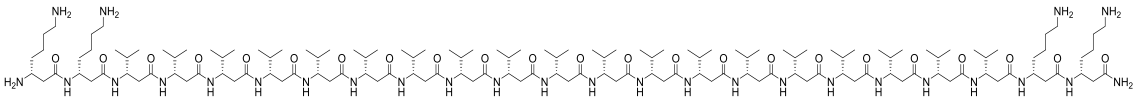

$C_{142}H_{268}N_{28}O_{23}$

2735.88 g/mol

41

The peptide was synthesised following SOP7 using Fmoc-D-β^3-Lys(Boc)-OH (**30**) (145 mg, 300 µmol, 4.00 eq) and Fmoc-D-β^3-Val-OH (**29**) (106 mg, 300 µmol, 4.00 eq). The cleavage was performed using SOP9 to obtain the crude peptide as a colourless solid which was purified by Semi-preparative HPLC to yield product **41** (8.00 mg, 2.92 µmol) as a colourless solid.

HPLC (Semi-preparative, gradient: 87-96% B in 30 min, λ in nm: 215, 254, 280): t_R = 16.89 min.
ESI-MS (*m/z*): 548.0 [M+5H]$^{5+}$, 684.8 [M+4H]$^{4+}$, 912.7 [M+3H]$^{3+}$, 1368.5 [M+2H]$^{2+}$.
HR-MS (ESI): calc. for [$C_{142}H_{270}N_{28}O_{23}$]$^{2+}$ ([M+2H]$^{2+}$): 1368.5419, found: 1368.5429; calc. for [$C_{142}H_{271}N_{28}O_{23}$]$^{3+}$ ([M+3H]$^{3+}$): 912.6970, found: 912.6974; calc. for [$C_{142}H_{272}N_{28}O_{23}$]$^{4+}$ ([M+4H]$^{4+}$): 684.7746, found: 684.7753; calc. for [$C_{142}H_{273}N_{28}O_{23}$]$^{5+}$ ([M+5H]$^{5+}$): 548.0211, found: 548.0216.

H-^{h}Lys$_2$-^{h}Val-^{h}Diiodo-^{h}Val$_{17}$-^{h}Lys$_2$-NH$_2$ (42)

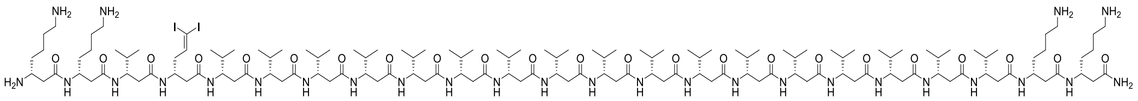

$C_{142}H_{264}I_2N_{28}O_{23}$

2985.66 g/mol

42

The peptide was synthesised following SOP7 using Fmoc-D-β^3-Lys(Boc)-OH (**30**) (145 mg, 300 µmol, 4.00 eq), Fmoc-D-β^3-Val-OH (**29**) (106 mg, 300 µmol, 4.00 eq) and Fmoc-D-β^3-6,6-diiodoallylhomoglycine (**2**) (182 mg, 300 µmol, 4.00 eq). The successful coupling of **2** was tested following SOP5. The cleavage was performed using SOP9 to obtain the crude peptide as a pale yellow solid which was purified by preparative HPLC to yield product **42** (32.0 mg, 10.7 µmol) as a colourless solid.

HPLC (preparative, gradient: 90-100% B in 30 min, λ in nm: 215, 254, 280): t_R = 10.59 min.
ESI-MS (*m/z*): 598.0 $[M+5H]^{5+}$, 747.2 $[M+4H]^{4+}$, 996.0 $[M+3H]^{3+}$, 1493.4 $[M+2H]^{2+}$.
HR-MS (ESI): calc. for $[C_{142}H_{266}I_2N_{28}O_{23}]^{2+}$ ($[M+2H]^{2+}$): 1493.4307, found: 1493.4315; calc. for $[C_{142}H_{267}I_2N_{28}O_{23}]^{3+}$ ($[M+3H]^{3+}$): 995.9562, found: 995.9569; calc. for $[C_{142}H_{268}I_2N_{28}O_{23}]^{4+}$ ($[M+4H]^{4+}$): 747.2190, found: 747.2198; calc. for $[C_{142}H_{269}I_2N_{28}O_{23}]^{5+}$ ($[M+5H]^{5+}$): 597.9767, found: 597.9771.

H-^{h}Lys$_2$-^{h}Val$_9$-^{h}Diiodo-^{h}Val$_9$-^{h}Lys$_2$-NH$_2$ (43)

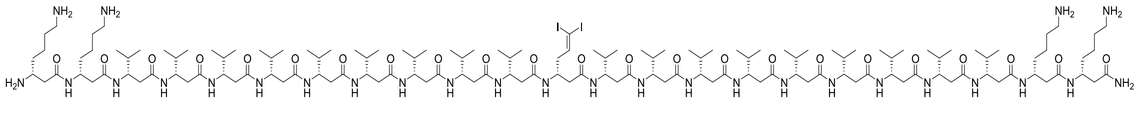

$C_{142}H_{264}I_2N_{28}O_{23}$

2985.66 g/mol

43

The peptide was synthesised following SOP7 using Fmoc-D-β^3-Lys(Boc)-OH (**30**) (145 mg, 300 µmol, 4.00 eq), Fmoc-D-β^3-Val-OH (**29**) (106 mg, 300 µmol, 4.00 eq) and Fmoc-D-β^3-6,6-diiodoallylhomoglycine (**2**) (182 mg, 300 µmol, 4.00 eq). The successful coupling of **2** was tested following SOP5. The cleavage was performed using SOP9 to obtain the crude peptide as a pale yellow solid which was purified by preparative HPLC to yield product **43** (22.0 mg, 7.37 µmol) as a colourless solid.

HPLC (preparative, gradient: 85-100% B in 30 min, λ in nm: 215, 254, 280): t_R = 19.44 min.
ESI-MS (*m/z*): 598.0 $[M+5H]^{5+}$, 747.2 $[M+4H]^{4+}$, 996.0 $[M+3H]^{3+}$, 1493.4 $[M+2H]^{2+}$.
HR-MS (ESI): calc. for $[C_{142}H_{266}I_2N_{28}O_{23}]^{2+}$ ($[M+2H]^{2+}$): 1493.4307, found: 1493.4323; calc. for $[C_{142}H_{267}I_2N_{28}O_{23}]^{3+}$ ($[M+3H]^{3+}$): 995.9562, found: 995.9578; calc. for $[C_{142}H_{268}I_2N_{28}O_{23}]^{4+}$ ($[M+4H]^{4+}$): 747.2190, found: 747.2206; calc. for $[C_{142}H_{269}I_2N_{28}O_{23}]^{5+}$ ($[M+5H]^{5+}$): 597.9767, found: 597.9773.

H-^{h}Lys$_2$-^{h}Trp$_2$-^{h}Val$_{19}$-^{h}Trp$_2$-^{h}Lys$_2$-NH$_2$ (44)

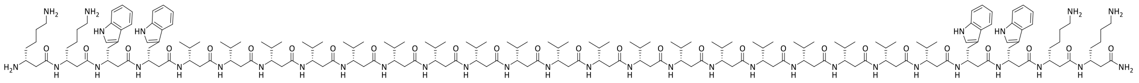

$C_{190}H_{316}N_{36}O_{27}$

3536.84 g/mol

44

The peptide was synthesised following SOP7 using Fmoc-D-β^3-Lys(Boc)-OH (**30**) (145 mg, 300 µmol, 4.00 eq), Fmoc-D-β^3-Trp(Boc)-OH (**33**) (162 mg, 300 µmol, 4.00 eq) and Fmoc-D-β^3-Val-OH (**29**) (106 mg, 300 µmol, 4.00 eq). Double coupling was performed for Fmoc-D-β^3-Trp(Boc)-OH (**33**). The cleavage was performed using SOP9 to obtain the crude peptide as a grey solid which was purified by preparative HPLC to yield product **44** (5.00 mg, 1.41 µmol) as a pale grey solid.

HPLC (preparative, gradient: 80-100% B in 30 min, λ in nm: 215, 254, 280): t_R = 21.78 min.
ESI-MS (*m/z*): 708.3 [M+5H]$^{5+}$, 885.1 [M+4H]$^{4+}$, 1179.8 [M+3H]$^{3+}$, 1769.2 [M+2H]$^{2+}$.
HR-MS (ESI): calc. for $[C_{190}H_{318}N_{36}O_{27}]^{2+}$ ([M+2H]$^{2+}$): 1769.2333, found: 1769.2320; calc. for $[C_{190}H_{319}N_{36}O_{27}]^{3+}$ ([M+3H]$^{3+}$): 1179.8246, found: 1179.8251; calc. for $[C_{190}H_{320}N_{36}O_{27}]^{4+}$ ([M+4H]$^{4+}$): 885.1203, found: 885.1207; calc. for $[C_{190}H_{321}N_{36}O_{27}]^{5+}$ ([M+5H]$^{5+}$): 708.2977, found: 708.2982.

H-^{h}Lys$_2$-^{h}Trp$_2$-^{h}Val-^{h}Diiodo-^{h}Val$_{17}$-^{h}Trp$_2$-^{h}Lys$_2$-NH$_2$ (45)

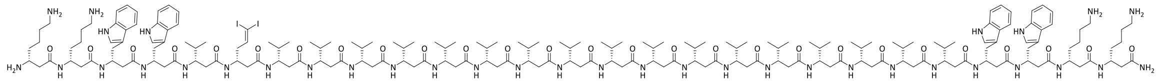

$C_{190}H_{312}I_2N_{36}O_{27}$

3786.62 g/mol

45

The peptide was synthesised following SOP7 using Fmoc-D-β^3-Lys(Boc)-OH (**30**) (145 mg, 300 µmol, 4.00 eq), Fmoc-D-β^3-Trp(Boc)-OH (**33**) (162 mg, 300 µmol, 4.00 eq), Fmoc-D-β^3-Val-OH (**29**) (106 mg, 300 µmol, 4.00 eq) and Fmoc-D-β^3-6,6-diiodoallylhomoglycine (**2**) (182 mg, 300 µmol, 4.00 eq). The successful coupling of **2** was tested following SOP5. Double coupling was performed for Fmoc-D-β^3-Trp(Boc)-OH (**33**). The cleavage was performed using SOP9 to obtain the crude peptide as a grey solid which was purified by preparative HPLC to yield product **45** (12.5 mg, 3.30 µmol) as a pale grey solid.

HPLC (preparative, gradient: 90-100% B in 40 min, λ in nm: 215, 254, 280): t_R = 23.30 min.
ESI-MS (*m/z*): 758.3 [M+5H]$^{5+}$, 947.6 [M+4H]$^{4+}$, 1263.1 [M+3H]$^{3+}$, 1894.1 [M+2H]$^{2+}$.

HR-MS (ESI): calc. for $[C_{190}H_{315}I_2N_{36}O_{27}]^{3+}$ ($[M+3H]^{3+}$): 1263.0839, found: 1263.0863; calc. for $[C_{190}H_{316}I_2N_{36}O_{27}]^{4+}$ ($[M+4H]^{4+}$): 947.5647, found: 947.5663; calc. for $[C_{190}H_{317}I_2N_{36}O_{27}]^{5+}$ ($[M+5H]^{5+}$): 758.2532, found: 758.2546.

H-^{h}Lys$_2$-^{h}Trp$_2$-^{h}Val$_9$-^{h}Diiodo-^{h}Val$_9$-^{h}Trp$_2$-^{h}Lys$_2$-NH$_2$ (46)

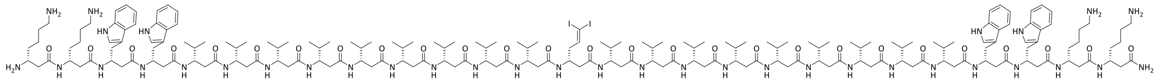

$C_{190}H_{312}I_2N_{36}O_{27}$

3786.62 g/mol

46

The peptide was synthesised following SOP7 using Fmoc-D-β^3-Lys(Boc)-OH (**30**) (145 mg, 300 µmol, 4.00 eq), Fmoc-D-β^3-Trp(Boc)-OH (**33**) (162 mg, 300 µmol, 4.00 eq), Fmoc-D-β^3-Val-OH (**29**) (106 mg, 300 µmol, 4.00 eq) and Fmoc-D-β^3-6,6-diiodoallylhomoglycine (**2**) (182 mg, 300 µmol, 4.00 eq). The successful coupling of **2** was tested following SOP5. Double coupling was performed for Fmoc-D-β^3-Trp(Boc)-OH (**33**). The cleavage was performed using SOP9 to obtain the crude peptide as a grey solid which was purified by preparative HPLC to yield product **46** (15.0 mg, 3.96 µmol) as a pale grey solid.

HPLC (preparative, gradient: 90-100% B in 30 min, λ in nm: 215, 254, 280): t_R = 18.88 min.
ESI-MS (*m/z*): 758.3 $[M+5H]^{5+}$, 947.6 $[M+4H]^{4+}$, 1263.1 $[M+3H]^{3+}$, 1894.1 $[M+2H]^{2+}$.
HR-MS (ESI): calc. for $[C_{190}H_{314}N_{36}O_{27}]^{2+}$ ($[M+2H]^{2+}$): 1894.1221, found: 1894.1223; calc. for $[C_{190}H_{315}I_2N_{36}O_{27}]^{3+}$ ($[M+3H]^{3+}$): 1263.0839, found: 1263.0864; calc. for $[C_{190}H_{316}I_2N_{36}O_{27}]^{4+}$ ($[M+4H]^{4+}$): 947.5647, found: 947.5665; calc. for $[C_{190}H_{317}I_2N_{36}O_{27}]^{5+}$ ($[M+5H]^{5+}$): 758.2532, found: 758.2548.

6.4.7.2 β-Glutamine functionalised β-peptides and their non-functionalised analogues

H-^{h}Lys(acetyl)-^{h}Lys$_{2}$-^{h}Trp$_{2}$-^{h}Val$_{19}$-^{h}Trp$_{2}$-^{h}Lys$_{2}$-NH$_{2}$ (48)

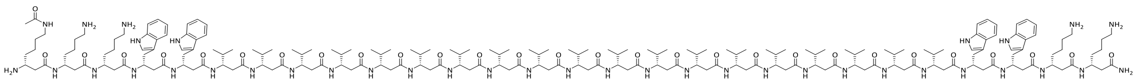

$C_{199}H_{332}N_{38}O_{29}$

3721.08 g/mol

48

The rink amide MBHA resin (44.0 mg, 25.0 µmol, 570 µmol/g, 1.00 eq) was preloaded with Fmoc-D-β^{3}-Lys(Boc)-OH (**30**) (60.0 mg, 125 µmol, 5.00 eq) following SOP3. The occupancy was tested following SOP4 and determined to be 510 µmol/g. The peptide was synthesised following SOP7 using Fmoc-D-β^{3}-Lys(Boc)-OH (**30**) (48.3 mg, 100 µmol, 4.00 eq), Fmoc-D-β^{3}-Trp(Boc)-OH (**33**) (54.0 mg, 100 µmol, 4.00 eq), Fmoc-D-β^{3}-Val-OH (**29**) (35.3 mg, 100 µmol, 4.00 eq) and Boc-D-β^{3}-Lys(Fmoc)-OH (**31**) (54.0 mg, 100 µmol, 4.00 eq). Double coupling was performed for Fmoc-D-β^{3}-Trp(Boc)-OH (**33**). After final Fmoc-deprotection the free *N*-terminus at the side chain was acetylated with DMF/Ac$_2$O/DIPEA (18:1:1, *v*/*v*/*v*, 1.50 mL) at rt for 10 min and afterwards, the resin was washed with DMF (10 × 2.00 mL), MeOH (10 × 2.00 mL) and DCM (5 × 2.00 mL) and dried overnight under reduced pressure. The cleavage was performed using SOP9 to obtain the crude peptide as a white solid which was purified by preparative HPLC to yield product **48** (2.43 mg, 652 nmol) as a colourless solid.

HPLC (preparative, gradient: 88-100% B in 30 min, λ in nm: 215, 254, 280): t_R = 12.30 min.

ESI-MS (*m*/*z*): 621.1[M+6H]$^{6+}$, 745.1 [M+5H]$^{5+}$, 931.2 [M+4H]$^{4+}$, 1241.2 [M+3H]$^{3+}$.

HR-MS (ESI): calc. for $[C_{199}H_{335}N_{38}O_{29}]^{3+}$ ([M+3H]$^{3+}$): 1241.1984, found: 1241.1998; calc. for $[C_{199}H_{336}N_{38}O_{29}]^{4+}$ ([M+4H]$^{4+}$): 931.1506, found: 931.1514; calc. for $[C_{199}H_{337}N_{38}O_{29}]^{5+}$ ([M+5H]$^{5+}$): 745.1219, found: 745.1224; calc. for $[C_{199}H_{338}N_{38}O_{29}]^{6+}$ ([M+6H]$^{6+}$): 621.1028, found: 621.1022.

H-^{h}Lys(NBD)-^{h}Lys$_{2}$-^{h}Trp$_{2}$-^{h}Val$_{19}$-^{h}Trp$_{2}$-^{h}Lys$_{2}$-NH$_{2}$ (49)

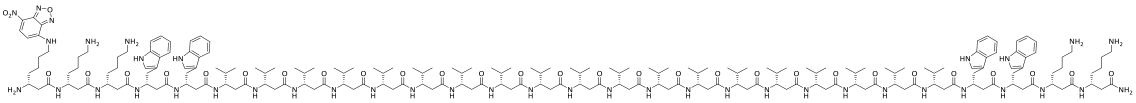

$C_{203}H_{331}N_{41}O_{31}$

3842.14 g/mol

49

The rink amide MBHA resin (44.0 mg, 25.0 µmol, 570 µmol/g, 1.00 eq) was preloaded with Fmoc-D-β^3-Lys(Boc)-OH (**30**) (60.0 mg, 125 µmol, 5.00 eq) following SOP3. The occupancy was tested following SOP4 and determined to be 510 µmol/g. The peptide was synthesised following SOP7 using Fmoc-D-β^3-Lys(Boc)-OH (**30**) (48.3 mg, 100 µmol, 4.00 eq), Fmoc-D-β^3-Trp(Boc)-OH (**33**) (54.0 mg, 100 µmol, 4.00 eq), Fmoc-D-β^3-Val-OH (**29**) (35.3 mg, 100 µmol, 4.00 eq) and Boc-D-β^3-Lys(Fmoc)-OH (**31**) (54.0 mg, 100 µmol, 4.00 eq). Double coupling was performed for Fmoc-D-β^3-Trp(Boc)-OH (**33**). After final Fmoc-deprotection the free *N*-terminus at the side chain was labelled with NBD–Cl (15.0 mg, 75.0 µmol, 3.00 eq) in DMF (345 µL), which was activated with DIPEA (83.0 µL, 500 µmol, 20.0 eq). The reaction mixture was allowed to react at rt overnight. Afterwards, the resin was washed with DMF (10 × 2.00 mL), MeOH (10 × 2.00 mL) and DCM (5 × 2.00 mL) and dried overnight under reduced pressure. The cleavage was performed using SOP9 to obtain the crude peptide as a brown solid which was purified by preparative HPLC to yield product **49** (538 µg, 140 nmol) as an orange solid.

HPLC (preparative, gradient: 80-100% B in 40 min, *λ* in nm: 215, 464, 280): t_R = 30.00 min.
ESI-MS (*m/z*): 769.3 $[M+5H]^{5+}$, 961.41 $[M+4H]^{4+}$, 1281.5 $[M+3H]^{3+}$.
HR-MS (ESI): calc. for $[C_{203}H_{334}N_{41}O_{31}]^{3+}$ ($[M+3H]^{3+}$): 1281.5288, found: 1281.5290; calc. for $[C_{203}H_{335}N_{41}O_{31}]^{4+}$ ($[M+4H]^{4+}$): 961.3984, found: 961.3987; calc. for $[C_{203}H_{336}N_{41}O_{31}]^{5+}$ ($[M+5H]^{5+}$): 769.3202, found: 769.3202.

H-^{h}Lys$_2$-^{h}Trp$_2$-^{h}Val$_{19}$-^{h}Trp$_2$-^{h}Lys$_2$-^{h}Lys(TAMRA)-NH$_2$ (50)

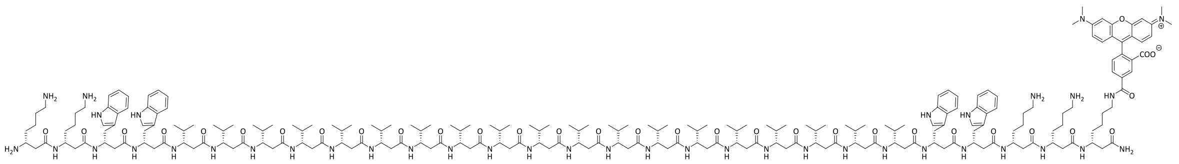

$C_{222}H_{350}N_{40}O_{32}$

4091.49 g/mol

50

The rink amide MBHA resin (44.0 mg, 25.0 µmol, 570 µmol/g, 1.00 eq) was preloaded with Fmoc-D-β^3-Lys(Alloc)-OH (**32**) (58.3 mg, 125 µmol, 5.00 eq) following SOP3. The occupancy was tested following SOP4 and determined to be 490 µmol/g. The peptide was synthesised following SOP7 using Fmoc-D-β^3-Lys(Boc)-OH (**30**) (48.3 mg, 100 µmol, 4.00 eq), Fmoc-D-β^3-Trp(Boc)-OH (**33**) (54.0 mg, 100 µmol, 4.00 eq), Fmoc-D-β^3-Val-OH (**29**) (35.3 mg, 100 µmol, 4.00 eq) and Boc-D-β^3-Lys(Boc)-OH (**57**) (36.0 mg, 100 µmol, 4.00 eq). Double coupling was performed for Fmoc-D-β^3-Trp(Boc)-OH (**33**). After Alloc-deprotection following SOP8 the free *N*-terminus was labelled with TAMRA (53.4 mg, 125 µmol, 5.00 eq) in DMF (340 µL), which was activated with PyBOP® (61.5 mg, 118 µmol, 4.70 eq) and DIPEA (41.7 µL, 245 µmol, 9.80 eq) and allowed to react at rt overnight. Afterwards, the resin was washed with DMF (10 × 2.00 mL), MeOH (10 × 2.00 mL) and DCM (5 × 2.00 mL) and dried overnight under reduced pressure. The cleavage was performed using SOP9 to obtain the crude peptide as a pink solid which was purified by preparative HPLC to yield product **50** (1.65 mg, 403 nmol) as a pink solid.

HPLC (preparative, gradient: 90-100% B in 30 min, λ in nm: 215, 540, 280): t_R = 11.20 min.
ESI-MS (*m/z*): 682.8 $[M+6H]^{6+}$, 819.1 $[M+5H]^{5+}$, 1023.7 $[M+4H]^{4+}$, 1364.6 $[M+3H]^{3+}$.
HR-MS (ESI): calc. for $[C_{222}H_{353}N_{40}O_{32}]^{3+}$ ($[M+3H]^{3+}$): 1364.5756, found: 1364.5769; calc. for $[C_{222}H_{354}N_{40}O_{32}]^{4+}$ ($[M+4H]^{4+}$): 1023.6835, found: 1023.6845; calc. for $[C_{222}H_{355}N_{40}O_{32}]^{5+}$ ($[M+5H]^{5+}$): 819.1483, found: 819.1490; calc. for $[C_{222}H_{356}N_{40}O_{32}]^{6+}$ ($[M+6H]^{6+}$): 682.7915, found: 682.7915.

H-^{h}Lys(acetyl)-^{h}Lys$_2$-^{h}Trp$_2$-^{h}Val$_9$-^{h}Gln-^{h}Val$_5$-^{h}Gln-^{h}Val$_3$-^{h}Trp$_2$-^{h}Lys$_2$-NH$_2$ (51)

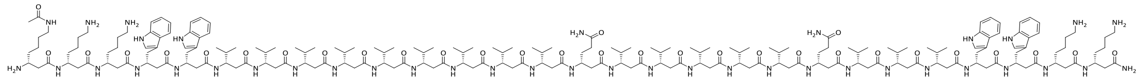

$C_{199}H_{330}N_{40}O_{31}$

3779.08 g/mol

51

The rink amide MBHA resin (44.0 mg, 25.0 µmol, 570 µmol/g, 1.00 eq) was preloaded with Fmoc-D-β^3-Lys(Boc)-OH (**30**) (60.0 mg, 125 µmol, 5.00 eq) following SOP3. The occupancy was tested following SOP4 and determined to be 500 µmol/g. The peptide was synthesised following SOP7 using Fmoc-D-β^3-Lys(Boc)-OH (**30**) (48.3 mg, 100 µmol, 4.00 eq), Fmoc-D-β^3-Trp(Boc)-OH (**33**) (54.0 mg, 100 µmol, 4.00 eq), Fmoc-D-β^3-Val-OH (**29**) (35.3 mg, 100 µmol, 4.00 eq), Fmoc-D-β^3-Gln(Trt)-OH (**34**) (62.4 mg, 100 µmol, 4.00 eq) and Boc-D-β^3-Lys(Fmoc)-OH (**31**) (54.0 mg, 100 µmol, 4.00 eq). Double coupling was performed for Fmoc-D-β^3-Trp(Boc)-OH (**33**). After final Fmoc-deprotection, the free *N*-terminus at the side chain was acetylated with DMF/Ac$_2$O/DIPEA (18:1:1, *v*/*v*/*v*, 1.50 mL) at rt for 10 min and afterwards, the resin was washed with DMF (10 × 2.00 mL), MeOH (10 × 2.00 mL) and DCM (5 × 2.00 mL) and dried overnight under reduced pressure. The cleavage was performed using SOP9 to obtain the crude peptide as a white solid which was purified by preparative HPLC to yield product **51** (3.22 mg, 852 nmol) as a colourless solid.

HPLC (preparative, gradient: 90-100% B in 30 min, λ in nm: 215, 254, 280): t_R = 14.12 min.

ESI-MS (*m*/*z*): 630.8 $[M+6H]^{6+}$, 756.7 $[M+5H]^{5+}$, 945.6 $[M+4H]^{4+}$, 1260.5 $[M+3H]^{3+}$.

HR-MS (ESI): calc. for $[C_{199}H_{333}N_{40}O_{31}]^{3+}$ ($[M+3H]^{3+}$): 1260.5251, found: 1260.5266; calc. for $[C_{199}H_{334}N_{40}O_{31}]^{4+}$ ($[M+4H]^{4+}$): 945.6457, found: 945.6457; calc. for $[C_{199}H_{335}N_{40}O_{31}]^{5+}$ ($[M+5H]^{5+}$): 756.7180, found: 756.7180; calc. for $[C_{199}H_{336}N_{40}O_{31}]^{6+}$ ($[M+6H]^{6+}$): 630.7662, found: 630.7664.

H-^{h}Lys(NBD)-^{h}Lys$_2$-^{h}Trp$_2$-^{h}Val$_9$-^{h}Gln-^{h}Val$_5$-^{h}Gln-^{h}Val$_3$-^{h}Trp$_2$-^{h}Lys$_2$-NH$_2$ (52)

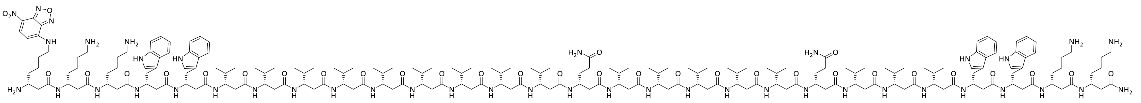

$C_{203}H_{329}N_{43}O_{33}$

3900.13 g/mol

52

The rink amide MBHA resin (44.0 mg, 25.0 µmol, 570 µmol/g, 1.00 eq) was preloaded with Fmoc-D-β^3-Lys(Boc)-OH (**30**) (60.0 mg, 125 µmol, 5.00 eq) following SOP3. The occupancy was tested following SOP4 and determined to be 500 µmol/g. The peptide was synthesised following SOP7 using Fmoc-D-β^3-Lys(Boc)-OH (**30**) (48.3 mg, 100 µmol, 4.00 eq), Fmoc-D-β^3-Trp(Boc)-OH (**33**) (54.0 mg, 100 µmol, 4.00 eq), Fmoc-D-β^3-Val-OH (**29**) (35.3 mg, 100 µmol, 4.00 eq), Fmoc-D-β^3-Gln(Trt)-OH (**34**) (62.4 mg, 100 µmol, 4.00 eq) and Boc-D-β^3-Lys(Fmoc)-OH (**31**) (54.0 mg, 100 µmol, 4.00 eq). Double coupling was performed for Fmoc-D-β^3-Trp(Boc)-OH (**33**). After final Fmoc-deprotection the free *N*-terminus at the side chain was labelled with NBD–Cl (15.0 mg, 75.0 µmol, 3.00 eq) in DMF (345 µL) which was activated with DIPEA (83.0 µL, 500 µmol, 20.0 eq). The reaction mixture was allowed to react at rt overnight. Afterwards, the resin was washed with DMF (10 × 2.00 mL), MeOH (10 × 2.00 mL) and DCM (5 × 2.00 mL) and dried overnight under reduced pressure. The cleavage was performed using SOP9 to obtain the crude peptide as a brown solid which was purified by preparative HPLC to yield product **52** (2.73 mg, 700 nmol) as an orange solid.

HPLC (preparative, gradient: 85-100% B in 30 min, *λ* in nm: 215, 464, 280): t_R = 23.66 min.
ESI-MS (*m/z*): 650.9 $[M+6H]^{6+}$, 780.9 $[M+5H]^{5+}$, 975.9 $[M+4H]^{4+}$, 1300.9 $[M+3H]^{3+}$.
HR-MS (ESI): calc. for $[C_{203}H_{332}N_{43}O_{33}]^{3+}$ ($[M+3H]^{3+}$): 1300.8555, found: 1300.8583; calc. for $[C_{203}H_{333}N_{43}O_{33}]^{4+}$ ($[M+4H]^{4+}$): 975.8935, found: 975.8952; calc. for $[C_{203}H_{334}N_{43}O_{33}]^{5+}$ ($[M+5H]^{5+}$): 780.9162, found: 780.9182; calc. for $[C_{203}H_{335}N_{43}O_{33}]^{6+}$ ($[M+6H]^{6+}$): 650.9314, found: 650.9315.

H-^{h}Lys$_{2}$-^{h}Trp$_{2}$-^{h}Val$_{3}$-^{h}Gln-^{h}Val$_{5}$-^{h}Gln-^{h}Val$_{9}$-^{h}Trp$_{2}$-^{h}Lys$_{2}$-^{h}Lys(TAMRA)-NH$_{2}$ (53)

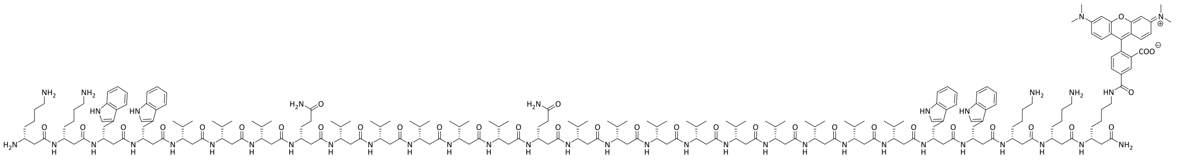

$C_{222}H_{348}N_{42}O_{34}$

4149.49 g/mol

53

The rink amide MBHA resin (44.0 mg, 25.0 µmol, 570 µmol/g, 1.00 eq) was preloaded with Fmoc-D-β^{3}-Lys(Alloc)-OH (**32**) (58.3 mg, 125 µmol, 5.00 eq) following SOP3. The occupancy was tested following SOP4 and determined to be 520 µmol/g. The peptide was synthesised following SOP7 using Fmoc-D-β^{3}-Lys(Boc)-OH (**30**) (48.3 mg, 100 µmol, 4.00 eq), Fmoc-D-β^{3}-Trp(Boc)-OH (**33**) (54.0 mg, 100 µmol, 4.00 eq), Fmoc-D-β^{3}-Val-OH (**29**) (35.3 mg, 100 µmol, 4.00 eq), Fmoc-D-β^{3}-Gln(Trt)-OH (**34**) (62.4 mg, 100 µmol, 4.00 eq) and Boc-D-β^{3}-Lys(Boc)-OH (**57**) (36.0 mg, 100 µmol, 4.00 eq). Double coupling was performed for Fmoc-D-β^{3}-Trp(Boc)-OH (**33**). After Alloc-deprotection following SOP8 the free *N*-terminus was labelled with TAMRA (53.4 mg, 125 µmol, 5.00 eq) in DMF (340 µL) which was activated with PyBOP® (61.5 mg, 118 µmol, 4.70 eq) and DIPEA (41.7 µL, 245 µmol, 9.80 eq) and allowed to react at rt overnight. Afterwards, the resin was washed with DMF (10 × 2.00 mL), MeOH (10 × 2.00 mL) and DCM (5 × 2.00 mL) and dried overnight under reduced pressure. The cleavage was performed using SOP9 to obtain the crude peptide as a pink solid which was purified by preparative HPLC to yield product **53** (5.04 mg, 1.21 µmol) as a pink solid.

HPLC (preparative, gradient: 86-100% B in 30 min, *λ* in nm: 215, 540, 280): t_R = 17.80 min.
ESI-MS (*m/z*): 692.5 $[M+6H]^{6+}$, 830.7 $[M+5H]^{5+}$, 1038.2 $[M+4H]^{4+}$, 1383.9 $[M+3H]^{3+}$.
HR-MS (ESI): calc. for $[C_{222}H_{351}N_{42}O_{34}]^{3+}$ ($[M+3H]^{3+}$): 1383.9024, found: 1383.9027; calc. for $[C_{222}H_{352}N_{42}O_{34}]^{4+}$ ($[M+4H]^{4+}$): 1038.1786, found: 1038.1790; calc. for $[C_{222}H_{353}N_{42}O_{34}]^{5+}$ ($[M+5H]^{5+}$): 830.7443, found: 830.7447; calc. for $[C_{222}H_{354}N_{42}O_{34}]^{6+}$ ($[M+6H]^{6+}$): 692.4549, found: 692.4548.

H-^{h}Lys(acetyl)-^{h}Lys$_2$-^{h}Trp$_2$-^{h}Val$_9$-^{h}Gln-^{h}Val$_2$-^{h}Gln-^{h}Val$_2$-^{h}Gln-^{h}Val$_3$-^{h}Trp$_2$-^{h}Lys$_2$-NH$_2$ (54)

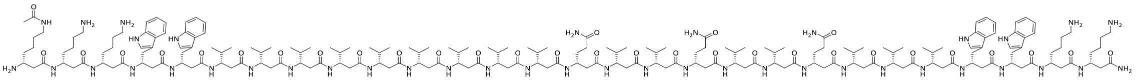

$C_{199}H_{329}N_{41}O_{32}$

3808.08 g/mol

54

The rink amide MBHA resin (44.0 mg, 25.0 µmol, 570 µmol/g, 1.00 eq) was preloaded with Fmoc-D-β^3-Lys(Boc)-OH (**30**) (60.0 mg, 125 µmol, 5.00 eq) following SOP3. The occupancy was tested following SOP4 and determined to be 480 µmol/g. The peptide was synthesised following SOP7 using Fmoc-D-β^3-Lys(Boc)-OH (**30**) (48.3 mg, 100 µmol, 4.00 eq), Fmoc-D-β^3-Trp(Boc)-OH (**33**) (54.0 mg, 100 µmol, 4.00 eq), Fmoc-D-β^3-Val-OH (**29**) (35.3 mg, 100 µmol, 4.00 eq), Fmoc-D-β^3-Gln(Trt)-OH (**34**) (62.4 mg, 100 µmol, 4.00 eq) and Boc-D-β^3-Lys(Fmoc)-OH (**31**) (54.0 mg, 100 µmol, 4.00 eq). Double coupling was performed for Fmoc-D-β^3-Trp(Boc)-OH (**33**). After final Fmoc-deprotection the free *N*-terminus at the side chain was acetylated with DMF/Ac_2O/DIPEA (18:1:1, *v*/*v*/*v*, 1.50 mL) at rt for 10 min and afterwards, the resin was washed with DMF (10 × 2.00 mL), MeOH (10 × 2.00 mL) and DCM (5 × 2.00 mL) and dried overnight under reduced pressure. The cleavage was performed using SOP9 to obtain the crude peptide as a white solid which was purified by preparative HPLC to yield product **54** (2.62 mg, 703 nmol) as a colourless solid.

HPLC (preparative, gradient: 90-100% B in 30 min, λ in nm: 215, 254, 280): t_R = 15.22 min.
ESI-MS (*m/z*): 635.6 $[M+6H]^{6+}$, 762.5 $[M+5H]^{5+}$, 952.9 $[M+4H]^{4+}$, 1270.2 $[M+3H]^{3+}$.
HR-MS (ESI): calc. for $[C_{199}H_{332}N_{41}O_{32}]^{3+}$ ($[M+3H]^{3+}$): 1270.1885, found: 1270.1913; calc. for $[C_{199}H_{333}N_{41}O_{32}]^{4+}$ ($[M+4H]^{4+}$): 952.8932, found: 952.8952; calc. for $[C_{199}H_{334}N_{41}O_{32}]^{5+}$ ($[M+5H]^{5+}$): 762.5160, found: 762.5183; calc. for $[C_{199}H_{335}N_{41}O_{32}]^{6+}$ ($[M+6H]^{6+}$): 635.5979, found: 635.5982.

H-^{h}Lys(NBD)-^{h}Lys$_2$-^{h}Trp$_2$-^{h}Val$_9$-^{h}Gln-^{h}Val$_2$-^{h}Gln-^{h}Val$_2$-^{h}Gln-^{h}Val$_3$-^{h}Trp$_2$-^{h}Lys$_2$-NH$_2$ (55)

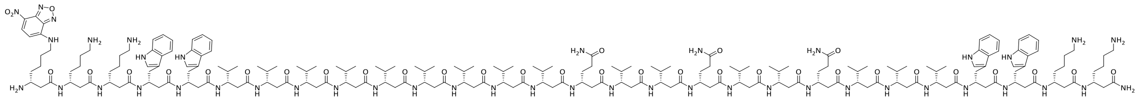

$C_{203}H_{328}N_{44}O_{34}$

3929.13 g/mol

55

The rink amide MBHA resin (44.0 mg, 25.0 µmol, 570 µmol/g, 1.00 eq) was preloaded with Fmoc-D-β^3-Lys(Boc)-OH (**30**) (60.0 mg, 125 µmol, 5.00 eq) following SOP3. The occupancy was tested following SOP4 and determined to be 480 µmol/g. The peptide was synthesised following SOP7 using Fmoc-D-β^3-Lys(Boc)-OH (**30**) (48.3 mg, 100 µmol, 4.00 eq), Fmoc-D-β^3-Trp(Boc)-OH (**33**) (54.0 mg, 100 µmol, 4.00 eq), Fmoc-D-β^3-Val-OH (**29**) (35.3 mg, 100 µmol, 4.00 eq), Fmoc-D-β^3-Gln(Trt)-OH (**34**) (62.4 mg, 100 µmol, 4.00 eq) and Boc-D-β^3-Lys(Fmoc)-OH (**31**) (54.0 mg, 100 µmol, 4.00 eq). Double coupling was performed for Fmoc-D-β^3-Trp(Boc)-OH (**33**). After final Fmoc-deprotection the free *N*-terminus at the side chain was labelled with NBD–Cl (15.0 mg, 75.0 µmol, 3.00 eq) in DMF (345 µL) which was activated with DIPEA (83.0 µL, 500 µmol, 20.0 eq). The reaction mixture was allowed to react at rt overnight. Afterwards, the resin was washed with DMF (10 × 2.00 mL), MeOH (10 × 2.00 mL) and DCM (5 × 2.00 mL) and dried overnight under reduced pressure. The cleavage was performed using SOP9 to obtain the crude peptide as a brown solid which was purified by preparative HPLC to yield product **55** (2.36 mg, 600 nmol) as an orange solid.

HPLC (preparative, gradient: 85-100% B in 30 min, *λ* in nm: 215, 464, 280): t_R = 23.38 min.

ESI-MS (*m*/*z*): 655.8 $[M+6H]^{6+}$, 786.7 $[M+5H]^{5+}$, 983.1 $[M+4H]^{4+}$, 1310.5 $[M+3H]^{3+}$.

HR-MS (ESI): calc. for $[C_{203}H_{331}N_{44}O_{34}]^{3+}$ ($[M+3H]^{3+}$): 1310.5189, found: 1310.5194; calc. for $[C_{203}H_{332}N_{44}O_{34}]^{4+}$ ($[M+4H]^{4+}$): 983.1410, found: 983.1415; calc. for $[C_{203}H_{333}N_{44}O_{34}]^{5+}$ ($[M+5H]^{5+}$): 786.7143, found: 786.7150; calc. for $[C_{203}H_{334}N_{44}O_{34}]^{6+}$ ($[M+6H]^{6+}$): 655.7631, found: 655.7627.

H-^{h}Lys$_2$-^{h}Trp$_2$-^{h}Val$_3$-^{h}Gln-^{h}Val$_2$-^{h}Gln-^{h}Val$_2$-^{h}Gln-^{h}Val$_9$-^{h}Trp$_2$-^{h}Lys$_2$-^{h}Lys(TAMRA)-NH$_2$ (56)

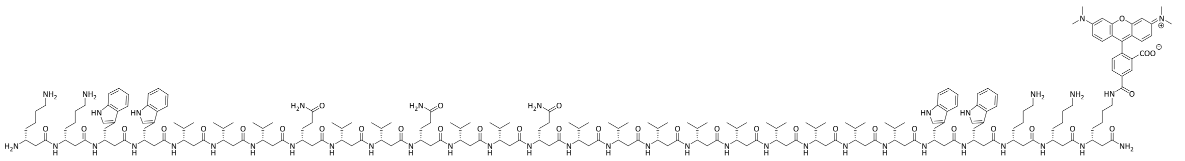

$C_{222}H_{347}N_{43}O_{35}$

4178.48 g/mol

56

The rink amide MBHA resin (44.0 mg, 25.0 µmol, 570 µmol/g, 1.00 eq) was preloaded with Fmoc-D-β^3-Lys(Alloc)-OH (**32**) (58.3 mg, 125 µmol, 5.00 eq) following SOP3. The occupancy was tested following SOP4 and determined to be 460 µmol/g. The peptide was synthesised following SOP7 using Fmoc-D-β^3-Lys(Boc)-OH (**30**) (48.3 mg, 100 µmol, 4.00 eq), Fmoc-D-β^3-Trp(Boc)-OH (**33**) (54.0 mg, 100 µmol, 4.00 eq), Fmoc-D-β^3-Val-OH (**29**) (35.3 mg, 100 µmol, 4.00 eq), Fmoc-D-β^3-Gln(Trt)-OH (**34**) (62.4 mg, 100 µmol, 4.00 eq) and Boc-D-β^3-Lys(Boc)-OH (**57**) (36.0 mg, 100 µmol, 4.00 eq). Double coupling was performed for Fmoc-D-β^3-Trp(Boc)-OH (**33**). After Alloc-deprotection following SOP8 the free *N*-terminus was labelled with TAMRA (53.4 mg, 125 µmol, 5.00 eq) in DMF (340 µL) which was activated with PyBOP® (61.5 mg, 118 µmol, 4.70 eq) and DIPEA (41.7 µL, 245 µmol, 9.80 eq) and allowed to react at rt overnight. Afterwards, the resin was washed with DMF (10 × 2.00 mL), MeOH (10 × 2.00 mL) and DCM (5 × 2.00 mL) and dried overnight under reduced pressure. The cleavage was performed using SOP9 to obtain the crude peptide as a pink solid which was purified by preparative HPLC to yield product **56** (3.45 mg, 825 nmol) as a pink solid.

HPLC (preparative, gradient: 85-100% B in 30 min, λ in nm: 215, 540, 280): t_R = 18.57 min.
ESI-MS (*m/z*): 697.3 $[M+6H]^{6+}$, 836.5 $[M+5H]^{5+}$, 1045.4 $[M+4H]^{4+}$, 1393.6 $[M+3H]^{3+}$.
HR-MS (ESI): calc. for $[C_{222}H_{350}N_{43}O_{35}]^{3+}$ ($[M+3H]^{3+}$): 1393.5658, found: 1393.5667; calc. for $[C_{222}H_{351}N_{43}O_{35}]^{4+}$ ($[M+4H]^{4+}$): 1045.4261, found: 1045.4271; calc. for $[C_{222}H_{352}N_{43}O_{35}]^{5+}$ ($[M+5H]^{5+}$): 836.5424, found: 836.5435; calc. for $[C_{222}H_{353}N_{43}O_{35}]^{6+}$ ($[M+6H]^{6+}$): 697.2865, found: 697.2874.

APPENDIX

7.1 Concentration dependent Fluorescence Emission Spectra of the KALPs 18-20 at a P/L-ratios 1/500 and 1/1000 at 25 °C

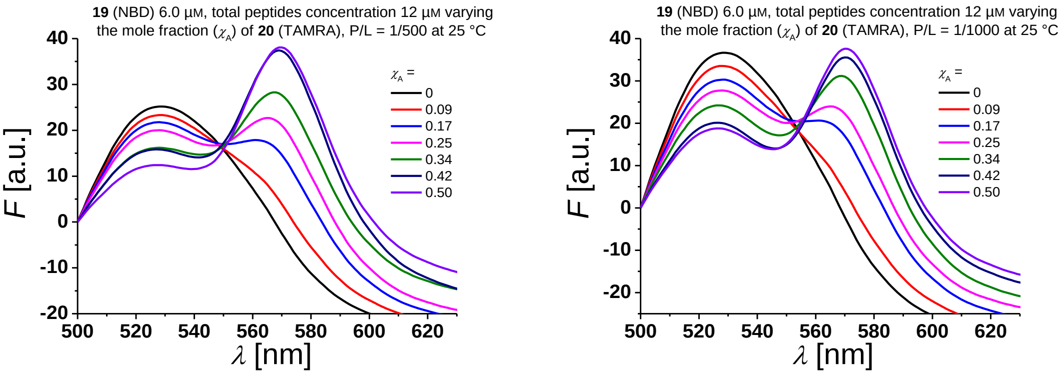

19 (NBD) 6.0 µM, total peptides concentration 12 µM varying the mole fraction (χ_A) of **20** (TAMRA), P/L = 1/500 at 25 °C

19 (NBD) 6.0 µM, total peptides concentration 12 µM varying the mole fraction (χ_A) of **20** (TAMRA), P/L = 1/1000 at 25 °C

Figure 51: Concentration dependent fluorescence spectra of compound 19 (NBD) at 6.0 µM with varying amounts of compound 29 (TAMRA) in DOPC LUVs at 25 °C. The P/L-ratio of 1/500 and 1/1000 and the total peptide concentration of 12 µM were kept constant by addition of the non-labelled peptide 18. The data points at 530 nm were used in the normalized fluorescence emission plots as a function of χ_A.

7.2 Concentration dependent Fluorescence Emission Spectra of the KALPs 21-23 at a P/L-ratios 1/100, 1/250, 1/500, and 1/1000 at 25 °C and at 60 °C

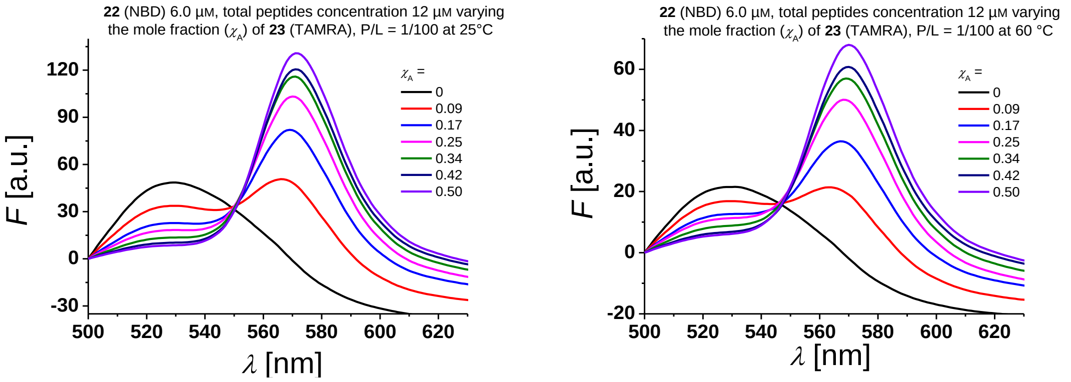

Figure 52: Concentration dependent fluorescence spectra of compound 22 (NBD) at 6.0 µM with varying amounts of compound 23 (TAMRA) in DOPC LUVs at 25 °C and 60 °C. The P/L-ratio of 1/100 and the total peptide concentration of 12 µM were kept constant by addition of the non-labelled peptide 21. The data points at 530 nm were used in the normalized fluorescence emission plots as a function of χ_A.

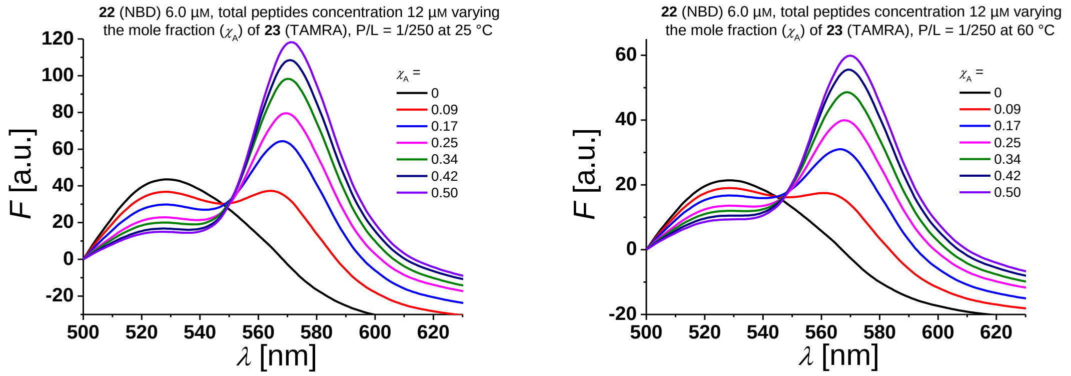

Figure 53: Concentration dependent fluorescence spectra of compound 22 (NBD) at 6.0 µM with varying amounts of compound 23 (TAMRA) in DOPC LUVs at 25 °C and 60 °C. The P/L-ratio of 1/250 and the total peptide concentration of 12 µM were kept constant by addition of the non-labelled peptide 21. The data points at 530 nm were used in the normalized fluorescence emission plots as a function of χ_A.

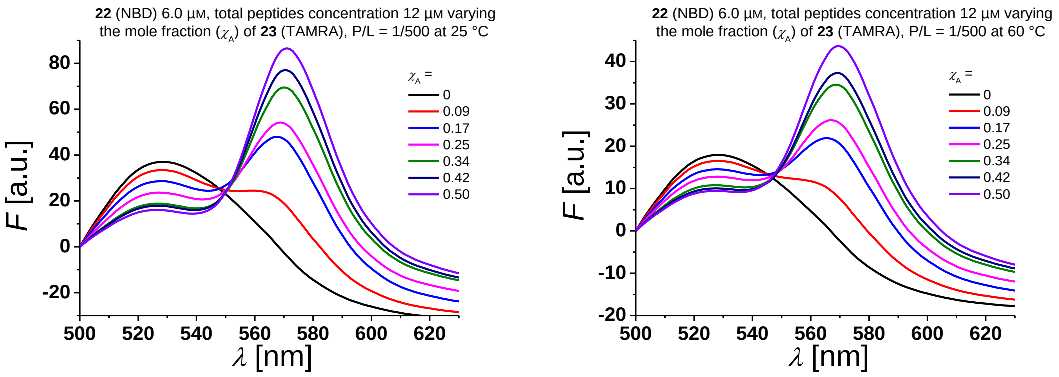

22 (NBD) 6.0 μM, total peptides concentration 12 μM varying the mole fraction (χ_A) of **23** (TAMRA), P/L = 1/500 at 25 °C

22 (NBD) 6.0 μM, total peptides concentration 12 μM varying the mole fraction (χ_A) of **23** (TAMRA), P/L = 1/500 at 60 °C

Figure 54: Concentration dependent fluorescence spectra of compound 22 (NBD) at 6.0 μM with varying amounts of compound 23 (TAMRA) in DOPC LUVs at 25 °C and 60 °C. The P/L-ratio of 1/500 and the total peptide concentration of 12 μM were kept constant by addition of the non-labelled peptide 21. The data points at 530 nm were used in the normalized fluorescence emission plots as a function of χ_A.

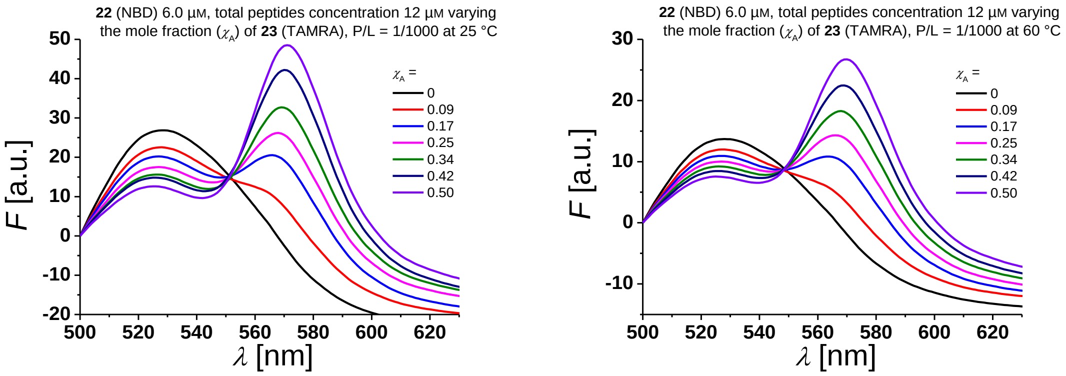

22 (NBD) 6.0 μM, total peptides concentration 12 μM varying the mole fraction (χ_A) of **23** (TAMRA), P/L = 1/1000 at 25 °C

22 (NBD) 6.0 μM, total peptides concentration 12 μM varying the mole fraction (χ_A) of **23** (TAMRA), P/L = 1/1000 at 60 °C

Figure 55: Concentration dependent fluorescence spectra of compound 22 (NBD) at 6.0 μM with varying amounts of compound 23 (TAMRA) in DOPC LUVs at 25 °C and 60 °C. The P/L-ratio of 1/1000 and the total peptide concentration of 12 μM were kept constant by addition of the non-labelled peptide 21. The data points at 530 nm were used in the normalized fluorescence emission plots as a function of χ_A.

7.3 Concentration dependent Fluorescence Emission Spectra of the β-Peptides 48-50, 51-53 and 54-56 at a P/L-ratio = 1/500 at 25 °C and 60 °C

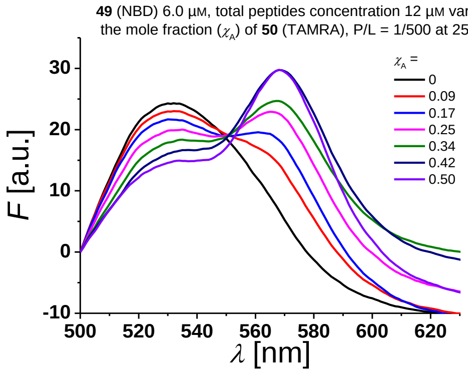

Figure 56: Concentration dependent fluorescence spectra of compound 49 (NBD) at 6.0 µM with varying amounts of compound 50 (TAMRA) in DOPC LUVs at 25 °C. The P/L-ratio of 1/500 and the total peptide concentration of 12 µM were kept constant by addition of the non-labelled peptide 48. The data points at 530 nm were used in the normalized fluorescence emission plots as a function of χ_A (Figure 44).

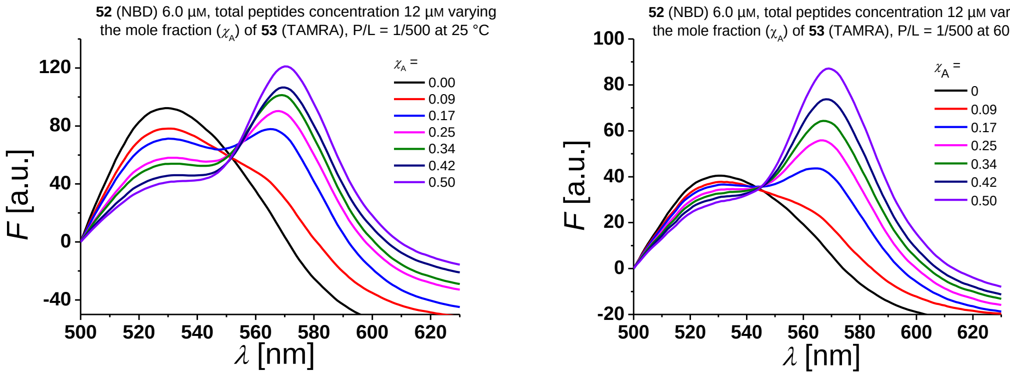

Figure 57: Concentration dependent fluorescence spectra of compound 52 (NBD) at 6.0 µM with varying amounts of compound 53 (TAMRA) in DOPC LUVs at 25 °C (left) and 60 °C (right). The P/L-ratio of 1/500 and the total peptide concentration of 12 µM were kept constant by addition of the non-labelled peptide 51. The data points at 530 nm (25 °C and 60 °C) were used in the normalized fluorescence emission plots as a function of χ_A (Figure 44).

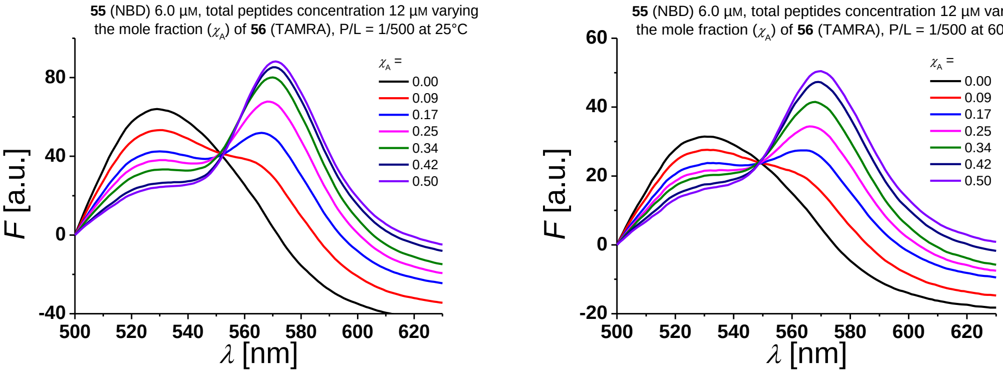

Figure 58: Concentration dependent fluorescence spectra of compound 55 (NBD) at 6.0 µM with varying amounts of compound 56 (TAMRA) in DOPC LUVs at 25 °C (left) and 60 °C (right). The P/L-ratio of 1/500 and the total peptide concentration of 12 µM were kept constant by addition of the non-labelled peptide 54. The data points at 530 nm (25 °C and 60 °C) were used in the normalized fluorescence emission plots as a function of χ_A (Figure 44).

7.4 Concentration dependent Fluorescence Emission Spectra of the β-Peptides 51-53 and 54-56 at the P/L-ratios 1/750 and 1/1000 at 25 °C

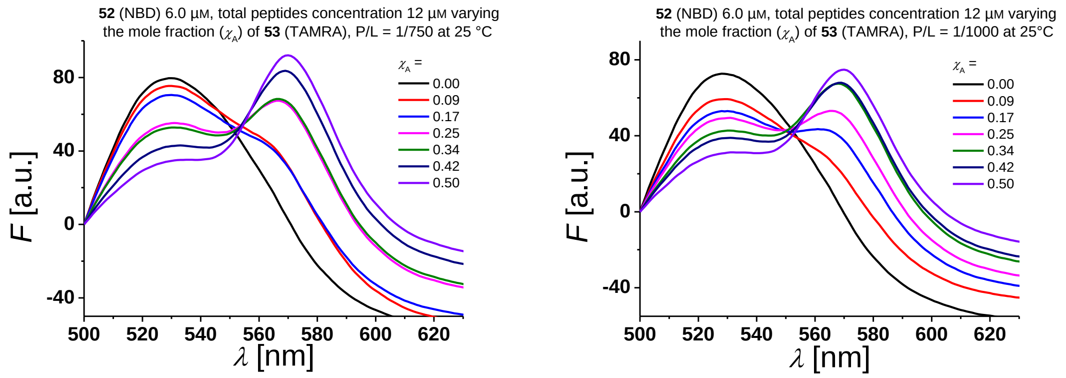

Figure 59: Concentration dependent fluorescence spectra of compound 52 (NBD) at 6.0 µM with varying amounts of compound 53 (TAMRA) in DOPC LUVs at 25 °C. The P/L-ratio of 1/750 (left) or 1/1000 (right) and the total peptide concentration of 12 µM were kept constant by addition of the non-labelled peptide 51. The data points at 530 nm were used in the normalized fluorescence emission plots as a function of χ_A (Figure 61).

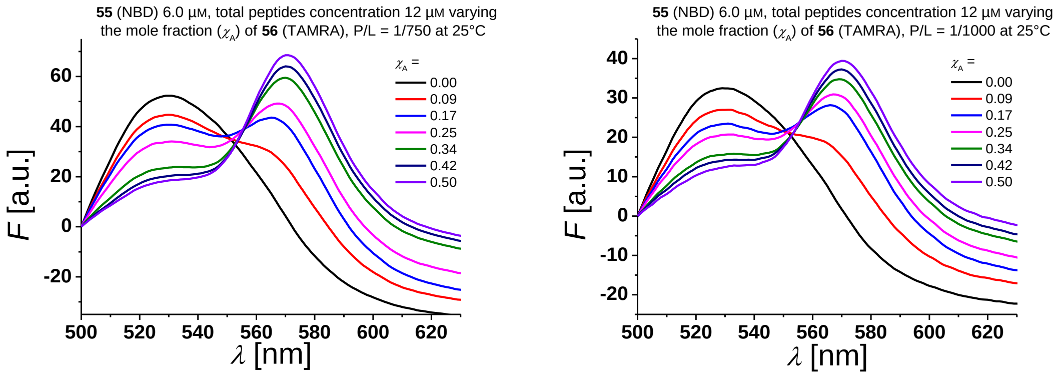

Figure 60: Concentration dependent fluorescence spectra of compound 55 (NBD) at 6.0 µM with varying amounts of compound 56 (TAMRA) in DOPC LUVs at 25 °C. The P/L-ratio of 1/750 (left) or 1/1000 (right) and the total peptide concentration of 12 µM were kept constant by addition of the non-labelled peptide 54. The data points at 530 nm were used in the normalized fluorescence emission plots as a function of χ_A (Figure 61).

7.5 Relative Changes in Donor Fluorescence Emission (F/F_0) as a Function of increasing Acceptor Concentration (β-Peptides 51-56)

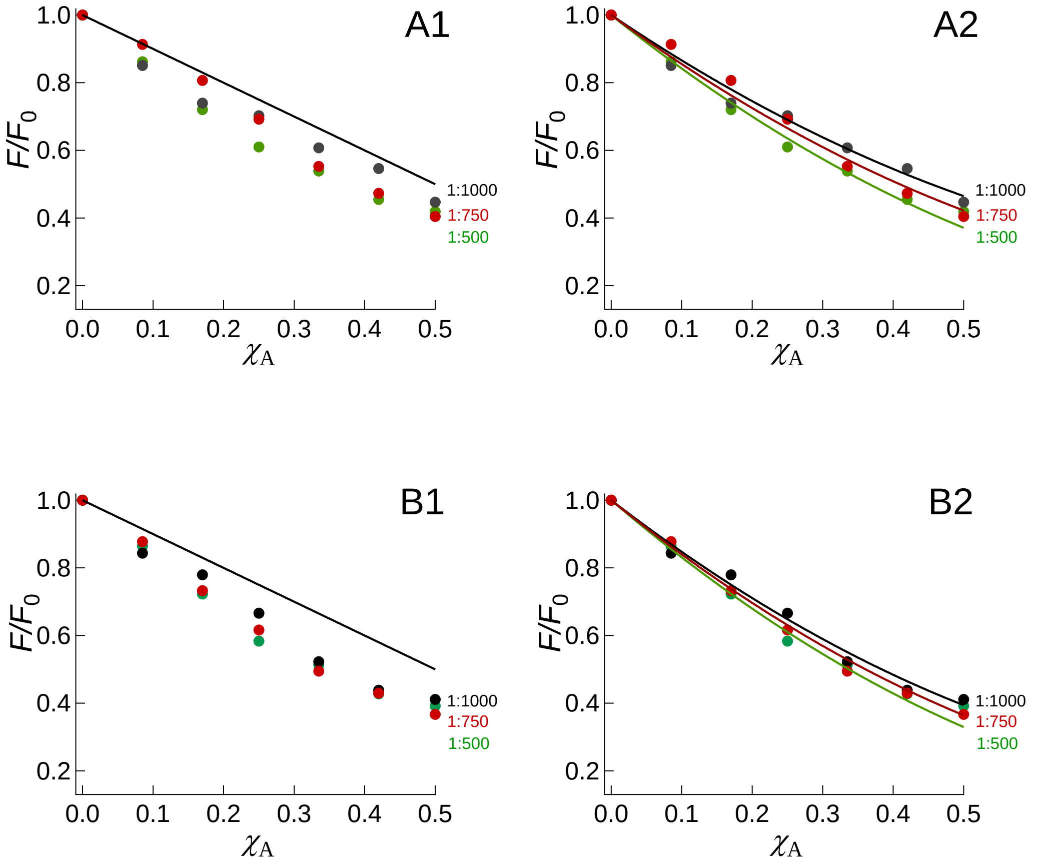

Figure 61: FRET analysis of A: two ^{h}Gln and B: three ^{h}Gln in 100 nm DOPC vesicles. The relative changes in NBD-fluorescence emission (F/F_0) as a function of increasing acceptor concentration χ_A are plotted. The solid lines are the results of a global fit analysis assuming (1) a monomer-dimer and (2) a monomer-trimer equilibrium. The FÖRSTER radius R_0 was determined to be $R_0 = 5.1$ nm as obtained from results with the β-peptides without recognition units assuming that only monomers are in the membrane and the FRET occurs statistically.[15,83] A monomer-dimer equilibrium does not explain the data. Even the assumption of a pure dimer (solid black line) does not explain the observed plots. For a monomer-trimer equilibrium, the following dissociation constants were obtained for two ^{h}Gln: A2: $K_D = (17.2 \pm 7.0) \cdot 10^{-8}$ MF^2 and three ^{h}Gln: B2: $K_D = (4.4 \pm 4.3) \cdot 10^{-8}$ MF^2.

ABBREVIATIONS

AI	azaindole
Alloc	allyloxycarbonyl
Boc	*tert*-butoxycarbonyl
CD	circular dichroism
DBU	1,8-diazabicyclo[5.4.0]undec-7-en
DCM	dichlormethane
DIBAL	diisobutylaluminiumhydride
DIC	*N*,*N*ʹ-diisopropylcarbodiimide
DIPEA	*N*,*N*-diisopropylethylamine
DMF	*N*,*N*-dimethylformamide
DMPC	1,2-dimyristoyl-*sn*-glycero-3-phosphocholine
DMSO	dimethyl sulfoxide
DOPC	1,2-dioleoyl-*sn*-glycero-3-phosphocholine
EDP	electron density profile
ESI	electrospray-ionisation
Fmoc	fluorenylmethoxycarbonyl
FRET	fluorescence resonance energy transfer
GID	gracing incidence diffraction
HATU	*O*-(7-azabenzotriazol-1-yl)-*N*,*N*,*N*ʹ,*N*ʹ-tetramethyluronium hexafluorophosphate
HBTU	*O*-(1*H*-benzotriazol-1-yl)-*N*,*N*,*N*ʹ,*N*ʹ-tetramethyluronium hexafluorophosphate
HOAt	1-hydroxy-7-azabenzotriazole
HOBt	1-hydroxybenzotriazole
HPLC	high performance liquid chromatography
HR-MS	high resolution mass spectrometry
KALP	peptides of general sequence: GKK(LA)$_n$LKKA
LUV	large unilamellar vesicle
MBHA	4-methylbenzhydrylamine
MF	mole fraction

NBD	7-nitrobenz-2-oxa-1,3-diazol-4-yl
NMP	*N*-methyl-pyrrolidone
NMR	nuclear magnetic resonance
OBzl	benzyloxy
PG	protecting group
P/L	peptide-to-lipid
ppm	parts per million
Ph	phenyl
PyBOP®	benzotriazole-1-yl-oxy-tris-pyrrolodino-phosphonium hexafluorophosphate
rt	room temperature
SOP	standard operating procedure
SPPS	solid phase peptide synthesis
SUV	small unilamellar vesicle
TAMRA	5(6)-carboxytetramethylrhodamine
Tert	tertiary
TFA	trifluoroacetic acid
TFE	trifluoroethanol
THF	tetrahydrofuran
TIS	triisopropylsilan
TMS	trimethylsilan
t_R	retention time
Trt	trityl
UV	ultraviolet
VIS	visual
v/*v*	volume to volume
WALP	peptides of general sequence: GWW(LA)$_n$LWWA

REFERENCES

[1] F. Hucho, C. Weise, *Angew. Chem.* **2001**, *113*, 3194–3211.

[2] D. Greenbaum, R. Jansen, M. Gerstein, *Bioinformatics* **2002**, *18*, 585–596.

[3] U. Rost, C. Steinem, U. Diederichsen, *Chem. Sci.* **2016**, *7*, 5900–5907.

[4] P. Chakraborty, U. Diederichsen, *Chem. Eur. J.* **2005**, *11*, 3207–3216.

[5] N. Naarmann, B. Bilgiçer, H. Meng, K. Kumar, C. Steinem, *Angew. Chem. Int. Ed.* **2006**, *45*, 2588–2591.

[6] Y. Guo, S. Pogodin, V. A. Baulin, *J. Chem. Phys.* **2014**, *140*, 174903.

[7] J. A. Killian, T. K. M. Nyholm, *Curr. Opin. Struct. Biol.* **2006**, *16*, 473–479.

[8] L. K. Tsou, C. D. Tatko, M. L. Waters, *J. Am. Chem. Soc.* **2002**, *124*, 14917–14921.

[9] M. Rueping, Y. R. Mahajan, B. Jaun, D. Seebach, *Chem. Eur. J.* **2004**, *10*, 1607–1615.

[10] E. M. Sletten, C. R. Bertozzi, *Angew. Chem. Int. Ed Engl.* **2009**, *48*, 6974–6998.

[11] H.-D. Arndt, D. Bockelmann, A. Knoll, S. Lamberth, C. Griesinger, U. Koert, *Angew. Chem. Int. Ed.* **2002**, *41*, 4062–4065.

[12] D. Liu, W. F. DeGrado, *J. Am. Chem. Soc.* **2001**, *123*, 7553–7559.

[13] P. E. Schneggenburger, A. Beerlink, B. Worbs, T. Salditt, U. Diederichsen, *ChemPhysChem* **2009**, *10*, 1567–1576.

[14] A. Küsel, Z. Khattari, P. E. Schneggenburger, A. Banerjee, T. Salditt, U. Diederichsen, *ChemPhysChem* **2007**, *8*, 2336–2343.

[15] P. E. Schneggenburger, S. Müllar, B. Worbs, C. Steinem, U. Diederichsen, *J. Am. Chem. Soc.* **2010**, *132*, 8020–8028.

[16] C. Choma, H. Gratkowski, J. D. Lear, W. F. DeGrado, *Nat. Struct. Mol. Biol.* **2000**, *7*, 161–166.

[17] A. M. Brückner, P. Chakraborty, S. H. Gellman, U. Diederichsen, *Angew. Chem. Int. Ed.* **2003**, *42*, 4395–4399.

[18] S. Takeuchi, T. Tahara, *Proc. Natl. Acad. Sci.* **2007**, *104*, 5285–5290.

[19] C.-P. Chang, H. Wen-Chi, K. Meng-Shin, P.-T. Chou, J. H. Clements, *J. Phys. Chem.* **1994**, *98*, 8801–8805.

[20] Y.-S. Wu, H.-C. Huang, J.-Y. Shen, H.-W. Tseng, J.-W. Ho, Y.-H. Chen, P.-T. Chou, *J. Phys. Chem. B* **2015**, *119*, 2302–2309.

[21] U. Koert, *Angew. Chem. Int. Ed. Engl.* **1997**, *36*, 1836–1837.

[22] U. Rost, Y. Xu, T. Salditt, U. Diederichsen, *ChemPhysChem* **2016**, *17*, 2525–2534.

[23] N. Naarmann, B. Bilgiçer, K. Kumar, C. Steinem, *Biochemistry (Mosc.)* **2005**, *44*, 5188–5195.

[24] A. G. Lee, *Biochim. Biophys. Acta* **2004**, *1666*, 62–87.

[25] S. H. White, W. C. Wimley, *Annu. Rev. Biophys. Biomol. Struct.* **1999**, *28*, 319–365.

[26] L. Popot, D. M. Engelman, *Biochemistry (Mosc.)* **1990**, *29*, 4031–4037.

[27] C. Landolt-Marticorena, K. A. Williams, C. M. Deber, R. A. F. Reithmeier, *J. Mol. Biol.* **1993**, *229*, 602–608.

[28] D. Langosch, J. Heringa, *Proteins* **1998**, *31*, 150–159.

[29] A. R. Curran, D. M. Engelman, *Curr. Opin. Struct. Biol.* **2003**, *13*, 412–417.

[30] N. HyunJoong Joh, A. Min, S. Faham, J. P. Whitelegge, D. Yang, V. L. Woods, J. U. Bowie, *Nature* **2008**, *453*, 1266–1270.

[31] A. M. Stanley, K. G. Fleming, *J. Mol. Biol.* **2007**, *370*, 912–924.

[32] H. Gratkowski, J. D. Lear, W. F. DeGrado, *Proc. Natl. Acad. Sci.* **2001**, *98*, 880–885.

[33] F. X. Zhou, H. J. Merianos, A. T. Brunger, D. M. Engelman, *Proc. Natl. Acad. Sci. U. S. A.* **2001**, *98*, 2250–2255.

[34] P. Cosson, S. P. Lankford, J. S. Bonifacino, R. D. Klausner, *Nature* **1991**, *351*, 414–416.

[35] Y. Chen, R. L. Rich, F. Gai, J. W. Petrich, *J. Phys. Chem.* **1993**, *97*, 1770–1780.

[36] M. Negrerie, F. Gai, S. M. Bellefeuille, J. W. Petrich, *J. Phys. Chem.* **1991**, *95*, 8663–8670.

[37] M. Negrerie, S. M. Bellefeuille, S. Whitham, J. W. Petrich, R. W. Thornburg, *J. Am. Chem. Soc.* **1990**, *112*, 7419–7421.

[38] C. F. Chapman, M. Maroncelli, *J. Phys. Chem.* **1992**, *96*, 8430–8441.

[39] J. W. Young, Z. D. Pozun, K. D. Jordan, D. W. Pratt, *J. Phys. Chem. B* **2013**, *117*, 15695–15700.

[40] W.-S. Yu, C.-C. Cheng, C.-P. Chang, G.-R. Wu, C.-H. Hsu, P.-T. Chou, *J. Phys. Chem. A* **2002**, *106*, 8006–8012.

[41] C. A. Taylor, M. A. El-Bayoumi, M. Kasha, *Proc. Natl. Acad. Sci.* **1969**, *63*, 253–260.

[42] C.-C. Hsieh, K.-Y. Chen, W.-T. Hsieh, C.-H. Lai, J.-Y. Shen, C.-M. Jiang, H.-S. Duan, P.-T. Chou, *ChemPhysChem* **2008**, *9*, 2221–2229.

[43] S. Takeuchi, T. Tahara, *J. Phys. Chem. A* **1998**, *102*, 7740–7753.

[44] J. Guharay, P. K. Sengupta, *Biochem. Biophys. Res. Commun.* **1996**, *219*, 388–392.

[45] F. Gai, Y. Chen, J. W. Petrich, *J. Am. Chem. Soc.* **1992**, *114*, 8343–8345.

[46] J. R. Lakowicz, *Principles of Fluorescence Spectroscopy*, Springer Science & Business Media, **2007**.

[47] L. Stryer, *Science* **1968**, *162*, 526–533.

[48] J. W. Lichtman, J.-A. Conchello, *Nat. Methods* **2005**, *2*, 910–919.

[49] D. Frackowiak, *J. Photochem. Photobiol. B* **1988**, *2*, 399.

[50] T. Förster, *Ann. Phys.* **1948**, *437*, 55–75.

[51] M. Kritsanida, P. Magiatis, A.-L. Skaltsounis, Y. Peng, P. Li, L. P. Wennogle, *J. Nat. Prod.* **2009**, *72*, 2199–2202.

[52] B. A. Wallace, *Protein Sci.* **2003**, *12*, 875–884.

[53] "Fmoc-DL-7-azatryptophan AldrichCPR | Sigma-Aldrich," can be found under http://www.sigmaaldrich.com/catalog/product/aldrich/cds019272?lang=de&region=DE, **31.05.2016**.

[54] "DL-7-Azatryptophan hydrate | Sigma-Aldrich," can be found under http://www.sigmaaldrich.com/catalog/product/sigma/a1632?lang=de&region=DE, **31.05.2016**.

[55] "Fmoc-DL-7-azatryptophan | VWR," can be found under https://us.vwr.com/store/catalog/product.jsp?product_id=8998664, **31.05.2016**.

[56] V. De Filippis, S. De Boni, E. De Dea, D. Dalzoppo, C. Grandi, A. Fontana, *Protein Sci.* **2004**, *13*, 1489–1502.

[57] "Fmoc-(S)-7-Azatryptophan from AnaSpec, EGT Group | Biocompare.com," can be found under http://www.biocompare.com/11119-Chemicals-and-Reagents/4664256-Fmoc-S-7-Azatryptophan/, **31.05.2016**.

[58] "FMOC-L-7-AZATRP | 737007-45-3," can be found under http://www.chemicalbook.com/ChemicalProductProperty_EN_CB2465977.htm, **31.05.2016**.

[59] R.-F. V. LECOINTE L, *Tetrahedron Asymmetry* **1998**, *9*, 1753.

[60] B. P. Noichl, P. M. Durkin, N. Budisa, *Pept. Sci.* **2015**, *104*, 585–600.

[61] W.-G. Su, H. Jia, G. Dai, *Certain Triazolopyridines and Triazolopyrazines, Compositions Thereof and Methods of Use Therefor*, **2011**.

[62] H. Salman, Y. Abraham, S. Tal, S. Meltzman, M. Kapon, N. Tessler, S. Speiser, Y. Eichen, *Eur. J. Org. Chem.* **2005**, *2005*, 2207–2212.

[63] L. Zhang, G. S. Kauffman, J. A. Pesti, J. Yin, *J. Org. Chem.* **1997**, *62*, 6918–6920.

[64] T. M. Weiss, P. C. A. van der Wel, J. A. Killian, R. E. Koeppe II, H. W. Huang, *Biophys. J.* **2003**, *84*, 379–385.

[65] M. R. R. de Planque, J. A. W. Kruijtzer, R. M. J. Liskamp, D. Marsh, D. V. Greathouse, R. E. Koeppe, B. de Kruijff, J. A. Killian, *J. Biol. Chem.* **1999**, *274*, 20839–20846.

[66] M. R. de Planque, E. Goormaghtigh, D. V. Greathouse, R. E. Koeppe, J. A. Kruijtzer, R. M. Liskamp, B. de Kruijff, J. A. Killian, *Biochemistry (Mosc.)* **2001**, *40*, 5000–5010.

[67] M. R. R. de Planque, J. A. Killian, *Mol. Membr. Biol.* **2003**, *20*, 271–284.

[68] D. P. Siegel, V. Cherezov, D. V. Greathouse, R. E. Koeppe, J. A. Killian, M. Caffrey, *Biophys. J.* **2006**, *90*, 200–211.

[69] S. K. Kandasamy, R. G. Larson, *Biophys. J.* **2006**, *90*, 2326–2343.

[70] J. A. Killian, G. von Heijne, *Trends Biochem. Sci.* **2000**, *25*, 429–433.

[71] M. R. R. de Planque, B. B. Bonev, J. A. A. Demmers, D. V. Greathouse, R. E. Koeppe, F. Separovic, A. Watts, J. A. Killian, *Biochemistry (Mosc.)* **2003**, *42*, 5341–5348.

[72] J. A. Killian, *FEBS Lett.* **2003**, *555*, 134–138.

[73] S. H. Park, S. J. Opella, *J. Mol. Biol.* **2005**, *350*, 310–318.

[74] J. A. Killian, *Biochim. Biophys. Acta* **1998**, *1376*, 401–415.

[75] S. M. Kelly, T. J. Jess, N. C. Price, *Biochim. Biophys. Acta BBA - Proteins Proteomics* **2005**, *1751*, 119–139.

[76] M. J. Janiak, D. M. Small, G. G. Shipley, *Biochemistry (Mosc.)* **1976**, *15*, 4575–4580.

[77] P. Manavalan, W. C. Johnson, *Nature* **1983**, *305*, 831–832.

[78] D. M. Lilley, T. J. Wilson, *Curr. Opin. Chem. Biol.* **2000**, *4*, 507–517.

[79] M. Schindler, C. Banning, *BIOspectrum* **2010**, *10*, 298–302.

[80] J. Szöllosi, S. Damjanovich, L. Mátyus, *Cytometry* **1998**, *34*, 159–179.

[81] Z. Fazekas, M. Petrás, Á. Fábián, Z. Pályi-Krekk, P. Nagy, S. Damjanovich, G. Vereb, J. Szöllősi, *Cytometry A* **2008**, *73A*, 209–219.

[82] E. A. Jares-Erijman, T. M. Jovin, *Nat. Biotechnol.* **2003**, *21*, 1387–1395.

[83] P. K. Wolber, B. S. Hudson, *Biophys. J.* **1979**, *28*, 197–210.

[84] R. Roy, S. Hohng, T. Ha, *Nat. Methods* **2008**, *5*, 507–516.

[85] M. Li, L. G. Reddy, R. Bennett, N. D. Silva, L. R. Jones, D. D. Thomas, *Biophys. J.* **1999**, *76*, 2587–2599.

[86] J. D. Lear, H. Gratkowski, W. F. DeGrado, *Biochem. Soc. Trans.* **2001**, *29*, 559–564.

[87] B. Bilgiçer, K. Kumar, *Proc. Natl. Acad. Sci. U. S. A.* **2004**, *101*, 15324–15329.

[88] B. D. Adair, D. M. Engelman, *Biochemistry (Mosc.)* **1994**, *33*, 5539–5544.

[89] N. Naarmann, "Charakterisierung und Kontrolle selbstorganisierter Peptidhelixbündel in Phospholipidmembranen," can be found under http://epub.uni-regensburg.de/10369/, **2006**.

[90] P. L. Kastritis, A. M. J. J. Bonvin, *J. R. Soc. Interface* **2013**, *10*, 20120835.

[91] L. A. Chung, J. D. Lear, W. F. DeGrado, *Biochemistry (Mosc.)* **1992**, *31*, 6608–6616.

[92] J. M. Sanderson, *Org. Biomol. Chem.* **2005**, *3*, 201.

[93] S. Sindbert, S. Kalinin, H. Nguyen, A. Kienzler, L. Clima, W. Bannwarth, B. Appel, S. Müller, C. A. M. Seidel, *J. Am. Chem. Soc.* **2011**, *133*, 2463–2480.

[94] N. Kucerka, S. Tristram-Nagle, J. F. Nagle, *J. Membr. Biol.* **2005**, *208*, 193–202.

[95] N. Castillo, L. Monticelli, J. Barnoud, D. P. Tieleman, *Chem. Phys. Lipids* **2013**, *169*, 95–105.

[96] E. Gazit, *FASEB J.* **2002**, *16*, 77–83.

[97] C. A. Hunter, J. K. M. Sanders, *J. Am. Chem. Soc.* **1990**, *112*, 5525–5534.

[98] K. J. Thomas, R. B. Sunoj, J. Chandrasekhar, V. Ramamurthy, *Langmuir* **2000**, *16*, 4912–4921.

[99] R. C. Dougherty, *J. Chem. Phys.* **1998**, *109*, 7372–7378.

[100] H. A. Scheraga, G. Nemethy, I. Z. Steinberg, *J. Biol. Chem.* **1962**, *237*, 2506–2508.

[101] M. O. Sinnokrot, E. F. Valeev, C. D. Sherrill, *J. Am. Chem. Soc.* **2002**, *124*, 10887–10893.

[102] Andrew G. Myers, James L. Gleason, *Org. Synth.* **1999**, *76*, 57–76.

[103] G. Guichard, S. Abele, D. Seebach, *Helv. Chim. Acta* **1998**, *81*, 187–206.

[104] P. I. Arvidsson, J. Frackenpohl, D. Seebach, *Helv. Chim. Acta* **2003**, *86*, 1522–1553.

[105] D. H. Appella, L. A. Christianson, D. A. Klein, D. R. Powell, X. Huang, J. J. Barchi, S. H. Gellman, *Nature* **1997**, *387*, 381–384.

[106] U. Arnold, M. P. Hinderaker, J. Köditz, R. Golbik, R. Ulbrich-Hofmann, R. T. Raines, *J. Am. Chem. Soc.* **2003**, *125*, 7500–7501.

[107] S. H. Gellman, *Acc. Chem. Res.* **1998**, *31*, 173–180.

[108] D. J. Hill, M. J. Mio, R. B. Prince, T. S. Hughes, J. S. Moore, *Chem. Rev.* **2001**, *101*, 3893–4012.

[109] D. Seebach, J. L. Matthews, *Chem. Commun.* **1997**, 2015–2022.

[110] R. P. Cheng, S. H. Gellman, W. F. DeGrado, *Chem. Rev.* **2001**, *101*, 3219–3232.

[111] W. f. DeGrado, J. p. Schneider, Y. Hamuro, *J. Pept. Res.* **1999**, *54*, 206–217.

[112] Y.-D. Wu, W. Han, D.-P. Wang, Y. Gao, Y.-L. Zhao, *Acc. Chem. Res.* **2008**, *41*, 1418–1427.

[113] A. Glättli, D. Seebach, W. F. van Gunsteren, *Helv. Chim. Acta* **2004**, *87*, 2487–2506.

[114] S. Ahmed, K. Kaur, *Chem. Biol. Drug Des.* **2009**, *73*, 545–552.

[115] E. Juaristi, D. Quintana, B. Lamatsch, D. Seebach, *J. Org. Chem.* **1991**, *56*, 2553–2557.

[116] D. Seebach, M. Overhand, F. N. Kühnle, B. Martinoni, L. Oberer, U. Hommel, H. Widmer, *Helv. Chim. Acta* **1996**, *79*, 913–941.

[117] G. Cardillo, C. Tomasini, *Chem Soc Rev* **1996**, *25*, 117–128.

[118] D. Seebach, A. K. Beck, D. J. Bierbaum, *Chem. Biodivers.* **2004**, *1*, 1111–1239.

[119] E. Juaristi, V. A. Soloshonok, *Enantioselective Synthesis of Beta-Amino Acids*, John Wiley & Sons, **2005**.

[120] D. Seebach, K. Gademann, J. V. Schreiber, J. L. Matthews, T. Hintermann, B. Jaun, L. Oberer, U. Hommel, H. Widmer, *Helv. Chim. Acta* **1997**, *80*, 2033–2038.

[121] T. Hintermann, D. Seebach, *Synlett* **1997**, *1997*, 437–438.

[122] B. S. Patil, G.-R. Vasanthakumar, V. V. S. Babu, *Lett. Pept. Sci.* **2002**, *9*, 231–233.

[123] J. Podlech, D. Seebach, *Liebigs Ann.* **1995**, *1995*, 1217–1228.

[124] R. Bhushan, H. Brückner, *Amino Acids* **2004**, *27*, 231–247.

[125] G. Szókán, G. Mezö, F. Hudecz, *J. Chromatogr. A* **1988**, *444*, 115–122.

[126] R. Bhushan, H. Brückner, V. Kumar, *Biomed. Chromatogr.* **2007**, *21*, 1064–1068.

[127] P. Marfey, *Carlsberg Res. Commun.* **1984**, *49*, 591–596.

[128] O. Flögel, J. D. C. Codée, D. Seebach, P. H. Seeberger, *Angew. Chem. Int. Ed.* **2006**, *45*, 7000–7003.

[129] D. Seebach, J. V. Schreiber, S. Abele, X. Daura, W. F. van Gunsteren, *Helv. Chim. Acta* **2000**, *83*, 34–57.

[130] X. Daura, D. Bakowies, D. Seebach, J. Fleischhauer, W. F. van Gunsteren, P. Krüger, *Eur. Biophys. J.* **2003**, *32*, 661–670.

[131] X. Daura, W. F. van Gunsteren, D. Rigo, B. Jaun, D. Seebach, *Chem. Eur. J.* **1997**, *3*, 1410–1417.

[132] J. R. Allison, M. Müller, W. F. van Gunsteren, *Protein Sci. Publ. Protein Soc.* **2010**, *19*, 2186–2195.

[133] D. Seebach, D. F. Hook, A. Glättli, *Biopolymers* **2006**, *84*, 23–37.

[134] A. Banerjee, P. Balaram, *Curr. Sci.* **1997**, *73*, 1067–1077.

[135] N. Rathore, S. H. Gellman, J. J. de Pablo, *Biophys. J.* **2006**, *91*, 3425–3435.

[136] J. A. Kritzer, J. Tirado-Rives, S. A. Hart, J. D. Lear, W. L. Jorgensen, A. Schepartz, *J. Am. Chem. Soc.* **2005**, *127*, 167–178.

[137] D. Seebach, S. Abele, K. Gademann, B. Jaun, *Angew. Chem.* **1999**, *111*, 1700–1703.

[138] R. F. Epand, L. Raguse, S. H. Gellman, R. M. Epand, *Biochemistry (Mosc.)* **2004**, *43*, 9527–9535.

[139] T. L. Raguse, J. R. Lai, S. H. Gellman, *Helv. Chim. Acta* **2002**, *85*, 4154–4164.

[140] B. W. Gung, D. Zou, A. M. Stalcup, C. E. Cottrell, *J. Org. Chem.* **1999**, *64*, 2176–2177.

[141] Y. Hamuro, J. P. Schneider, W. F. DeGrado, *J. Am. Chem. Soc.* **1999**, *121*, 12200–12201.

[142] T. L. Raguse, J. R. Lai, P. R. LePlae, S. H. Gellman, *Org. Lett.* **2001**, *3*, 3963–3966.

[143] A. J. de Jesus, T. W. Allen, *Biochim. Biophys. Acta BBA - Biomembr.* **2013**, *1828*, 864–876.

[144] K. He, S. J. Ludtke, Y. Wu, H. W. Huang, *Biophys. J.* **1993**, *64*, 157–162.

[145] B. Bechinger, *Biophys. J.* **2001**, *81*, 2251–2256.

[146] P. E. Schneggenburger, A. Beerlink, B. Weinhausen, T. Salditt, U. Diederichsen, *Eur. Biophys. J.* **2011**, *40*, 417–436.

[147] D. M. Petrović, K. Leenhouts, M. L. van Roosmalen, F. KleinJan, J. Broos, *Anal. Biochem.* **2012**, *428*, 111–118.

[148] F. S. Abrams, E. London, *Biochemistry (Mosc.)* **1993**, *32*, 10826–10831.

[149] S. Stoller, G. Sicoli, T. Y. Baranova, M. Bennati, U. Diederichsen, *Angew. Chem.* **2011**, *123*, 9917–9920.

[150] D. Pan, W. Wang, W. Liu, L. Yang, H. W. Huang, *J. Am. Chem. Soc.* **2006**, *128*, 3800–3807.

[151] D. Vaknin, P. Krüger, M. Lösche, *Phys. Rev. Lett.* **2003**, *90*, 178102.

[152] A. B. Ramesha, G. M. Raghavendra, K. N. Nandeesh, K. S. Rangappa, K. Mantelingu, *Tetrahedron Lett.* **2013**, *54*, 95–100.

[153] D. Wernic, J. DiMaio, J. Adams, *J. Org. Chem.* **1989**, *54*, 4224–4228.

[154] M. Mentzel, H. M. R. Hoffmann, *J. Für Prakt. ChemieChemiker-Ztg.* **1997**, *339*, 517–524.

[155] C. Douat, A. Heitz, J. Martinez, J.-A. Fehrentz, *Tetrahedron Lett.* **2001**, *42*, 3319–3321.

[156] M. Paris, C. Pothion, A. Heitz, J. Martinez, J.-A. Fehrentz, *Tetrahedron Lett.* **1998**, *39*, 1341–1344.

[157] J.-C. Meillon, N. Voyer, *Angew. Chem.* **1997**, *109*, 1004–1006.

[158] D. A. Kelkar, A. Chattopadhyay, *Biochim. Biophys. Acta BBA-Biomembr.* **2007**, *1768*, 2011–2025.

[159] J. K. Murray, S. H. Gellman, *Org. Lett.* **2005**, *7*, 1517–1520.

[160] M. A. Andrade, P. Chacon, J. J. Merelo, F. Moran, *Protein Eng.* **1993**, *6*, 383–390.

[161] J. Gardiner, R. I. Mathad, B. Jaun, J. V. Schreiber, O. Flögel, D. Seebach, *Helv. Chim. Acta* **2009**, *92*, 2698–2721.

[162] R. W. Woody, *Eur. Biophys. J. EBJ* **1994**, *23*, 253–262.

[163] R. W. Woody, *Biopolymers* **1978**, *17*, 1451–1467.

[164] A. Chakrabartty, T. Kortemme, S. Padmanabhan, R. L. Baldwin, *Biochemistry (Mosc.)* **1993**, *32*, 5560–5565.

[165] H. E. Auer, *J. Am. Chem. Soc.* **1973**, *95*, 3003–3011.

[166] H. T. Tien, E. A. Dawidowicz, *J. Colloid Interface Sci.* **1966**, *22*, 438–453.

[167] S. Mann, J. P. Hannington, R. J. P. Williams, *Nature* **1986**, *324*, 565–567.

[168] Y. Lyatskaya, Y. Liu, S. Tristram-Nagle, J. Katsaras, J. F. Nagle, *Phys. Rev. E Stat. Nonlin. Soft Matter Phys.* **2001**, *63*, 11907.

[169] M. Seul, M. J. Sammon, *Thin Solid Films* **1990**, *185*, 287–305.

[170] A. M. Seddon, P. Curnow, P. J. Booth, *Biochim. Biophys. Acta* **2004**, *1666*, 105–117.

[171] T. Salditt, *Curr. Opin. Struct. Biol.* **2003**, *13*, 467–478.

[172] C. Li, D. Constantin, T. Salditt, *J. Phys. Condens. Matter* **2004**, *16*, S2439.

[173] A. Spaar, T. Salditt, *Biophys. J.* **2003**, *85*, 1576–1584.

[174] S. Aeffner, T. Reusch, B. Weinhausen, T. Salditt, *Eur. Phys. J. E* **2009**, *30*, 205–214.

[175] W. T. Heller, A. J. Waring, R. I. Lehrer, T. A. Harroun, T. M. Weiss, L. Yang, H. W. Huang, *Biochemistry (Mosc.)* **2000**, *39*, 139–145.

[176] W. C. Hung, F. Y. Chen, H. W. Huang, *Biochim. Biophys. Acta BBA - Biomembr.* **2000**, *1467*, 198–206.

[177] T. Salditt, C. Li, A. Spaar, *Biochim. Biophys. Acta BBA - Biomembr.* **2006**, *1758*, 1483–1498.

[178] K. Hristova, S. H. White, *Biophys. J.* **1998**, *74*, 2419–2433.

[179] B. Weinhausen, S. Aeffner, T. Reusch, T. Salditt, *Biophys. J.* **2012**, *102*, 2121–2129.

[180] A. Spaar, C. Münster, T. Salditt, *Biophys. J.* **2004**, *87*, 396–407.

[181] J. S. Hub, T. Salditt, M. C. Rheinstädter, B. L. de Groot, *Biophys. J.* **2007**, *93*, 3156–3168.

[182] M. A. Lemmon, D. M. Engelman, *FEBS Lett.* **1994**, *346*, 17–20.

[183] D. H. Appella, Barchi Joseph J., S. R. Durell, S. H. Gellman, *J. Am. Chem. Soc.* **1999**, *121*, 2309–2310.

[184] J. T. Vivian, P. R. Callis, *Biophys. J.* **2001**, *80*, 2093–2109.

[185] J. Ren, S. Lew, Z. Wang, E. London, *Biochemistry (Mosc.)* **1997**, *36*, 10213–10220.

[186] S. Lew, J. Ren, E. London, *Biochemistry (Mosc.)* **2000**, *39*, 9632–9640.

[187] J. Ren, S. Lew, J. Wang, E. London, *Biochemistry (Mosc.)* **1999**, *38*, 5905–5912.

[188] C. D. Geddes, *Reviews in Fluorescence 2007*, Springer Science & Business Media, **2009**.

[189] H. Butenschön, K. P. Vollhardt, N. E. Schore, *Organische Chemie*, Wiley-VCH, Weinheim, **2000**.

[190] D. Voet, J. G. Voet, *Biochemistry*, John Wiley & Sons, Hoboken, NJ, **2011**.

[191] N. J. Greenfield, *Nat. Protoc.* **2007**, *1*, 2876–2890.

[192] A. Pingoud, C. Urbanke, *Arbeitsmethoden der Biochemie*, Walter De Gruyter, **1997**.

[193] *Novabiochem® Peptide Synthesis*, Peptide Synthesis Protocols, **2012**.

[194] M. Gude, J. Ryf, P. D. White, *Lett. Pept. Sci.* **2002**, *9*, 203–206.

[195] E. Kaiser, R. L. Colescott, C. D. Bossinger, P. I. Cook, *Anal. Biochem.* **1970**, *34*, 595–598.

[196] B. Blankemeyer-Menge, M. Nimtz, R. Frank, *Tetrahedron Lett.* **1990**, *31*, 1701–1704.

[197] H. Wu, Y. Li, G. Bai, Y. Niu, Q. Qiao, J. D. Tipton, C. Cao, J. Cai, *Chem. Commun.* **2014**, *50*, 5206–5208.

[198] H. Choi, J. v. Aldrich, *Int. J. Pept. Protein Res.* **1993**, *42*, 58–63.

[199] D. S. King, C. G. Fields, G. B. Fields, *Int. J. Pept. Protein Res.* **1990**, *36*, 255–266.

[200] R. C. MacDonald, R. I. MacDonald, B. P. M. Menco, K. Takeshita, N. K. Subbarao, L. Hu, *Biochim. Biophys. Acta BBA - Biomembr.* **1991**, *1061*, 297–303.

ACKNOWLEDGEMENTS

Mein besonderer Dank gilt Prof. Dr. Ulf Diederichsen für sein Vertrauen, die interessante Themenstellung, die gewährte wissenschaftliche Freiheit, die gute Betreuung, die entspannte Arbeitsatmosphäre und die Unterstützung während der gesamten Zeit meiner Promotion.

Ebenso danke ich Prof. Dr. Claudia Steinem für die produktive Kooperation, ihre stetige Diskussionsbereitschaft sowie für die gemeinsame Arbeit am Paper und die Übernahme des Korreferats.

Prof. Dr. Kai Tittmann, Prof. Dr. Dietmar Stalke, Dr. Franziska Thomas und Dr. Inke Siewert danke ich für die Bereitschaft meiner Prüfungskommission anzugehören.

Meinen Kooperationspartnern Yihui Xu und Prof. Dr. Tim Salditt danke ich für die gute Zusammenarbeit am Diiodo-Projekt.

Dr. Holm Frauendorf und seinen Mitarbeitern sowie Dipl.-Chem. Reinhold Machinek, Dr. Michael John und der gesamten NMR-Abteilung danke ich für die Aufnahmen der Massen- und NMR-Spektren.

Juliane Gräfe (jetzt Schuster☺), Angela Heinemann und Aoife Neville danke ich für ihre Hilfe in allen organisatorischen Belangen.

Für das Korrekturlesen meiner Arbeit danke ich von ganzem Herzen Peter Stollberg, Dr. Hanna Radzey, Raik Artschwager, Aoife Neville, Markus Wiegand und Denis Pahlke.

Allen aktuellen und ehemaligen Mitgliedern des AK Diederichsen danke ich für die abwechslungsreiche Zeit während meiner Diplom- und Doktorarbeit.

Insbesondere möchte ich meinen aktuellen und ehemaligen Laborkollegen Dr. Annika Groschner, Dr. Hanna Radzey, Dr. Samit Guha, Dr. Zeynep Kanlidere, Dr. Marta Gascon Moya, Dr. Tatiana Baranova, Dr. Marta Anna Cal, Atida Nasufovska, Denis Pahlke, Dominik Herkt, Florian Rüping, Markus Wiegand, Janine Wegner und Julia Schneider für den immer witzigen und niemals langweilig werdenden Laboralltag danken.

Den zahlreichen von mir betreuten Bachelor- und Masterstudenten, Abteilungspraktikanten sowie Austauschstudenten danke ich für die Unterstützung meiner Forschungsarbeit und die große Freude, die ich mit euch allen hatte.

HOLGER TUCHOLLA danke ich für seine stetige Hilfsbereitschaft sowie für die netten Telefonate und Pläuschchen abseits des Laboralltages. WOLFRAM MATHIS, FRANK PETERS, HEIKO RENZIEHAUSEN und seinem Team sowie allen Mitarbeitern vom Gebäudemanagement danke ich für die schnelle und stets freundliche Hilfe bei handwerklichen und technischen Problemen jeglicher Art. DANIEL FRANK danke ich für seine Hilfe im Laboralltag und bei den zahlreichen Computerfragen.

Bei meinen 'Jungs' FLORIAN CZERNY, NILS MEYER, DENIS PAHLKE, MARKUS WIEGAND, MATHIS RINK, MATTHIAS KRULL, DR. EIKE SACHS und DR. STEFAN MÜLLAR sowie den 'Ladies' DR. HANNA RADZEY, GERALIN HÖGER UND ANASTASIYA SCHIRMACHER möchte ich mich für die netten Kaffeepausen, das Kickern, den Spaß und das ein oder andere Feierabendbier bedanken.

Bei den Volleyballern sowie meinen Freunden aus der Heimat und aus Göttingen möchte ich mich für die schöne gemeinsame Zeit außerhalb der Arbeit bedanken.

Ein besonderer Dank geht hierbei an DR. HANNA 'HÄNNA' RADZEY, die mit ihrer offenen nordischen Art einfach alles hat so leicht erscheinen lassen. Das Quatschen hinter der Säule, das Rumalbern beim Volleyball sowie die normalen Gespräche sind und waren einfach unbezahlbar und ich danke dir für deine Freundschaft.

DR. ANNIKA GROSCHNER möchte ich an dieser Stelle von ganzem Herzen für ihre Freundschaft danken. Von Anfang an lagen wir auf einer Wellenlänge und noch heute ist es so, dass bei jedem Treffen die Zeit mit dir wie im Flug vergeht. Das Klackern deiner High Heels wird mir hoffentlich bis ins hohe Alter ein Lächeln ins Gesicht zaubern.

FLORIAN CZERNY danke ich für die Umsetzung unseres Plans 'ich bleibe, wenn du bleibst'. Unsere Freundschaft wird immer etwas Besonderes bleiben und ich danke dir für deine charmante, humorvolle und stets freundliche Art.

SARINA TERHARDT danke ich für die tolle Freundschaft, die nun seit fast 20 Jahren besteht und ewig halten wird, weil das Lachen mit dir einfach noch immer wie früher ist.

Meinem Chemielehrer HERRN V. GÖTZE danke ich für den Schubser in die richtige Richtung.

Der ˈSippeˈ und ganz besonders ANJA und KLAUS danke ich für die Unterstützung und die tolle gemeinsame Zeit in den letzten 11 Jahren.

Meiner Schwester BIRGIT danke ich für ihre Freundschaft und einfach dafür, dass sie meine geliebte Schwester ist.

PETER, dir danke ich für deine Liebe, deinen tollen Humor und die schöne gemeinsame Zeit, die wir zusammen verbringen. Es wird einfach nie langweilig bei uns und ich genieße wirklich jeden Tag, den wir miteinander haben. <3

Meiner Familie und ganz besonders meinen Eltern danke ich für alles, was sie in den letzten Jahren für mich getan haben. Ohne euch wäre der lange Weg des Chemiestudiums nicht möglich gewesen. Ihr habt dabei immer an mich geglaubt und ich konnte mir eurer Unterstützung und Liebe stets sicher sein. DANKE SCHÖN !

CURRICULUM VITAE

Personal Data

Name:	Ulrike Rost
Date of birth:	04 June 1984
Place of birth:	Leipzig
Nationality:	German

Work Experience

Since 10/2012

Research associate at the Institute of Organic and Biomolecular Chemistry at the Georg-August-University, Göttingen.

- *Development and realisation of different lab courses and tutorials*
- *Mentoring of students during their Bachelor- and Master thesis*

07/2012 - 08/2016

Lecturer at the XLAB, Experimentallabor für junge Leute e.V., Göttingen.

- *Teaching of national and international students in natural science courses*
- *Teaching and supervision of international students in natural science courses during ”International Science Camp (ISC)“*

01/2012 - 09/2012

Research assistant at the Institute of Organic and Biomolecular Chemistry at the Georg-August-University, Göttingen.

- *Mentoring of a student during her Bachelor thesis*
- *Tutor in ”Experimentalchemie I“*

Academic Education

01/2012-08/2016

PhD thesis within the research group of Prof. Dr. Ulf Diederichsen at the Institute of Organic and Biomolecular Chemistry at the Georg-August-University, Göttingen.

Title: *”Organisation and Recognition of Artificial Transmembrane Peptides”*

01/2011 – 11/2011	Diploma thesis within the research group of Prof. Dr. Ulf Diederichsen at the Institute of Organic and Biomolecular Chemistry at the Georg-August-University, Göttingen. Title: *"Organisation von D/L-alternierend konfigurierten Transmembranhelices durch Wasserstoffbrückenerkennung"* ***grade: very good***
10/2004 – 11/2011	Studies of Chemistry at the Georg-August-University, Göttingen ***grade: good***

Education

06/2004	General matriculation standard at the Geschwister-Scholl Gymnasium in Fürstenwalde/Spree

Qualifications

Awards	Award for the best independent teaching at the Institute of Organic and Biomolecular Chemistry at the Georg-August-University, Göttingen: winter semester 2013/2014, summer semester 2014 and winter semester 2014/2015.
Publications	Three publications in professional journals - K. Menck *et al.*, *J. Mol. Cell Biol*. **2015**, *7*, 143–153. - U. Rost *et al.*, *ChemPhysChem* **2016**, *17*, 2525–2534. - U. Rost *et al.*, *Chem. Sci*. **2016**, *7*, 5900–5907.

Languages & IT

Languages	German (native speaker), English (fluent)
IT	MS Office Paket, SciFinder, ChemOffice, Origin

Freizeitaktivitäten

Recreation	Kitesurfing, volleyball

Göttingen, 15.06.2016

Ulrike Rost